Testosterone: impact on peripheral human T cells in health and autoimmunity

Dissertation

to obtain the degree

Doctor *rerum naturalium* (Dr. rer. nat.)

at the Faculty of Mathematics, Informatics and Natural Sciences

of the University of Hamburg

submitted by

Lara Henze

August, 2021

This dissertation was performed at the research laboratories for Immunoregulation and Liver Inflammation in the I. Department of Medicine, University Medical Center Hamburg-Eppendorf (UKE) and thankfully supervised by Prof. Dr. Christoph Schramm and Dr. Dorothee Schwinge to obtain the academic degree of Doctor of Natural Sciences (Dr. rer. nat.) at the Faculty of Mathematics, Informatics and Natural Sciences, University Hamburg.

Disputation: 05.04.2022

Reviewers:

Prof. Dr. Christoph Schramm, I. Department of Medicine University, University Medical Center Hamburg-Eppendorf (UKE)

Jun.-Prof. Dr. Esther Diekhof, Neuroendocrinology, Institute of Cell and Systems Biology of Animals, University Hamburg

Contents

Abstract

Women are more prone to develop autoimmune diseases (AID), including the autoimmune liver diseases primary biliary cholangitis (PBC) and autoimmune hepatitis (AIH). The mechanisms that cause this female predominance are still unknown, but dysregulated immune responses have been described as a major hallmark. There is increasing evidence suggesting an important and so far underexplored role for testosterone in mediating sex differences in immune responses. In this study, we aimed to unravel the effects of testosterone on the phenotype and function of T cells *in vivo* and *in vitro* and how this contributes to the pathogenesis of autoimmune liver diseases.

We confirmed that immune cells are able to respond to testosterone through the detection of the cytosolic androgen receptor (AR) and the membrane androgen receptor ZIP9 on *ex vivo* human lymphocyte populations, including CD4 and CD8 T cells. Using *in vitro* assays, we demonstrated that the stimulation of human T cells in the presence of testosterone had no effect on their proliferative capacity but resulted in decreased secretion of the proinflammatory cytokines TNFα and IFNγ. This finding is of particular interest because the involvement of IFN/TNF-producing cells has been studied for many AIDs, including AIH. To analyze the direct effects of testosterone *in vivo*, we recruited a unique cohort of transgender patients undergoing high doses of testosterone treatment. Sample collection was performed before treatment (BL), as well as 3 months (3M) and 6 months (6M) after the start of testosterone administration, and increased serum testosterone levels were confirmed after 3M and 6M. The characterization of the immune cells in blood was performed by flow cytometry-based deep immunophenotyping combined with CITE-Sequencing of T cells. Using these in-depth analyses, we revealed that testosterone treatment was associated with changes in distinct T cell subpopulations. Thus, a reduction in effector memory (EM) T cells, especially CD8 EM T cells and TH17 cells, was observed under testosterone treatment. On the other hand, using flow cytometry, the frequencies of CD4 and CD8 TEMRA (effector memory re-expressing CD45RA T cells) T cell populations and of CD4 regulatory T cells (Treg) were shown to increase under testosterone treatment. Importantly, CITE-Seq analysis validated the increase in CD8 TEMRA cells. Mechanistically, altered gene expression upon testosterone treatment in specific T cell clusters could be detected. Invariant γδ T cells and mucosal-associated invariant T cells (MAITs) had the greatest differential gene expression upon *in vivo*

testosterone treatment, while most T cell clusters showed an increased GIMAP7 expression. The role of GIMAP7 in T cells is so far completely unknown.

To confirm the role of testosterone in AID, we collected peripheral blood samples of patients with autoimmune liver diseases and healthy age- and sex-matched controls through a translational approach. Interestingly, female AIH and PBC patients showed decreased bioavailable testosterone levels in serum compared to age-matched controls. In addition, these patients showed increased TH1/Treg and TH17/Treg ratios compared to healthy controls. Of note, these ratios were significantly reduced in our trans men cohort after testosterone treatment.

In general, our data demonstrate that testosterone is able to shape immune cell responses and likely tips the balance towards a more anti-inflammatory immune response. This finding might be one of the reasons why males are less likely to develop autoimmune diseases. Further elucidation of the mechanisms underlying the impact testosterone has on T cell function and differentiation will help us understand the sex dimorphism in immunity and why females are more prone to develop autoimmune diseases.

Zusammenfassung

Frauen sind anfälliger für die Entwicklung von Autoimmunerkrankungen, einschließlich der autoimmunen Lebererkrankungen Primär biliäre Cholangitis (PBC) und Autoimmune Hepatitis (AIH). Die Mechanismen für die weibliche Prädominanz sind noch unbekannt, aber dysregulierte Immunantworten wurden als ein Hauptmerkmal beschrieben. Es gibt zunehmend Hinweise darauf, dass Testosteron eine bedeutende und bisher wenig erforschte Rolle bei der Vermittlung von Geschlechtsunterschieden in der Immunantwort spielt. In dieser Studie wollten wir die Auswirkungen von Testosteron auf den Phänotyp und die Funktion von T-Zellen *in vivo* und *in vitro* entschlüsseln und untersuchen, wie dies zur Pathogenese von Autoimmunerkrankungen der Leber beiträgt.

Wir bestätigten, dass Immunzellen in der Lage sind, auf Testosteron zu reagieren, indem wir den zytosolischen Androgenrezeptor AR und den membranständigen Androgenrezeptor ZIP9 auf *ex vivo* isolierten primären menschlichen Lymphozytenpopulationen nachwiesen, einschließlich CD4- und CD8-T-Zellen. In *in-vitro*-Assays konnten wir zeigen, dass die Stimulation humaner T-Zellen in Gegenwart von Testosteron keinen Einfluss auf ihre proliferative Kapazität hatte, aber zu einer verminderten Sekretion der pro-inflammatorischen Zytokine TNFα und IFNγ führte. Dies ist von besonderem Interesse, da eine Beteiligung von IFN/TNF-produzierenden Zellen für viele Autoimmunerkrankungen einschließlich AIH pathogenetisch bedeutsam ist. Um die direkten Effekte von Testosteron *in vivo* im Menschen zu analysieren, wurde eine Kohorte von Transgender-Patienten rekrutiert, die sich einer hochdosierten Testosteronbehandlung unterzog. Die Proben wurden vor der Behandlung (BL) sowie drei Monate (3M) und sechs Monate (6M) nach Beginn der Testosterongabe entnommen und die erhöhten Testosteronspiegel im Serum wurden nach 3M und 6M bestätigt. Die Charakterisierung der Immunzellen im Blut wurde mittels einer ausführlichen durchflusszytometrischen Immunphänotypisierung in Kombination mit CITE-Sequenzierung von T-Zellen durchgeführt. Mit dieser umfassenden Analyse konnten wir feststellen, dass die Testosteronbehandlung mit Veränderungen in verschiedenen T-Zell-Subpopulationen verbunden war. So wurde unter Testosteronbehandlung eine Reduktion der Effektor-Memory (EM)-T-Zellen beobachtet, insbesondere der CD8-EM-T-Zellen und der TH17-Zellen. Auf der anderen Seite konnten eine Zunahme der T-Zellpopulationen CD4- und CD8-TEMRA (Effektor-Gedächtniszellen, die CD45RA exprimieren) sowie eine

Zunahme der regulatorischen T-Zellen (Treg) mittels durchflusszytometrischer Analyse nachgewiesen werden. Bedeutend ist, dass der Anstieg der CD8-TEMRA-Zellen durch eine CITE-Seq-Analyse validiert werden konnte. Mechanistisch konnte eine veränderte Genexpression nach Testosteronbehandlung in spezifischen T-Zell-Clustern nachgewiesen werden. Invariante γδ-T-Zellen und MAIT-Zellen hatten die stärkste differentielle Genexpression nach *in-vivo*-Testosteronbehandlung, während die meisten T-Zell-Cluster eine erhöhte GIMAP7-Expression aufwiesen. Die Rolle von GIMAP7 in T-Zellen ist bisher noch unbekannt.

Um die Rolle von Testosteron bei Autoimmunerkrankungen zu bestätigen, wurden in einem translationalen Ansatz periphere Blutproben von Patienten mit autoimmunen Lebererkrankungen und gesunden alters- und geschlechtsgematchten Kontrollen gesammelt. Interessanterweise zeigten weibliche AIH- und PBC-Patienten im Vergleich zu altersgleichen Kontrollen verminderte bioverfügbare Testosteronspiegel im Serum. Darüber hinaus zeigten diese Patienten im Vergleich zu den gesunden Kontrollen tendenziell erhöhte TH1/Treg- und TH17/Treg-Ratios. Diese Ratios waren nach der Testosteronbehandlung in unserer Transgender-Kohorte signifikant reduziert.

Zusammengenommen deuten unsere Daten darauf hin, dass Testosteron in der Lage ist, Immunzellantworten zu formen, was zu einem weniger inflammatorisch ausgerichteten peripheren Immunsystem führen kann. Dieser Befund könnte ein Grund dafür sein, dass Männer weniger anfällig für die Entwicklung von Autoimmunkrankheiten sind. Die weitere Aufklärung der Mechanismen, über die Testosteron die Funktion und Differenzierung von T-Zellen beeinflusst, wird uns helfen, die Unterschiede zwischen den Immunzellantworten von Männern und Frauen weiter zu verstehen und erklären zu können, warum Frauen anfälliger für die Entwicklung von Autoimmunkrankheiten sind.

Publication List

IL-17A/F enable cholangiocytes to restrict T cell-driven experimental cholangitis via PD-1/PD-L1 interaction. Stein S, **Henze L**, Poch T, Carambia A, Krech T, Preti M, Amrei Schuran F, Reich M, Keitel V, Fiorotto R, Strazzabosco M, Fischer L, Li J, Müller LM, Wagner J, Gagliani N, Herkel J, Schwinge D, Schramm C. J HEPATOL. 2020 Nov 13. https://doi.org/10.1016/j.jhep.2020.10.035

The Effects of Androgens on T Cells: Clues to Female Predominance in Autoimmune Liver Diseases? Henze L, Schwinge D, Schramm C. Frontiers in Immunology. 2020 Jul 29;11. https://doi.org/10.3389/fimmu.2020.01567

Monocytes as potential mediators of pathogen-induced Th17 differentiation in patients with primary sclerosing cholangitis (PSC). Kunzmann, LK, Schoknecht, T, Poch, T, **Henze, L**, Stein, S, Kriz, M, Grewe, I, Preti, M, Hartl, J, Pannicke, N, Peiseler, M, Sebode, M, Zenouzi, R, Horvatits, T, Böttcher, M, Petersen, B-S, Weiler-Normann, C, Hess, LU, Elise Ahrenstorf, A, Lunemann, S, Martrus, G, Fischer, L, Li, J, Carambia, A, Kluwe, J, Huber, S, Lohse, AW, Franke, A, Herkel, J, Schramm, C & Schwinge, D. HEPATOLOGY. 2020 Jan 23. https://doi.org/10.1002/hep.31140

TNF-Producing Th1 Cells Are Selectively Expanded in Liver Infiltrates of Patients with Autoimmune Hepatitis. Bovensiepen, CS, Schakat, M, Sebode, M, Zenouzi, R, Hartl, J, Peiseler, M, Li, J, **Henze, L**, Woestemeier, A, Schramm, C, Lohse, AW, Herkel, J & Weiler-Normann, C. J IMMUNOL. 2019 Dez 15;203(12):3148-3156. https://doi.org/10.4049/jimmunol.1900124

1. Introduction

1.1. Basic principles of the immune system

The immune system can be divided into the innate and the adaptive immune system, both fighting potentially harmful pathogens and antigens, such as microorganisms or toxins. Furthermore, the specific architecture of organs, as well as their chemical or physical barriers, are important for the maintenance of our bodies. The quick (first line of defense) response is the innate immune system, which can mount an immune reaction within minutes or hours. It is mainly composed of monocytes, macrophages, dendritic cells, natural killer cells and innate lymphoid cells (ILCs)[1,2]. The foreign antigen or pathogen is destroyed by antimicrobial peptides and phagocytosis, while the secretion of cytokines and chemokines attract more innate cells and enhance the innate immune response. The adaptive immune response takes longer than the innate response but is more specific. The secretion of chemokines and cytokines by the innate immune system can recruit cells associated with the adaptive immune system. These consist mainly of T and B cells, which express highly specific T and B cell receptors on their surface. Adaptive immune cells are able to specifically detect foreign antigens and non-self molecules and lead to the specific deletion of the foreign antigen[2-4].

T cells are a major part of the adaptive immune system and are involved in many AIDs. T cells are named after their origin in the thymus and have a variety of T cell receptors (TCRs) on their surface to interact with the major histocompatibility complex (MHC) molecules. TCRs consist of two different chains, most frequently the TCRα and TCRβ chain and less commonly the TCRγ and TCRδ chain. Different chains leading to the ability to fight different foreign antigens or pathogens arise from the VDJ recombination of the constant C region, the variable V, D and J region in each chain. Together with the TCR co-receptor CD3 and its domains (CD3γε/CD3δε/CD3ζζ), they are referred to as the TCR complex[5,6].

T cells can be divided into helper (TH), cytotoxic (TC) and regulatory T Cells (Tregs). Conventionally, CD4 T cells are referred to as TH cells and CD8 T cells as the cytotoxic component. More specifically, several CD4, CD8 positive, double positive and negative subpopulations have been described in the last decades[7]. Most of them are explained in more detail in the following chapter.

1.1.1. T cell subpopulations orchestrate different functions of the immune system

The classical subpopulation of T cells includes TH1, TH2, TH17, Tregs and TC cells. In addition to these conventional T cells, unconventional T cells with a more innate phenotype exist, including MAITs (mucosal-associated invariant T cells), γδ T cells, and NKT cells. Moreover, most T cells can be assigned to their effector status, such as naïve, central memory or effector/TEMRA (effector memory re-expressing CD45RA T cells) cells[7,8] (Fig. 1). Naïve T cells express an isoform of the leukocyte common antigen CD45RA and concurrently express CD197 (CCR7) and CD62L. The lack of CD45RA characterizes their central memory (CM) phenotype. Effector cells, also called effector memory RA (TEMRA) cells, express CD45RA and not CD62L/CD197. If they express neither, they are effector memory (EM) cells[8] (Fig. 1).

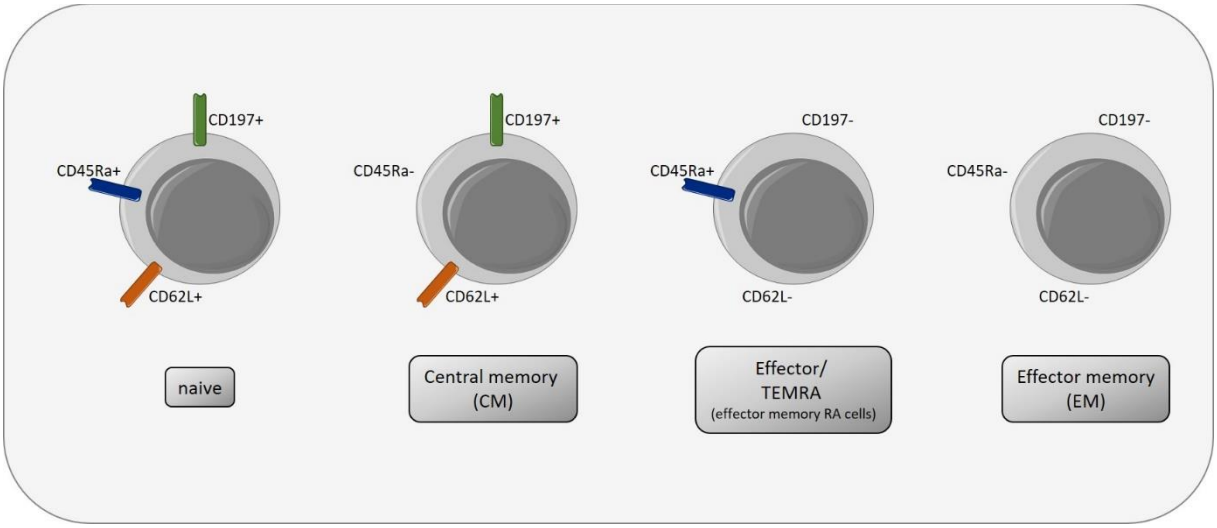

Figure 1. Schematic presentation of the naïve, effector and memory T cell subset characteristics. Naïve T cells express CD45RA+, CD62L+, and CD197+; central memory T Cells (CM) do not express CD45RA+; TEMRA T cells express CD45RA only; and effector memory T cells (EM) express neither.

Depending on the TCR's affinity for the antigen-MHC II complex on the antigen-presenting cell (APC) and in the surrounding environment (including cytokines and chemokines), naïve T cells can differentiate into other T cell subsets and can be characterized by their production of specific cytokines and master transcription factor. Figure 2A outlines some of these differentiations for CD4 T cells. TH1, TH2 and TH17 are called T helper cells, while CD4 Tregs are responsible for tolerance. Though TH1 cells primarily produce IFNγ, they also produce IL-2 and TNF and are likewise part of cellular immunity. IL-4 and IL-13 are

the major cytokines of TH2 cells and IL-17 is the major cytokine of TH17 cells. TH2 cells are part of humoral immunity and have been associated with the defense against parasites and the development of allergies, while TH17 cells have been implicated in multiple autoimmune diseases. These subsets also have major transcription factors that initiate or maintain their differentiation state: TBET for TH1 cells, GATA-3 for TH2 cells, RORC/RORγt for TH17 cells and FOXP3 for Tregs[9,10].

Similar populations have recently been described for CD8 T cells, such as TC1, TC2 and TC17 cells, in addition to the classic TC cells, which mainly produce Granzyme B[7,8]. Furthermore, there are invariant T cells with specific T cell receptor chains, including NKT cells, MAITs, and γδ T cells, whose main features are outlined in Figure 2B.

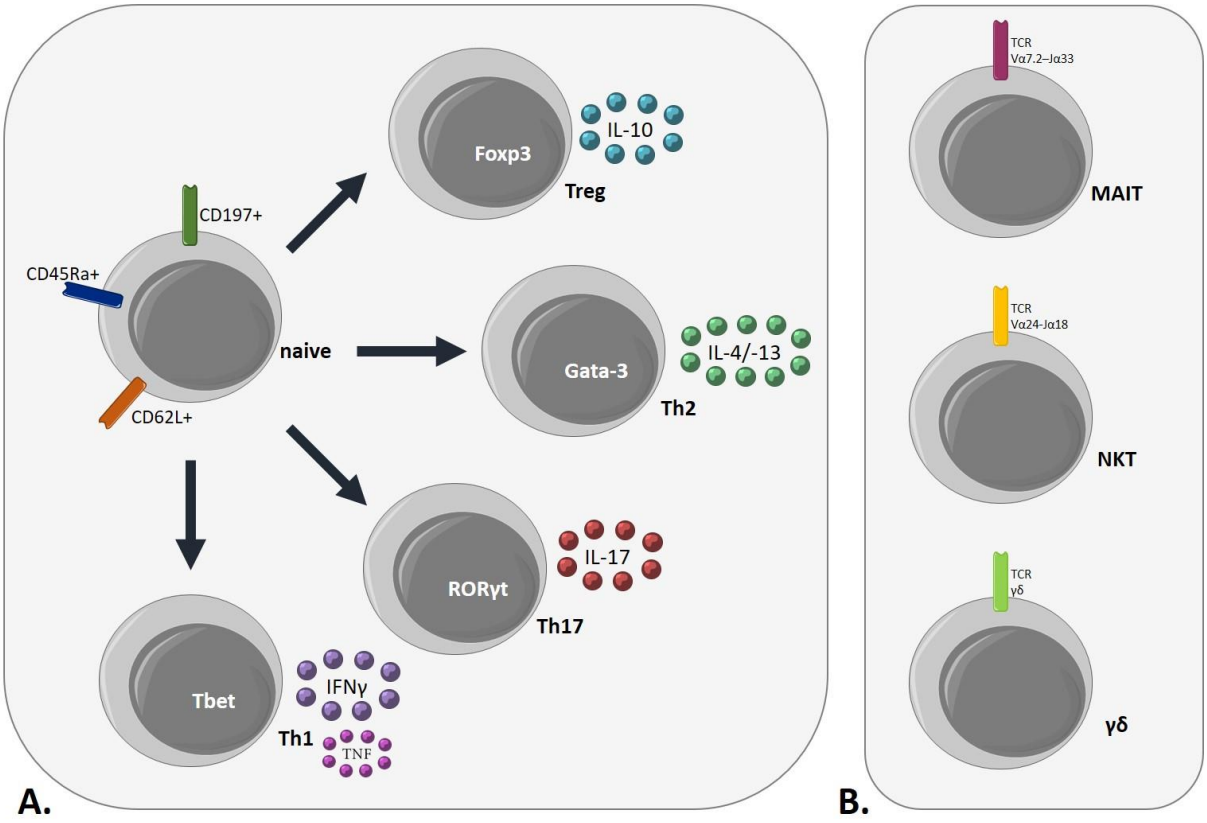

Figure 2. Schematic representation of T cell subtypes. A. CD4 T cell helper subtypes and their main transcription factors and cytokines. Naïve CD4 T cells can differentiate into TH1 cells, with their main transcription factor TBET and produce mainly IFNγ and TNF. Furthermore, they can differentiate into TH17 cells, expressing RORγt and producing IL-17. They can also differentiate into TH2 cells marked by GATA-3 expression and IL-4 and IL-13 production. Lastly, naïve cells can differentiate into Tregs, which express FOXP3 and mainly produce IL-10[7,8]. **B**. Invariant T cell subtypes and their invariant TCR chains: Vα7.2-Jα33 for human mucosal-associated invariant T cells (MAITs), Vα24-Jα18 for natural killer T cells (NKT) and TCRγδ for γδ T cells[11-13].

However, there is an ongoing discussion about the assignment of specific surface markers or transcription factors to a specific T cell subset, and there is considerable plasticity between the different subtypes. The nomenclature this study uses is outlined in this Introduction and in Chapter 5.1.

In addition to cytokines, immune cells and T cells can produce chemokines and express chemokine receptors. For example, CCL20 is a typical cytokine produced by cholangiocytes whose corresponding receptor is CCR6 (CD196), which is expressed by DCs and B cells but also by T cells[14]. Table 1 summarizes the chemokines and matching receptors that this study investigates. Furthermore, T cells express activator, co-activator, and inhibitory molecules, which can influence their interaction with other cells and ultimately their immunomodulatory function. The most prominent example of a co-receptor is CD28; Table 1 describes some of the other molecules this thesis considers.

Table 1. Surface molecules of T cells and their proposed counterparts and function.

On T cell	Proposed counterparts	Presumably involved in….
CD196/CCR6	CCL20	TH17, homing to gut/inflamed skin/lung[8,14]
CD183/CXCR3	CXCL9, CXCL10, CXCL11, CXCL4	CD4+, CD8+, TH1, homing to inflamed sites[7,8]
CD161/KLRB1	LLT1/CLEC2D	CD4+, CD8+, TH17, NKT[7,8,11]
CD279/PD-1	PD-L1, PD-L2	Exhaustion marker, inhibitory receptor[8]
CD272/BTLA	HVEM	Inhibitory receptor[8]
CD25	IL-2	Marker of activation[7,15,16]
CD57	CD62L, CD62P	CD4+, CD8+, adhesion, TEMRA/EM[7,8]
CD103	ITGB7, E-cadherin	T cell homing, tissue-resident memory T cells[17,18]
CD49a/VLA-1	Collagen, PSGL-1	Homing to lung/skin, CD8, tissue-resident memory[17,19]
CD49b/VLA-2	Collagen, laminin, fibronectin	Tr1, homing to gut, TH17[20]

CD39		T cell stability, activation, ATP/adenosine modulation, immunosuppression[8,21,22]
CD73		ATP/adenosine modulation, immunosuppression[8,21]
CD223/LAG-3	MHC class II, FGL1, LSECtin	Treg, Tr1, NK cells, TC, immunosuppressive[23-25]
CD127/IL7R	IL-7	Memory T cells, stem-like, low in Tregs[16,26,27]

T cells are influenced by their surrounding milieu and accordingly change their expression profile and differentiate into the subtypes outlined above. The main drivers of a T cell subset are cytokines and chemokines produced by other T cells and immune cells, such as antigen-presenting cells. This change allows the immune system to specifically adapt to its current conditions.

1.2. Sex bias in disease

Overall, women have a higher risk of autoimmune diseases (AIDs), a lower risk for most infectious diseases[28-30], and a greater ability to clear viral infections[31] than men. The involvement of sex hormones and sex chromosomal alterations in disease development and immunological processes is widely accepted[29,32-34]. However, the mechanism and signaling cascades in different cell types and the resulting consequences remain unclear.

Men have a higher incidence of infectious diseases, including parasitic infections such as Leishmaniasis[29], which are also often more severe than in women. For example, older males are more vulnerable to influenza compared to adult males and older females, possibly due to declined testosterone levels in aging[35]. Furthermore, men have a higher incidence of cryptococcosis infection than women[36]. In men, urinary tract infections are often more severe and persistent, despite their higher incidence in women[37].

Women, on the other hand, are more prone to autoimmune diseases, although some of these diseases are more severe in men (see Chapter 1.3). Autoimmune diseases are disorders characterized by an immune response against healthy self-cells and can be found in nearly all parts of the body. Most patients with AIDs have antibodies against parts

of the body, called autoantibodies. The pathophysiology of most AIDs is very complex and has environmental, genetic, and epigenetic components (Fig. 3). Several AIDs, including multiple sclerosis (MS) and systemic lupus erythematodes (SLE), have been shown to occur predominantly in women. Importantly, given the high prevalence of AIDs such as SLE in women, the role of estrogen has been widely investigated. However, the role of testosterone on immune cells has been underestimated, especially in women.

To date, research has shown that in men and women, a higher amount of total and bioavailable testosterone is associated with higher levels of hemoglobin[38,39], leading to a significantly higher risk of anemia in men and women with low testosterone levels[39]. Moreover, it has recently been reported that the microbiome can influence testosterone levels, adding another layer of interaction between the different possible reasons for sex bias in diseases[40].

In addition to hormones, some studies have suggested that in women, incomplete X inactivation (XCI) contributes to the higher incidence of AIDs due to the higher expression of genes that escape XCI. Numerous genes are involved in immune pathways encoded on the X chromosome. Those known to be involved in AID disease development include, for example, *TLR7*, *CD40L*, *FOXP3* and *IL2RG*. MicroRNAs, such Mir-18b, Mir-223 and Mir-106a[41], are also involved. A study showed that in SLE *TLR7* in pDCs, monocytes and B cells escape XCI[42,43]. In three AIDs with a high female frequency, autoimmune thyroid disease, systemic sclerosis, and PBC, an enhanced rate of X monosomy in PBMCs, possibly including T and B cells, was found compared to healthy women. Meanwhile, XCI was random and similar to the control groups, though it increased with age[44-46]. Both X chromosome encoded genes and XCI likely have an influence and therefore the effect of hormones should always be observed in the context of the sex chromosome background (XX or XY).

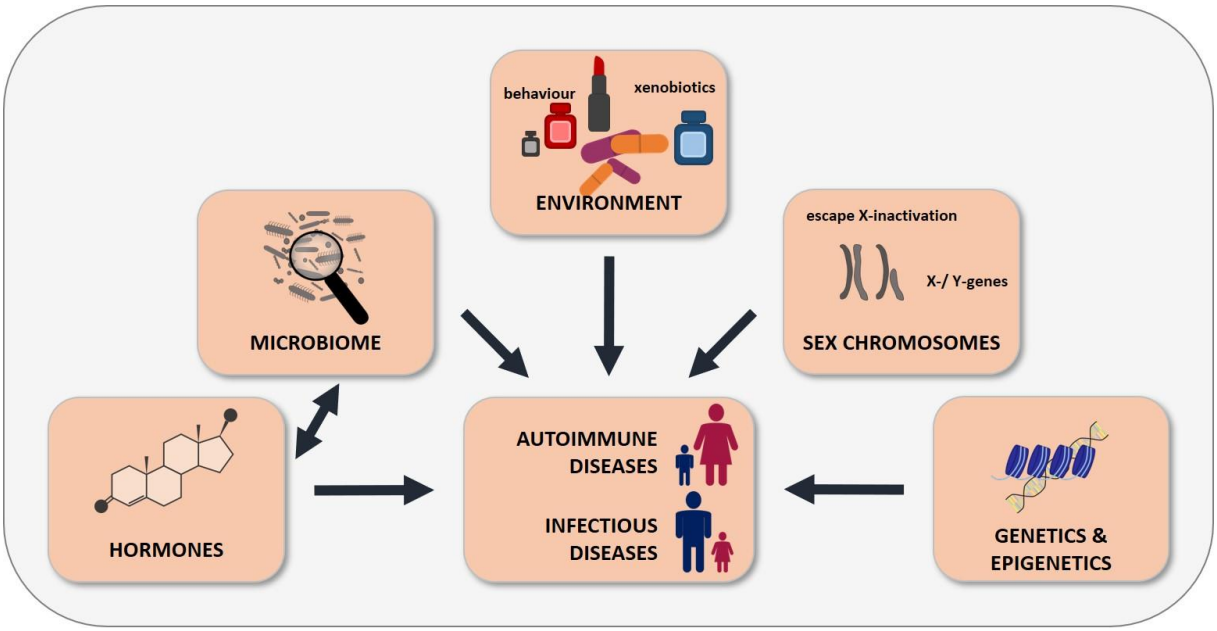

Figure 3. Schematic presentation of possible reasons for sex bias in diseases. Many autoimmune diseases affect more women than men, although in some infectious diseases, it is the other way around. This sex bias could be due to or at least influenced by the individual's environment, including behaviors commonly expressed by the same gender as well as xenobiotic influences. Different genes are encoded on the X and Y chromosomes, and some genes escape X inactivation. Most diseases also have a genetic component and are further influenced by epigenetics. Research has found that the microbiomes of men and women are different and could therefore influence diseases. It has also been reported that microbiomes can influence testosterone levels. Lastly, hormones are thought to play a role in the sex bias of diseases.

1.2.1. Sex bias in autoimmune diseases (AID) and autoimmune liver diseases (AILD)

Most autoimmune diseases are predominant in females[47]. A prominent example is MS, a heterogeneous AID of the brain, spinal cord and nerves, with a female to male sex ratio of approximately 3:1[48]. The pathogenesis is unknown, but autoreactive T cells against myelin antigens have been identified as an early driver of this disease. Thus, multiple subsets of T cells seem to be involved, including TH1 and TH17 cells, as well as Tregs, CD8+ T cells and B cells[49,50]. In addition, the interaction of distinct microbiota, X chromosome dosage and sex hormones probably contribute to the disease. Of interest, a lower level of testosterone in men with MS compared to healthy men has been reported and correlated to disease severity[51]. Some small studies have shown disease improvement upon testosterone treatment of male MS patients[51,52].

Another prominent example of an AID with a high female to male ratio (9:1) is systemic lupus erythematosus (SLE)[53,54]. Men have a more severe disease progression and

outcome and more often develop end-stage renal disease[55]. Enhanced expression of type I interferons is regularly found in patients with SLE, demonstrating the involvement of the immune system[56]. Females have a higher prevalence of developing juvenile SLE after puberty, which indicates the involvement of sex hormones[57]. In women with SLE, lower amounts of testosterone than in healthy women have been reported[58].

Autoimmune liver diseases (AILD) have been shown to have a high female to male ratio. Three different AILD are currently known: primary sclerosing cholangitis (PSC), primary biliary cholangitis (PBC) and autoimmune hepatitis (AIH). Of these three autoimmune liver diseases, PBC and AIH show a strong female dominance[59,60].

Due to its special localization and constant blood flow, the liver has unique immunological functions and must continuously balance between tolerance and immune responsiveness. In autoimmune liver diseases, this balance is disturbed, and excessive immune activation occurs in the liver [61,62].

PBC has a female to male ratio of up to 9:1[63]. Inflammatory responses are directed against intrahepatic cholangiocytes. Chronic disease progression includes portal inflammation with granuloma formation, the destruction of the small bile ducts and ductopenia. If left untreated, PBC leads to liver cirrhosis and death. This rare AILD is characterized by the presence of specific antinuclear antibodies and anti-mitochondrial antibodies, most of them against the pyruvate dehydrogenase complex (PDC-E2)[63,64]. PBC has not only HLA associations but also associations with other genetic risk loci. CD4+ and CD8+ T cells are highly enriched in portal triads, suggesting T cells play a role in disease development[64]. Men with PBC have a more severe disease course than women, shown in higher serum alkaline phosphatase and a higher mortality rate[63,65]. Additionally, Abdulkarim et al. reported a delayed diagnosis and worse prognosis in men with PBC[66].

In AIH, the incidence is higher in females than in males (3:1). Men and women seem to exhibit no differences in clinical manifestations at presentation, but men are more likely to experience a relapse in disease activity after the initial treatment response and be diagnosed at a younger age[60,67]. AIH is characterized by an immune response against hepatocytes, and patients often present with non-organ specific autoantibodies, elevated serum transaminase and IgG levels, and hypergammaglobulinemia. Risk factors that are known but not crucial include the human leukocyte antigen alleles (HLA)-DRB1*03:01 and HLA-DRB1*04:01[60,68]. CD4+ and CD8+ T cells are involved in the disease

pathogenesis [64,69]. Recently, an elevated population of CD4+ TNFα+ (most of them also IFNγ+) in AIH patients compared to healthy controls has been reported[70]. Besides the obvious sex bias, the age of onset and the disease alterations during pregnancy indicate the involvement of sex hormones in disease pathogenesis. Disease modulation by pregnancy is exemplified by the reduced disease activity of AIH during pregnancy and frequent flares after delivery[71-74].

1.3. The importance of androgens and androgen signaling in a variety of biological functions

Androgen metabolism and signaling are very complex and tissue dependent. In general, there are four major androgenic steroid hormones: dehydroepiandrostenone (DHEA), androstenedione, dihydrotestosterone (DHT) and testosterone. They are generated from cholesterol, and testosterone can also be converted into estrogen by the enzyme aromatase, depending on the tissue. DHT is metabolized from testosterone through the 5α-reductase and cannot be further converted into estrogen[75-78]. Only 0.5–3% of testosterone is freely in the blood; the rest is either bound to albumin (around 30–35%) or sex hormone-binding globulin (SHGB) (65–70%)[79]. The amount of bioavailable testosterone can therefore be estimated by the concentrations of total testosterone, SHGB and albumin serum levels[80]. The androgen levels of total testosterone range from 0.35 to 2.94 nmol/l in women, while the typical range is 6.2 to 32.1 nmol/l in men[79,81,82]. The amount of total and bioavailable testosterone is significantly higher in males, but in both sexes, it declines significantly with age. Furthermore, in women, there might be a slight peak of testosterone at midcycle, while in men, there is a slight daily decrease towards the afternoon[81-84].

Testosterone is involved in the regulation of a variety of processes, including libido, fat distribution, bone mass, production of sperm, red blood cells and muscle mass and strength. Moreover, some testosterone actions have been attributed to its conversion to estrogen, such as its effects on male bone mass[78,85,86].

Currently, two types of androgen receptors have been identified, the classical cytosolic androgen receptor (AR) and the non-classical membrane bound receptors (mAR)[78,87].

Similarly, there are two cytosolic estrogen receptors, the transcription factors ER1 and ER2, and membrane bound estrogen receptors such as GPER1[88,89].

DHT has a high affinity to AR and a low occurrence of dissociation, while its affinity for mARs is probably lower than that of testosterone[78]. The expression of the AR has been shown in many different tissues, including epithelial, endothelial and immune cells in mice and humans[90-92]. Conversely, the expression of ZIP9, one of the mARs, has only been reported in some tissues, and other proposed mARs such as GPRC6A have only been detected in prostate-related tissue[78,93-96].

The cytoplasmic AR is a transcription factor and can be ligand dependent and independent[97,98]. The human AR gene is located on the X chromosome, has eight exons and a DNA-binding domain, a ligand-binding domain and an N-terminal domain. In the cytoplasm, it resides in a complex with heat-shock proteins, cytoskeletal proteins and chaperons, and after a conformational change due to ligand binding, the receptor dimerizes and translocates to the nucleus[99,100]. The receptor recognizes androgen response elements on the genes and executes its transcriptional activity[99,101]. AR signaling can undergo ligand-independent modulation through ubiquitination, methylation and phosphorylation[99,101,102].

In addition, the AR can not only be modulated independently of ligands but also signal independently of androgenic ligands. For example, it has been shown that IL-6 interferes with the signaling of PKA/PKC/MAPK through the AR, and IL-8 has been found to promote AR-dependent growth[78,100,103-105]. This further complicates AR signaling depending on both the organ, tissue and cell type and on the inflammation milieu that can occur in an autoimmune injury.

The AR has been shown to interact in some cells with the gene transcription of *PI3K*, *RAS* GTPase and *SRC* family kinase, leading to MAPK/ERK signaling that in turn initiates, for example, cell survival and proliferation[99,100]. Non-genomic AR signaling has been suggested for mTOR, FOXO1, FOXO3a, HDAC3, AKT, EGFR and STAT3[99,106-110].

The signaling of the mARs is even more unclear. The zinc transporter ZIP9 (SLC39A9) has been shown to interact with several kinase pathways, such as the ERK1/2 pathway, in specific cell types[111-114].

In general, the signaling and activation of the AR and mARs are complex and highly tissue and context dependent.

1.4. T cells are influenced by androgens

There have been several suggestions that androgens influence the immune system and T cells in particular[115,116]. However, the mechanisms and the consequences of androgen actions on T cells remain unknown.

The expression of the AR has been found on a variety of mice and human innate and adaptive immune cells, including macrophages, monocytes, neutrophils, mast cells and ILCs[88,117-121]as well as CD4+ and CD8+ T cells[117,122-124]. In addition, T cells were shown to express an mAR in the 1990s, although the specific mAR was not known[93,95].

To date, studies investigating the effects of androgens and T cells have mainly compared male and female T cells *ex vivo*, although some studies have used *in vitro* stimulation assays and mice models to assess the impact of androgens. After treating T cells with DHT *in vitro*, an increased expression of *FOXP3* was reported. One study also found increased Treg frequencies in men and in eight-year-old boys[15,125,126]. Furthermore, in adult men, a negative correlation between testosterone serum levels and CD3+, CD4+ and CD8+ T cells was found[127]. A microarray analysis of stimulated cells showed a lower expression of proinflammatory genes such as G*NLY, GZMA, LTß, IL12Rß2* and *IFNγ* in male T cells compared to female T cells and a higher expression of *IL-17A*, *IL-5* and *IL-10*[128]. Furthermore, a study reported that male human-derived naïve CD4+ T cells produced higher levels of IL-17a and lower levels of IFNγ upon CD3/CD28 stimulation, and the authors suggested that PPARα and PPARγ functioned as the mechanistic link[129-131].

Further insights into the influence of androgens were reported through an analysis of men undergoing hormone replacement therapies. For example, a study found an increase in IL-10 and a decrease in IL1ß and TNF in the serum of hypogonadal men receiving testosterone replacement therapy. However, the study did not investigate the responsible cell population[132]. In a single case study of a hypogonadal man, researchers observed an increase of naïve CD4+CD45RA+ cells after treatment with androgen[133]. Additionally, using a 5a-reductase type II inhibitor with finasteride to treat the prostate tissue of benign prostatic hyperplasia patients, who exhibit reduced intraprostatic DHT levels, showed a

high infiltration of CD8+ T cells and CCL5 expression. *In vitro* studies have found that in a low androgen concentration, CD8+ T cells promoted prostate epithelial cell proliferation, presumably through the CCND1/JAK-STAT5/CCL5 pathway[134,135].

Moreover, the analysis of transgender individuals can give insight into the influence of androgens on XX women. Currently, only Giltay et al. have reported a change in immune parameters after hormone replacement therapy with testosterone. They found an increased IFNγ/IL-4 ratio and a higher TNF production of peripheral blood mononuclear cells (PBMCs) stimulated with phytohemagglutinin, which both indicate a possibly increased TH1 differentiation. However, this result should be further validated, and T cell populations should be investigated in more detail[136].

Studies on mice have revealed a similar picture as those on humans. For example, DHT-selected female T cell lines showed an increased IL-10 and a decreased IFNγ production[123]. Furthermore, *in vitro* treatment of peripheral female T cells with DHT showed an increase in IL-10 and a decrease in IL-12 cytokine production under aCD3 stimulation[122]. Another study performed a microarray analysis of splenic derived CD4+ T cells from castrated and control mice, revealing an upregulation of *Ifnγ*, *IL-12R*, *T-bet* and *Cxcr3*. This finding suggests that testosterone has an influence on TH1 differentiation as well as tissue homing[137]. Further treatment with synthetic testosterone *in vitro* led to a decrease of Tbet and IFNγ in splenic CD4+ T cells and a reduction of Stat4 phosphorylation with additional IL-12 stimulation[137].

As in human T cells, mice CD4+ T cells cultured in a testosterone-rich medium showed an increase in *Foxp3* expression as well as higher IL-10 production[121,123]. Similarly, male visceral adipose tissue had higher CD4+ Foxp3+ Treg frequencies compared to female tissue. These male Tregs also exhibit differences in their transcriptional landscapes, chromatin accessibility and phenotype; for example, in male visceral adipose tissue Tregs, *Ccr2* expression was increased compared to female Tregs. Female mice then treated with testosterone showed an increase in *Ccl2*, the ligand for CCR2, in the visceral adipose tissue[138].

While some researchers have posited that a shift towards TH2 leads to reduced TH1 cells, a previous report suggested enhanced autophagy in TH1 and TH17 T cells after *in vitro* androgen and aCD3 stimulation[139]. Furthermore, testosterone caused a direct reduction

of TH1 and TH17 differentiation in combination with aromatase inhibitors to prevent estrogen production[140].

Studies on autoimmunity have indicated the influence of androgens on the immune system and also possibly on T cells in autoimmune mice models. The K14-OVAp mouse model, a T cell-driven acute cholangitis model with similarities to human PBC, has a sex bias similar to that in human PBC patients. The authors showed that female mice treated with testosterone had decreased disease parameters compared to male mice. This finding occurred concurrently with reduced *Il-17a* expression and lower chemokine expression of *Cxcl-9* and *10*[141]. In experimental autoimmune encephalomyelitis (EAE) mice, a murine MS model, comparable effects have been observed upon testosterone treatment. Studies found enhanced IL-10 and suppressed IFNγ production by T cells and determined that testosterone had a protective effect on disease outcomes[123,142,143].

Taken together, these and other data regarding the influence of androgens on the immune system and especially on T cells (e.g. reviewed by Gubbels Bupp et al.[116] & Henze et al.[115]) clearly show that androgens directly and indirectly affect T cell differentiation and maturation as well as cytokine production and proliferation. However, the partly contradictory data also shows that much remains unknown and that androgen signaling in T cells is highly complex, dependent on both tissue type and inflammation levels. Overall, androgens seem to induce a more suppressive T cell phenotype and shift from TH1 to regulatory T cells, as summarized in Figure 4.

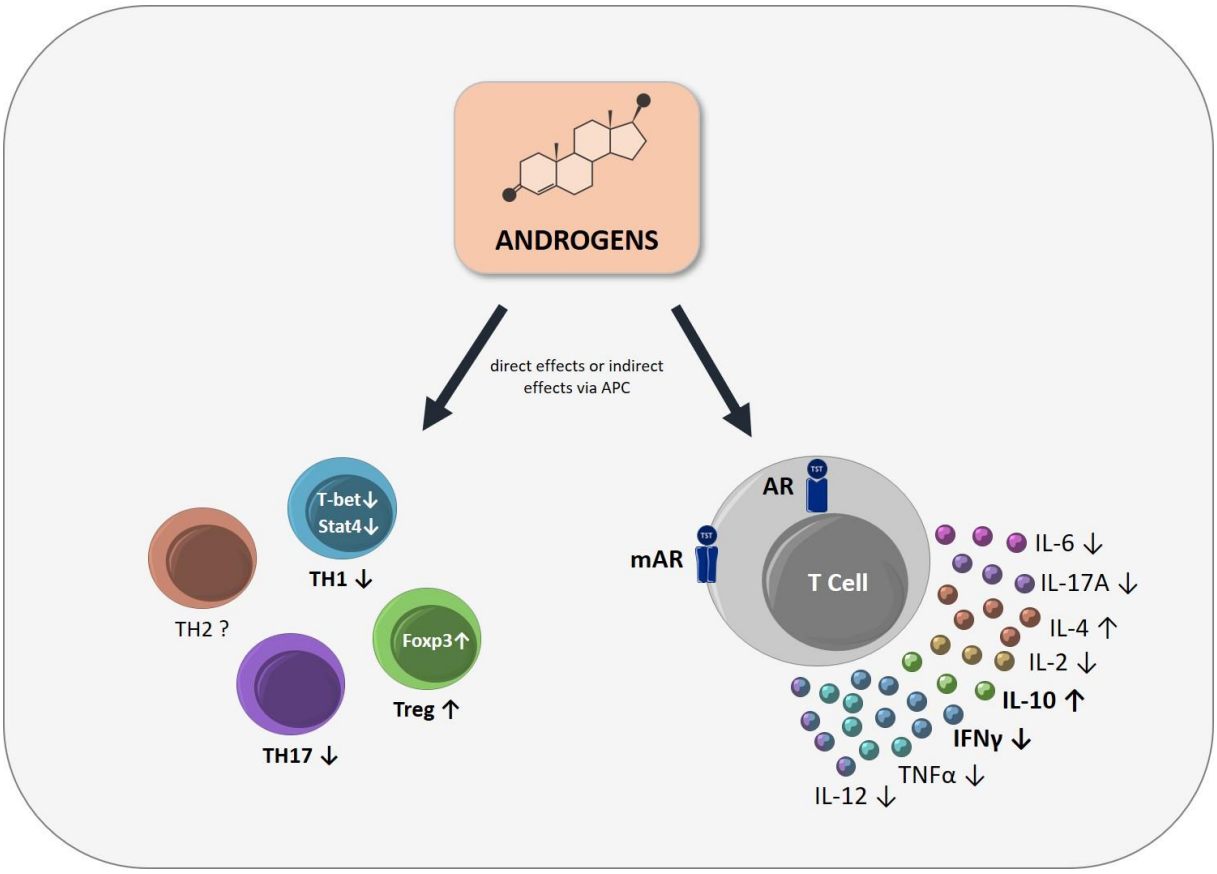

Figure 4. Schematic representation of direct and indirect effects of androgen on T cell differentiation, maturation and cytokine production. Androgens seem to directly or indirectly lead to higher numbers of Tregs and lower numbers of TH17 and TH1 T cells, although the effect on TH2 is less clear. Androgens also seem to enhance the production of IL-10 and IL-4, while lowering the release of IFNγ, TNFα, IL-12, IL-2, IL-6 and IL-17a[115].

2. AIM

There is compelling evidence that androgens influence the immune system. However, the mechanism and impact of androgens and especially of testosterone on immune cells and T cells in particular is insufficiently understood. Thus, further investigations in this field are needed. In this study, we therefore aim to investigate the influence of testosterone on the activation and differentiation of T cells regarding cytokine production and T cell subset formation. Understanding the impact of testosterone on immune cells might help decipher the impact of sex hormones on the pathogenesis and progression of autoimmune diseases. In addition, we aim to transfer that knowledge into the context of the autoimmune liver diseases PBC and AIH. This study will deepen our knowledge of T cells and might allow us to identify potential immunotherapeutic treatments.

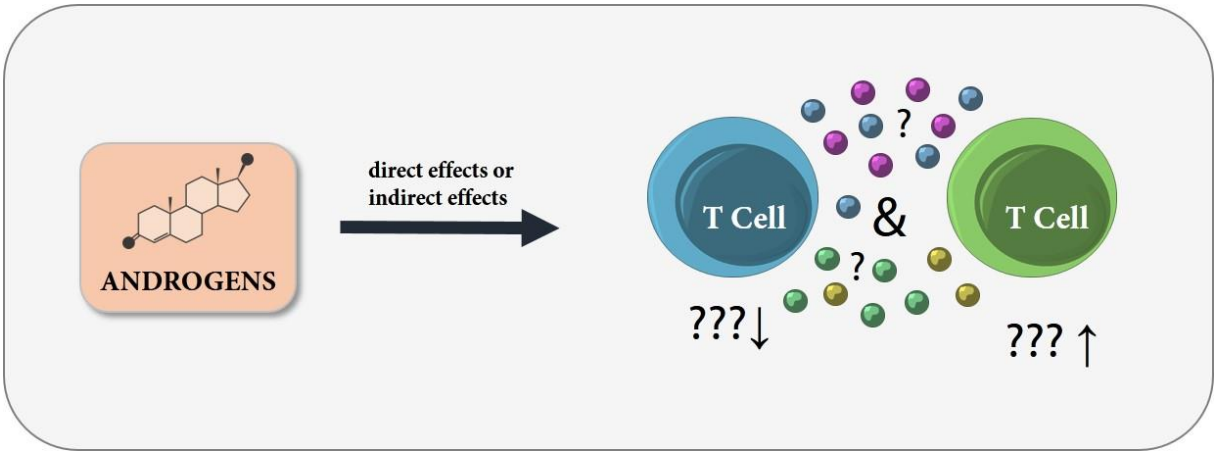

Figure 5. Schematic representation of the aim of this thesis. We aim to investigate the influence of testosterone on the activation and differentiation of T cells regarding cytokine production and T cell subset formation.

3. Results

Many autoimmune diseases, including autoimmune hepatitis and primary biliary cholangitis, have a female predominance. The mechanisms behind the observed gender differences are largely unknown, largely due to a lack of understanding of the pathogenesis of these diseases. One hallmark of autoimmune diseases is the disruption of immune balance, leading to an attack against self-cells. Here, a strong involvement of dysregulated T cell responses against organ resident cells (such as cholangiocytes) has been described (see the Introduction for more details). We aimed to investigate whether testosterone might directly alter immune cell function or impact the activation of target cells. To that end, we investigated the effect of testosterone on T cells *in vitro* and *in vivo*. Moreover, we translated our findings to patients with AILDs. Understanding these mechanisms will be fundamental for understanding disease pathogenesis and developing targeted treatment options.

3.1. Different immune cells express hormone receptors in humans

T cells orchestrate immune responses and play an important role in the pathogenesis of autoimmune diseases. Currently, knowledge of the direct effects of androgens on T cells is limited. The ability to respond to stimulation with sex hormones is dependent on the expression of specific hormone receptors. We therefore analyzed the expression of AR and ER receptors on immune cells and immune cell subpopulations associated with the development of autoimmune diseases. To that end, the expression of hormone receptors in human PBMCs (peripheral blood mononuclear cells) (n = 10), CD4 and CD8 T cells (n = 6–16), monocytes (n = 6) and DC enriched cells (n = 8) from healthy females and males was analyzed (Fig. 6). We detected the expression of AR, the expression of the mAR ZIP9, ER1 and ER2 in PBMCs, CD4 and CD8 T cells, monocytes and DCs. Importantly, receptor expression was independent of the sex of the donors, as no significant expression difference between males and females in this cohort was observed (Fig. 6A–E). Of note, the expression of GPRC6A, another proposed mAR, was not detected in any of those cells.

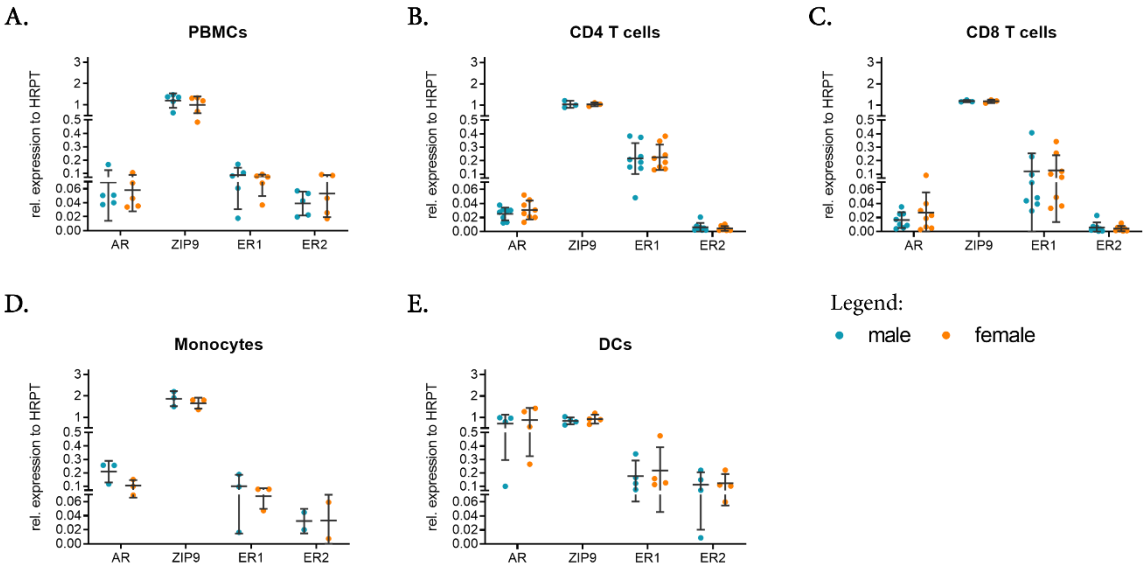

Figure 6. Human PBMCs, T cells, monocytes and dendritic cells express androgen and estrogen hormone receptors. Relative mRNA gene expression of the hormone receptors *AR*, *ZIP9*, *ER1* and *ER2* was analyzed in PBMCs, (**A**) CD4+ T cells, (**B**) CD8+ T cells, (**C**) monocytes, (**D**) and dendritic cells (**E**). Cells were isolated from male (blue) and female (orange) blood. Bars represent mean ± SD. Data were analyzed for statistical significance between males and females with the two-way ANOVA test.

3.2. Testosterone did not influence immune cell proliferation *in vitro*

To decipher the influence of testosterone on the activation of lymphocytes, we investigated the proliferation capacity of PBMCs, CD3 positive T cells and CD3 negative T cells *in vitro*. T cell receptor specific (aCD3/aCD28) stimulated PBMCs were cultured in the presence of different concentrations of testosterone, estradiol as another hormone control or ethanol (EC) as a dilution control. On day 4 after stimulation, PrestoBlue™ (PB) absorption was measured to determine cell numbers. No significant difference in the cell numbers and therefore in their proliferation of male and female PBMCs upon testosterone and estradiol treatment was observed in the PB assay (Fig. 7A). Furthermore, hormone treatment (0.5–500 ng/ml) of female PBMCs altered neither the percentage of proliferated living cells nor the percentage of proliferated T cells (CD3+) based on flow cytometry dilution using CellTrace™ (CT) staining added on day 0 (Fig. 7B and C), regardless of whether cells were treated once or four times (not shown here).

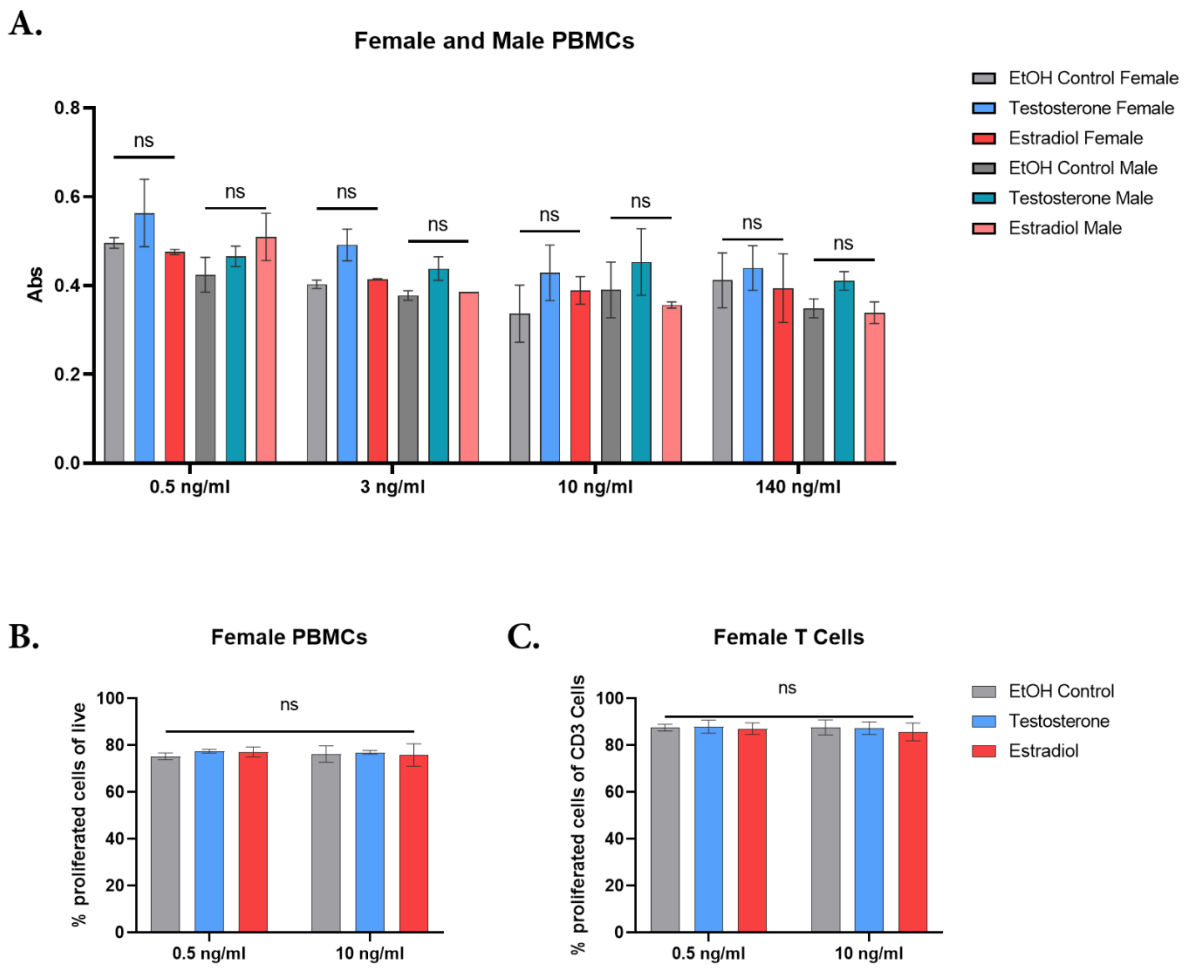

Figure 7. Proliferation of human lymphocytes is not altered by hormone treatment. A. Female and male PBMCs were treated with testosterone (blue) or estradiol (red) (0.5–140ng/ml) or corresponding dilution controls (grey). Absorption in supernatant was monitored after PrestoBlue™ incubation to determine the proliferation of living cells. **B and C** Female PBMCs were treated with testosterone (blue) or estradiol (red) (0.5 and 10 ng/ml) or corresponding dilution controls (grey). The percentage of proliferated cells from living cells was determined by flow cytometry analysis of intracellular CellTrace™ stained PBMCs (**B**) and additional CD3+ stained immune cells (**C**).

3.3. Testosterone treatment leads to a decreased proinflammatory immune cell response *in vitro*

In addition to contributing to the proliferation of immune cells, cell function and interaction with other cells are important for immune cell balance. These mechanisms can be investigated via the determination of lymphocyte cytokine production upon stimulation. We thus aimed to examine the influence of androgens on PBMC cytokine production and then observed T cell cytokine production *in vitro*.

PBMCs were incubated for 24 hours in the presence of testosterone, dihydrotestosterone (DHT) or dilution controls (ethanol [EC] and methanol [MC]) and then activated by unspecific stimulation with PMA/ionomycin for 4 hours. The release of TNFα and IFNγ release from PBMCs were analyzed in supernatants using ELISA. PBMCs isolated from female donors showed a slightly increased production of TNFα upon stimulation with PMA/Ionomycin compared to male-derived PBMCs (Fig. 8A; n = 32 from 6 different males and 9 different females). Pretreatment with testosterone (150 ng/ml) significantly reduced the secretion of TNFα compared to the dilution control (EC) independent of the donors' sex (Fig. 8B). For IFNγ, we detected a tendency for increased secretion upon stimulation with PMA/ionomycin compared to male-derived PBMCs. However, pretreatment with testosterone did not alter IFNγ expression (data not shown). In addition, treating PBMCs with DHT did not alter the secretion of TNFα and IFNγ compared to the dilution control (Fig. 8C; IFNγ not shown).

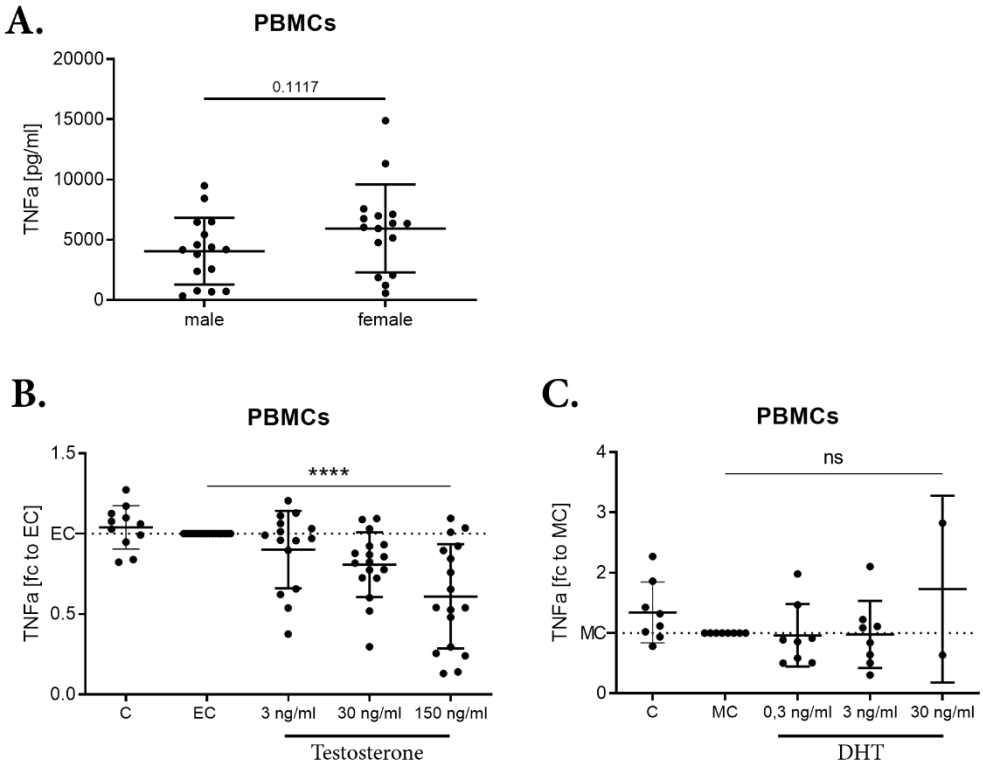

Figure 8. PBMC treated with androgens and stimulated with PMA/ionomycin show reduced levels of TNFα. Female and male PBMCs were treated with testosterone or dihydrotestosterone with the indicated concentrations or dilution control and stimulated with PMA and ionomycin (P/I). TNFα and IFNγ in the supernatant were measured. The fold change (fc) to the dilution control for each individual was calculated (EC = 1) and the significance was tested with an ordinary one-way ANOVA (**B and C**).

Since IFNγ and TNFα can be produced by T cells and have a known involvement in autoimmune diseases (see Introduction), we aimed to analyze the consequences of testosterone treatment on T cells alone. Therefore, we investigated the influence of testosterone treatment on female- and male-derived T cells upon TCR specific stimulation.

T cells derived from female donors showed significantly reduced levels of TNFα compared to EC controls in all tested testosterone concentrations. IFNγ expression was significantly reduced upon stimulation with high dose treatments of 30 and 150 ng/ml of testosterone (Fig. 9A and B). Importantly, we could not observe any effect on cytokine expression in T cells derived from male donors upon TCR specific stimulation in the presence of testosterone (Fig. 9C and D). In addition, treating female and male T cells with DHT did not alter the secretion of TNFα and IFNγ compared to the dilution control (not shown).

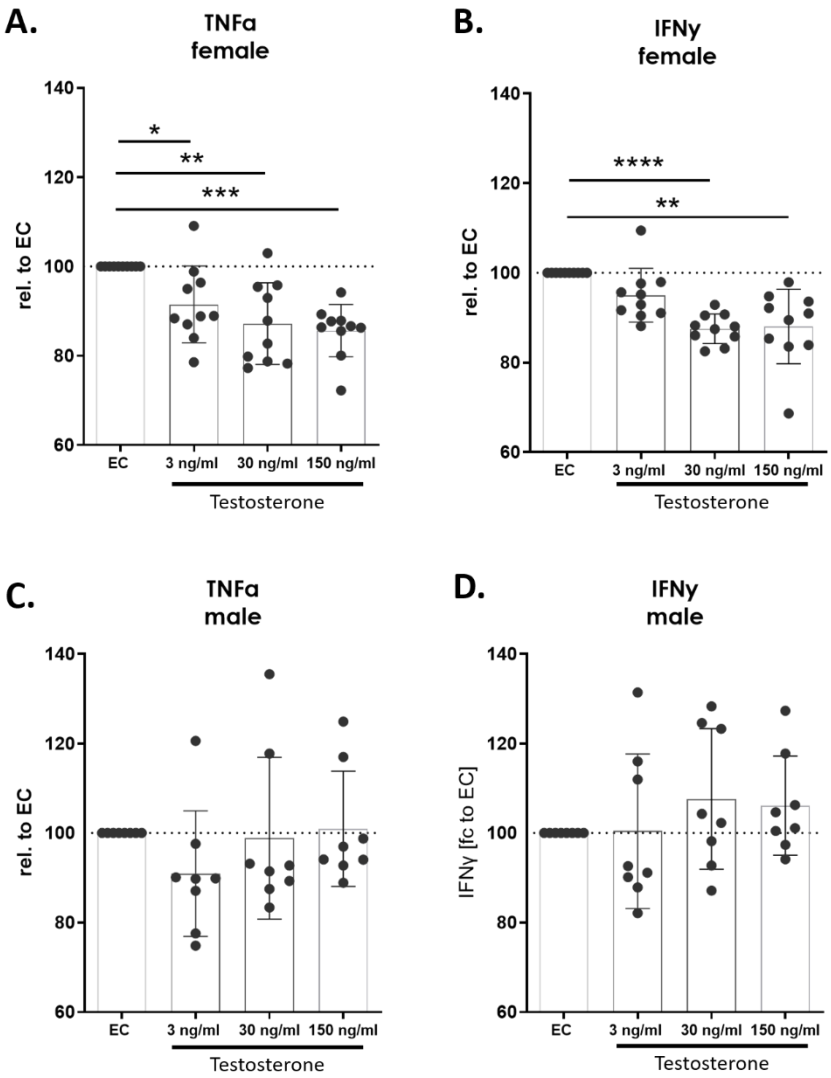

Figure 9. Testosterone treatment and TCR stimulation result in a lower release of TNFα and IFNγ from female T cells. Female (**A–B**) and male (**C–D**) T cells were treated with aCD3/aCD28 and either testosterone or their corresponding dilution control. The amount of TNFα (**A, C**) and IFNγ (**B, D**) was analyzed and the fold change to dilution control was calculated (EC = 100). Significant changes between the dilution control and testosterone-treated cells were tested with an ordinary one-way ANOVA.

To further analyze the impact of testosterone treatment on T cell activation, we analyzed the gene expression of testosterone-treated T cells. The expression of the androgen hormone receptors did not change upon testosterone treatment (Fig. 10A). Furthermore, the amount of expressed 5a-reductase, which was already low in the untreated samples (not shown), did not significantly change upon treatment with testosterone. This reductase is able to convert testosterone into dihydrotestosterone (see Introduction). Most importantly, aromatase (CYP19A1), which can convert testosterone to ß-estradiol, did not show a tendency towards increased gene expression upon stimulation with testosterone (Fig. 10A). From this result, the indirect influence of estradiol on these cells

can be excluded. In addition, we analyzed the gene expression of different cytokines but did not detect any significant changes upon testosterone stimulation (Fig. 10B). Compared to the dilution control (EC), the expression of TNFα was lower under testosterone (150 ng/ml) but only significantly reduced in female T cells (Fig. 10C). Finally, no change upon testosterone treatment on the expression of IFNγ was observed (Fig. 10D).

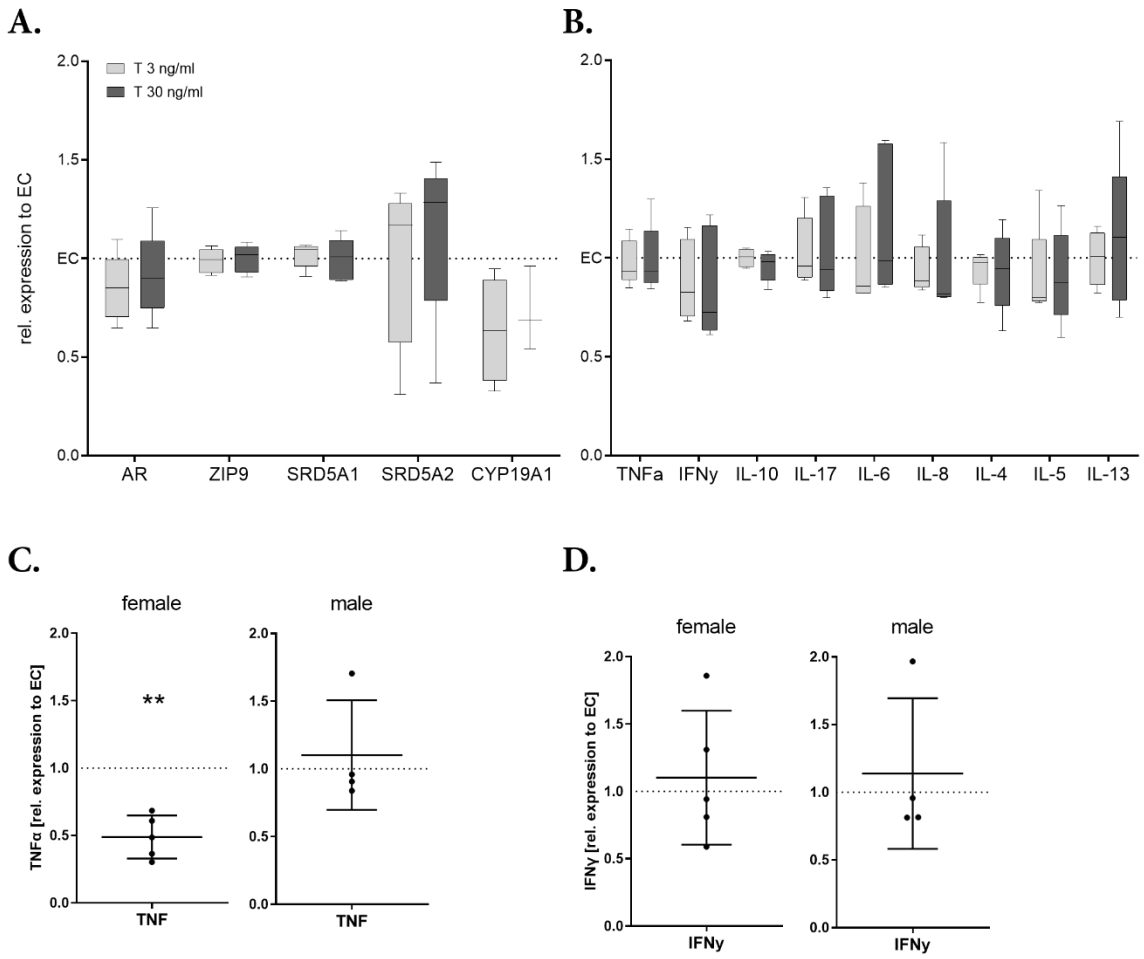

Figure 10. Testosterone-treated and TCR-stimulated female T cells show unchanged hormone receptor expression but decreased expression of TNFα. Female T cells were treated with testosterone and dilution control. The relative expression of androgen receptors and enzymes *AR*, *ZIP9*, *SRD5A1*, *SRD5A2* and *CYP19A1* upon testosterone treatment for 24 hours was analyzed. Fold change to dilution control is shown (EC= 1) (**A**). Relative expression of cytokines *TNFA*, *IFNG*, *IL-10*, *IL-17*, *IL-6*, *IL-8*, *IL-4*, *IL-5* and *IL-13* in T cells upon testosterone treatment for 24 hours was analyzed and fold change to dilution control was calculated (**B**). The relative expression upon testosterone treatment compared to the dilution controls of *TNFA* (**C**) and *IFNγ* (**D**). Significant changes between the dilution control and testosterone-treated cells were analyzed with an ordinary one-way ANOVA (**A, B**) or a t-test (**C, D**).

3.4. Blood parameter differences between healthy males and females

Next, we aimed to investigate the effect of sex hormones *in vivo.* First, we analyzed the differential blood count of healthy individuals *ex vivo* in order to obtain an idea of the overall influence of testosterone on the immune system *in vivo*. We did not detect any significant differences between males and females in the percentages of EVB, neutrophils, lymphocytes, monocytes or eosinophils in our cohort (see 5.2). However, a higher percentage of hematocrit and basophils in healthy males compared to females was observed (Fig. 11A). Furthermore, the absolute numbers of leucocytes, thrombocytes, neutrophils, lymphocytes, monocytes and eosinophils did not differ between the sexes, but the absolute number of erythrocytes was higher in male peripheral blood (Fig. 11B). What is more, the amount of MCV, MCH and MCHC did not differ between females and males, but the amount of hemoglobin was significantly higher in males (Fig. 11C). As expected, testosterone levels, including free and bioavailable testosterone levels, were significantly higher in healthy males than in females (Fig. 11D). Interestingly, the amount of ß-estradiol was only slightly higher but not significantly different in healthy middle-aged women compared to healthy middle-aged males (Fig. 11D).

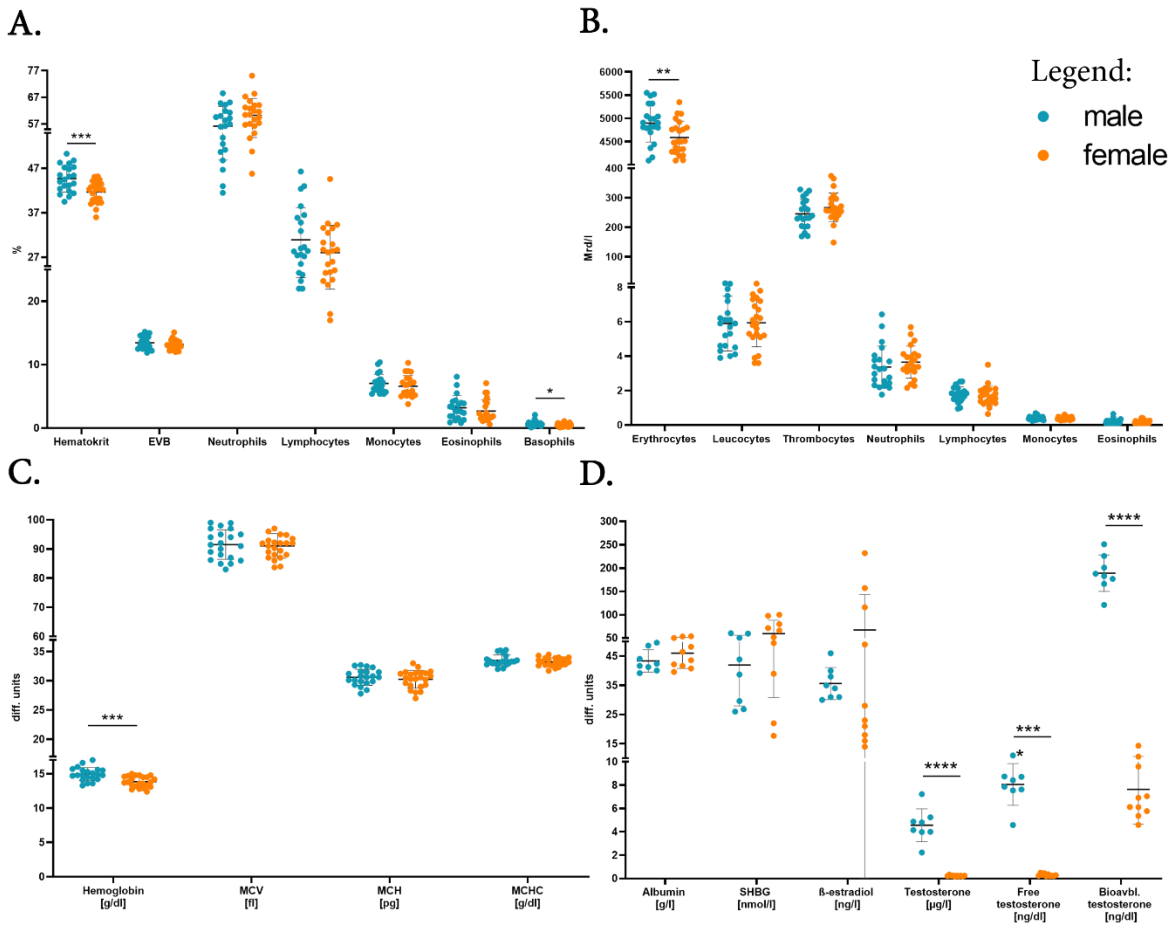

Figure 11. Blood parameter differences between healthy females and males. A. The percentage of hematocrit, EVB, neutrophils, lymphocytes, monocytes, eosinophils and basophils in peripheral blood. **B.** The absolute amount in Mrd/l of erythrocytes, leucocytes, thrombocytes, neutrophils, lymphocytes, monocytes and eosinophils. **C.** The levels of hemoglobin, MCV, MCH and MCHC in peripheral blood. **D.** Albumin, SHGB, ß-estradiol, testosterone, free testosterone and bioavailable testosterone levels in serum. An unpaired t-test between males (blue) and females (orange) was performed for each parameter individually (A–C: $n^{male} = 21$ $n^{female} = 23$; D: $n^{male} = 8$ $n^{female} = 10$).

3.5. Changes in blood parameters of women undergoing high dose testosterone treatment

In order to deepen our understanding of the effects of testosterone on T cells *in vivo*, we were fortunate to have a special patient cohort. Biosamples from birth sex females undergoing sex changes (trans men) were collected, and immune cells were analyzed *ex vivo*. The female-to-male (FTM) cohort data and collection time points are summarized in Table 3.

The differential blood count was investigated before patients started (baseline [BL]) hormone therapy (HRT) and 3 (3M) and 6 months (6M) after HRT. The hemoglobin,

hematocrit and erythrocyte parameters were significantly increased 3 and 6 months after testosterone treatment. The absolute number of lymphocytes was slightly significantly increased after 6 months, and the absolute numbers of monocytes were slightly increased after 3 months of testosterone treatment. All other parameters showed no significant changes compared to BL (Fig. 12).

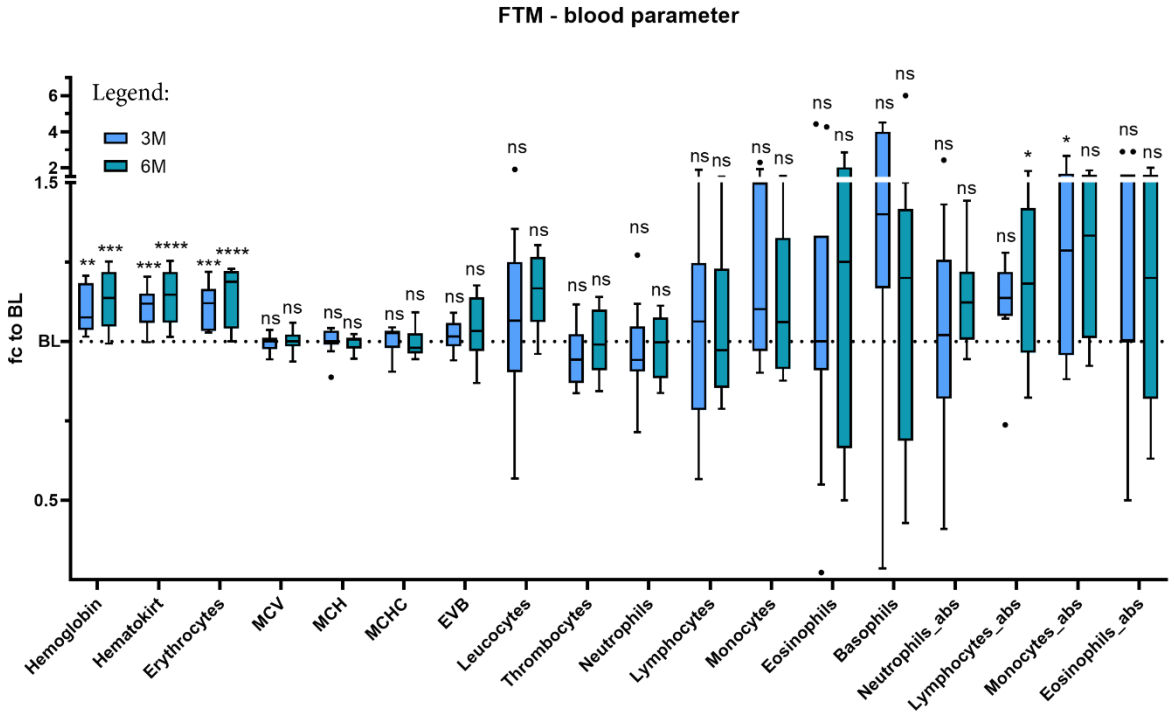

Figure 12. Blood parameters of female-to-male (FTM) subjects differ between baseline, 3 and 6 months of testosterone treatment. A differential blood count analysis of hemoglobin, hematocrit, erythrocytes, MCV, MCH, MCHC and EVB; the percentage of leukocytes, thrombocytes, neutrophils, lymphocytes, monocytes, eosinophils and basophils; and the absolute numbers of neutrophils, lymphocytes, monocytes and eosinophils (from left to right). The fold change at three (3M, blue) and six months (6M, green) after testosterone treatment compared to the baseline value (BL= 1) was calculated, and an ordinary one-way ANOVA was performed between BL, 3M and 6M for each parameter individually ($n^{3M} = 11$, $n^{6M} = 9$).

To validate the increase of testosterone at the time points 3M and 6M, we performed an ELISA to measure testosterone in the patients' serum. As shown in Fig. 13, the amount of testosterone significantly increased at least 2.5 fold in every trans man tested after 3 and 6 months of testosterone treatment.

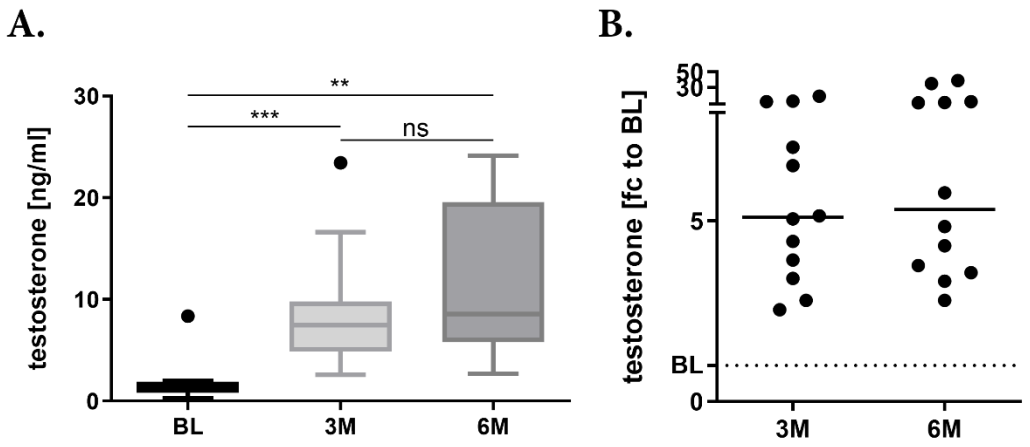

Figure 13. Testosterone levels of trans men increased after 3 and 6 months of testosterone treatment. A. Testosterone levels in ng/ml at BL, 3M and 6M and **B**. the individual change of testosterone levels at 3M and 6M compared to BL. The one-way ANOVA was performed to determine statistical differences between testosterone levels of BL, 3M and 6M.

3.6. Testosterone treatment induced anti-inflammatory phenotype of T cells in FTM individuals on a single cell protein level

To further analyze the effect of testosterone on specific cell populations in peripheral blood, we performed a multi-color flow cytometry-based analysis. Using markers for the detection of innate and adaptive cells, we performed deep immunophenotyping of these samples. The gating strategy and the antibodies used are described in sections 5.1.6. and 5.1.16.

In order to identify significant and relevant changes in the immune system, we separately investigated each cell population upon testosterone treatment. To that end, we examined the changes in frequency and absolute numbers between BL and approximately 6M after testosterone therapy began.

To detect the major effects of testosterone on non-T cell populations, which also interact with T cells (see Introduction), we examined peripheral immune cells belonging to the innate immune system and B cells. First, the percentage of CD45+ living cell populations was analyzed. There were no significant changes in the frequency of monocytes, B cells, dendritic cells (DCs) and NK cells (not shown). We did not detect significant changes in the absolute numbers of monocytes or monocyte subtypes, such as CD14hi, CD16hi and CD16intCD14hi (Fig. 14D, F–H), or B cells, such as B1-like B cells, naïve B cells, plasma cells, switched memory B cells and transitional B cell populations (Fig. 14E, L, N–Q).

Moreover, the absolute numbers of B cells expressing BAFF-R were not significantly changed upon testosterone treatment (Fig. 14M), while the percentage of BAFF-R expressing cells from B cells were significantly decreased (not shown). The absolute numbers of dendritic cells, including pDCs, cDC2s and mDCs, were not altered in peripheral blood after 6 months of testosterone treatment (Fig. 14I–K). Interestingly, the absolute numbers of NK cells and CD56dim NK cells, not CD56bright NK cells, were increased after 6 months of testosterone treatment (Fig. 14A–C).

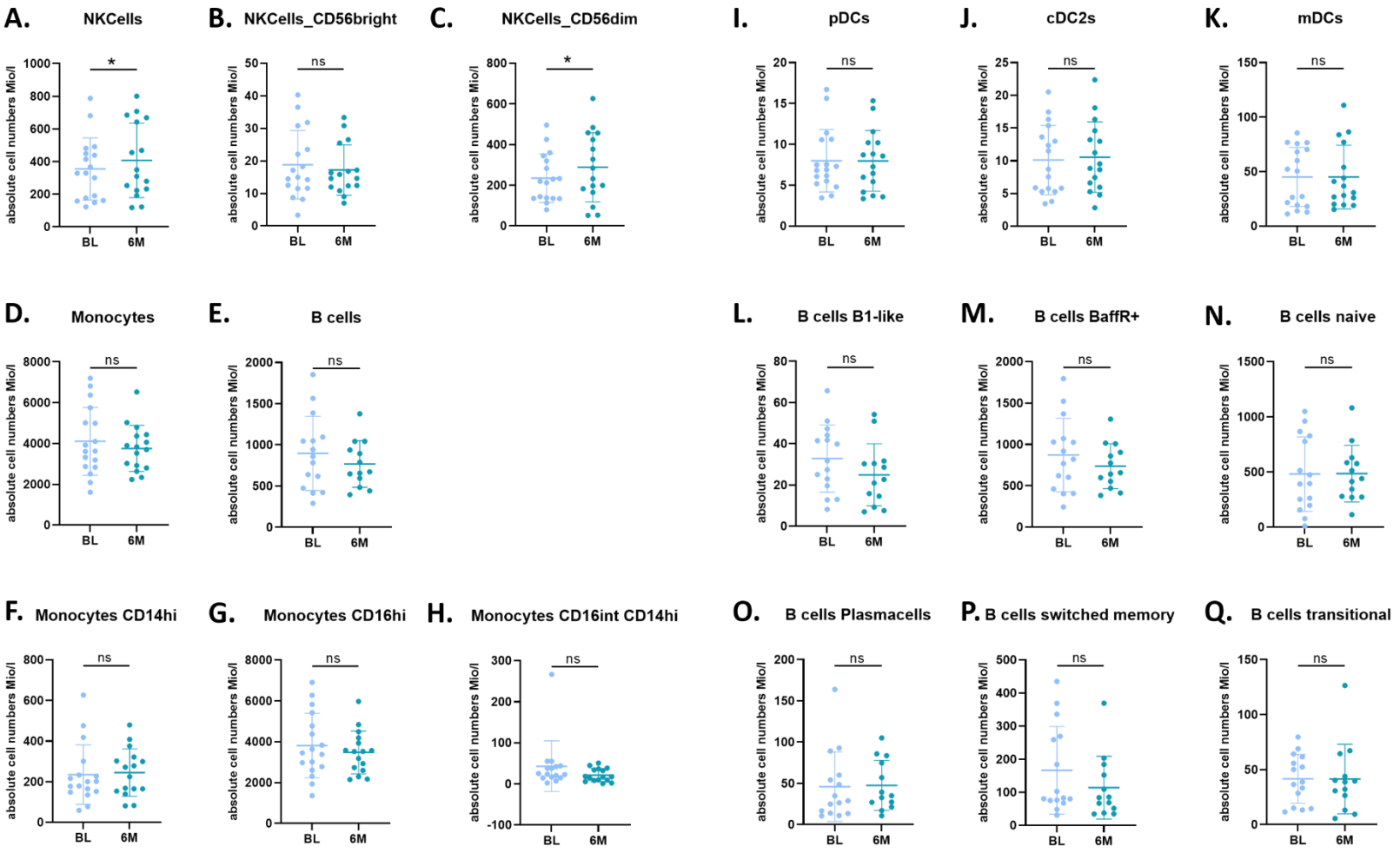

Figure 14. Absolute numbers of innate immune cells and B cells before and after 6 months of testosterone treatment. NK cells and their subtypes CD56bright and CD56dim were investigated. Monocytes and their subtypes CD14hi, CD16hi and CD16intCD14hi were examined. Changes in dendritic cells, reflected by numbers of pDCs, cDC2s and mDCs, were investigated. B cells and B cell subtypes, such as B1-like, BaffR+, naïve, plasma cells, switched memory and transitional B cells, were examined before and after 6 months of testosterone treatment. A subject paired t-test was performed for each population between BL and 6M samples.

Aside from the increase in NK cells, there were no striking differences in the innate immune system or in B cells in our trans men samples under testosterone.

To elucidate the indirect and direct consequences testosterone has on T cells, we next investigated different T cell populations in deep immunophenotyping flow cytometry panels. We analyzed the overall frequencies and absolute numbers of T cells and T cell subpopulations. We did not detect any significant differences in the frequencies or absolute numbers of CD3+, CD4+ or CD8+ single positive, double positive (DP) and double negative (DN) cell populations upon testosterone treatment for 6 months (Fig. 15; frequencies not shown).

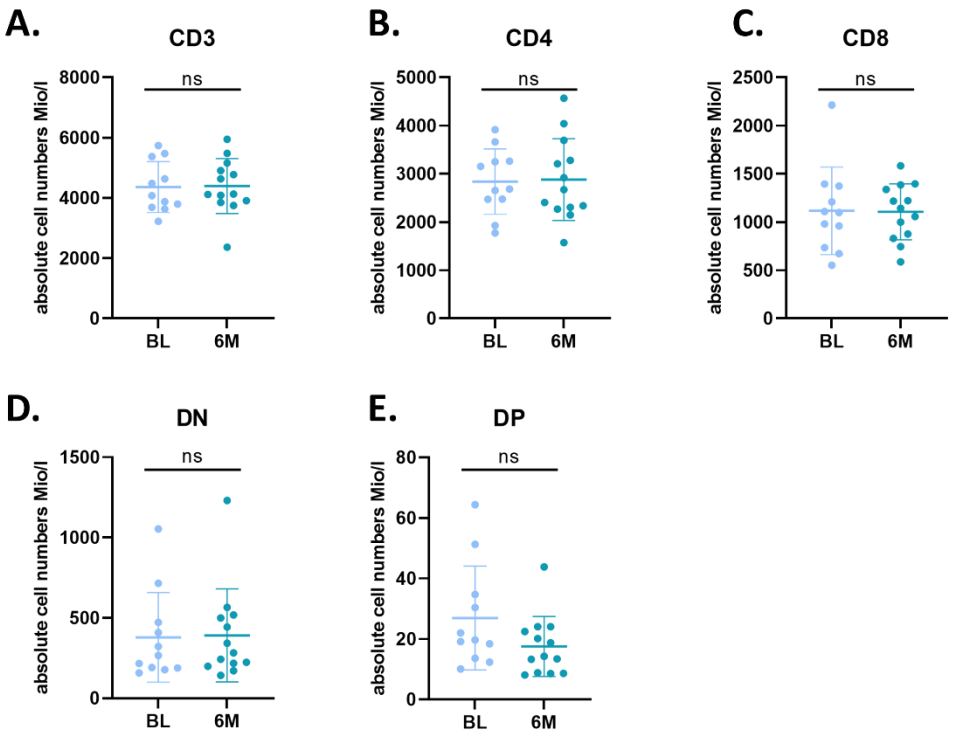

Figure 15. The absolute numbers of total T cells do not change after testosterone therapy. The absolute numbers before and 6 months after testosterone therapy of CD3 cells (A), CD4+ T cells (B), CD8+ T cells (C), CD4 and CD8 double negative (DN) T cells (D) and double positive (DP) T cells (E). A subject paired t-test was performed for each population between BL and 6M samples.

In order to obtain a deeper analysis of changes testosterone causes in T cells, we analyzed the protein expression of exhaustion, activation, inhibition and tissue homing markers. The percentage of each marker of CD4+, CD8+, DP and DN cells were gated. Then, fold changes after 6 months were calculated based on the cell frequencies of CD45 living cells and compared to BL (Fig. 16). Fold changes in the frequencies of CD8+ T cells expressing

CD69 and CD45Ra as well as TEMRA CD8+ T cells were significantly increased after 6 months of testosterone treatment (Fig. 16A, B). In contrast, fold changes in the frequencies of CD8+ T cells expressing CD28, CD57, CD160, CD161, CD272, CD279, CD25, CD44 CD49a, CD49b, CD62L and CD103 were not significantly altered (Fig. 16A, B). Unlike in the CD8+ T cells, the frequencies of CD161 expressing CD4+ T cells and TEMRA CD4+ T cells were significantly changed after 6 months of testosterone treatment (Fig. 16C, D). Fold changes in the frequencies of expression of CD28, CD57, CD160, CD272, CD279, CD25, CD44 CD49a, CD49b, CD62L, CD103, CD45Ra and CD69 on CD4+ T cells were not altered (Fig. 16C, D).

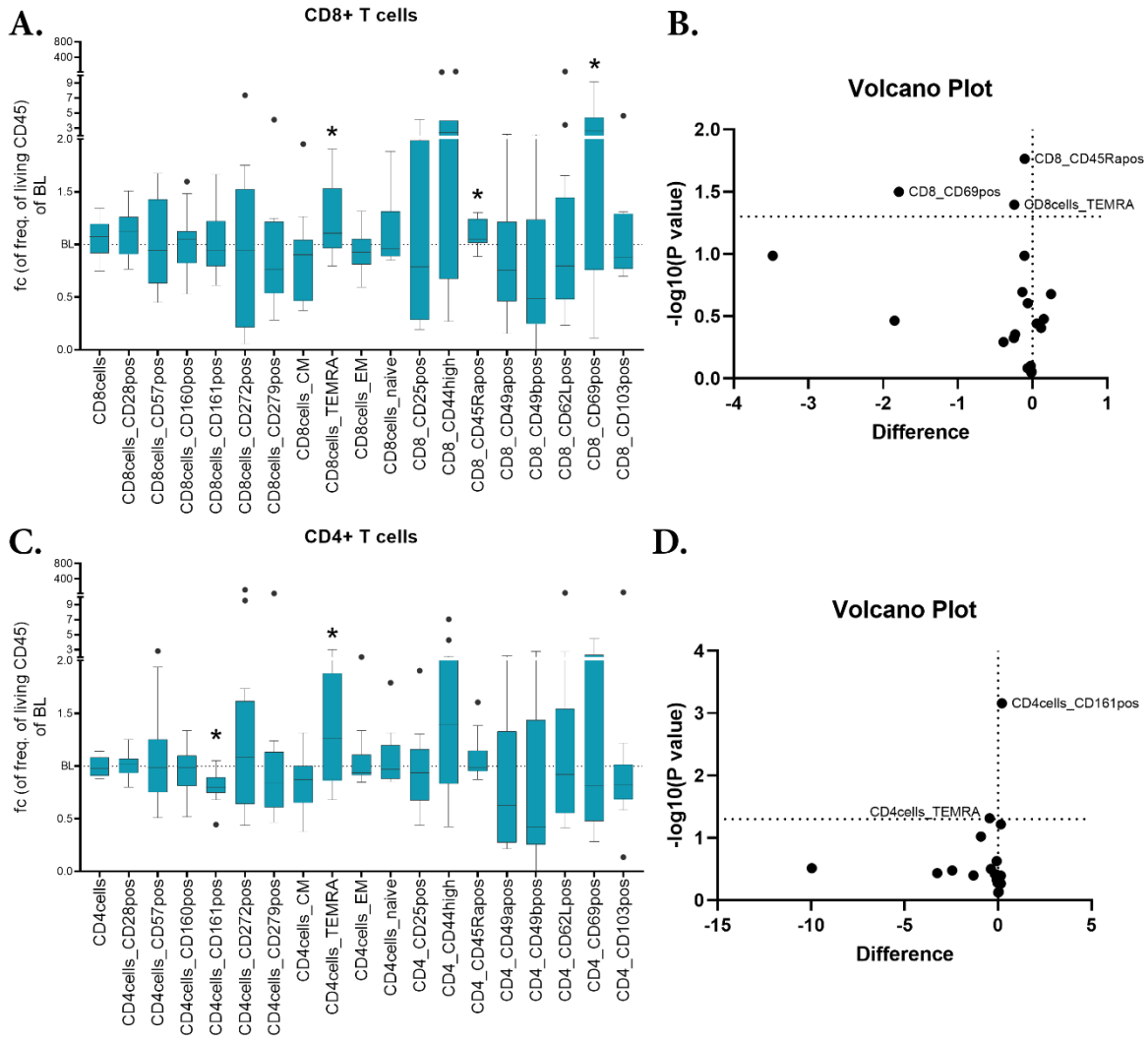

Figure 16. Frequencies of CD8+ and CD4+ T cell markers are altered upon testosterone treatment. A. Fold changes of CD28, CD57, CD160, CD161, CD272, CD279, CD25, CD44 CD49a, CD49b, CD62L, CD103, CD45Ra, CD69 on CD8+ T cells as well as TEMRA, EM, CM and naïve CD8+ T cells. Fold change is calculated between the baseline (BL) and 6 months (6M) values based on the frequencies of CD45 living cells. **C.** Same as in A but for CD4+ T cells. **B, D.** Volcano plot of paired t-tests between BL and 6M for each population graphed in A and C. The names of significant populations are shown; n=12–13.

To examine whether these changes were similar in absolute numbers, we next calculated the fold changes after 6M compared to BL based on absolute cell numbers (Fig. 17). Overall, the changes in absolute cell numbers at 6M of testosterone treatment compared to BL were similar to the changes observed in the frequencies. However, the increased expression of CD44hi CD8+ T cells was significant when measured in absolute numbers (Fig. 17B), while the expression of CD161 on CD4+ T cells in absolute cell numbers was no longer significant (Fig. 17D). The fold changes in absolute cell numbers of all other markers showed the same tendencies and significances as the frequencies (Fig. 17).

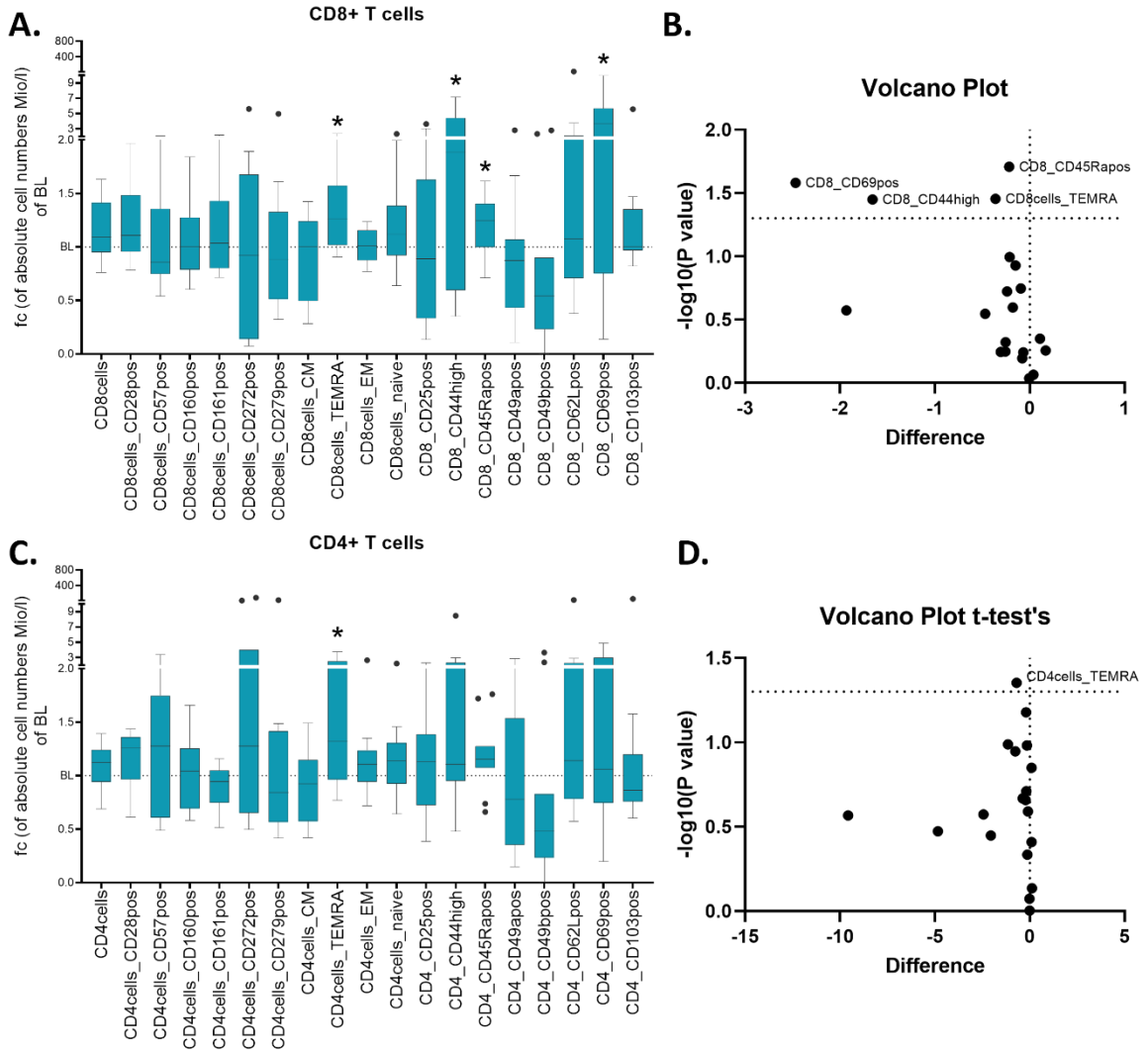

Figure 17. Absolute cell numbers of CD8+ and CD4+ T cell markers are altered upon testosterone treatment. A. Fold changes of CD28, CD57, CD160, CD161, CD272, CD279, CD25, CD44 CD49a, CD49b, CD62L, CD103, CD45Ra, CD69 on CD8+ T cells as well as of effector, EM, CM and naïve CD8+ T cells. Fold change was calculated between the baseline (BL) and 6 months (6M) values based on absolute cell numbers. **C.** Same as in A but for CD4+ T cells. **B, D.** Volcano plot of paired t-test between BL and 6M HRT for each population graphed in A and C. The names of significant populations are shown; n=10–11.

As Figures 17 and 18 indicate, a fold change in the effector and memory phenotype of CD8 and CD4+ T cells seems to occur during long-term treatment with testosterone. Therefore, the values of percentages of CD4+ and CD8+ as well as the absolute numbers of naïve, TEMRA, central memory and effector memory T cells before and after testosterone appliance were examined.

Percentages of EM, CM and naïve CD4+ T cells were not significantly changed, while TEMRA CD4+ cells were significantly increased upon testosterone treatment (Fig. 18A–D). The same trends, including a significant increase in the TEMRA population, was observed in absolute CD4 cell numbers (Fig. 18E, F).

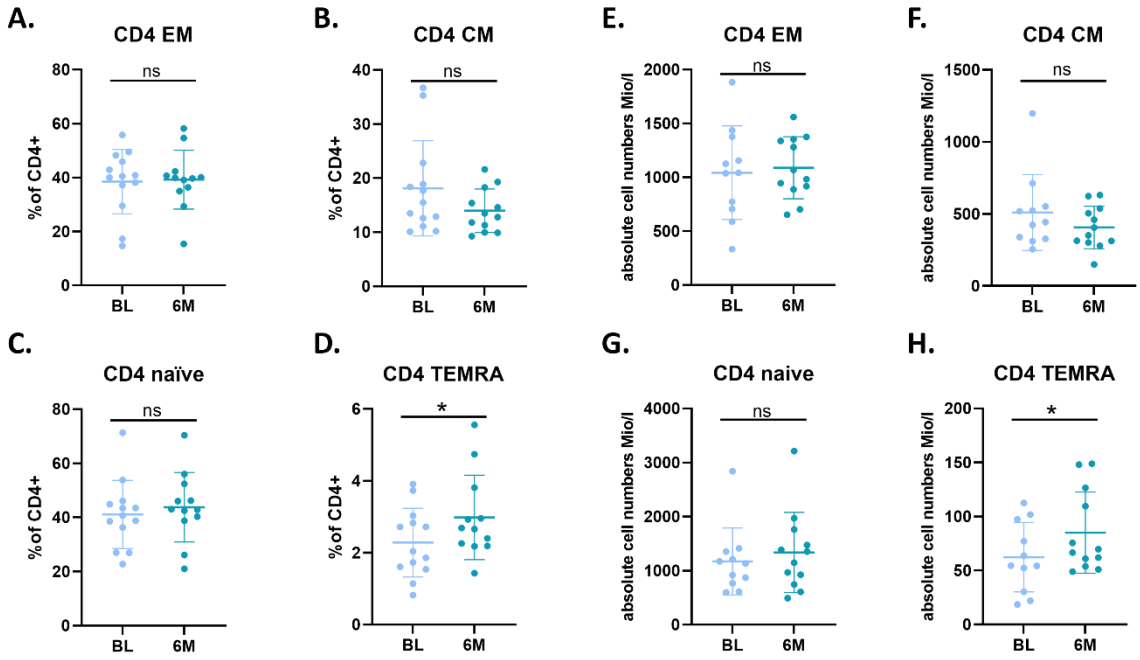

Figure 18. Effector and memory state of CD4+ T cells changes under testosterone therapy. The percentages of effector memory (**A**), central memory (**B**), naïve (**C**) and TEMRA (**D**) cells of CD4+ T cells. The absolute cell numbers of effector memory (**E**), central memory (**F**), naïve (**G**) and CD4+ TEMRA (**H**) T cells. A subject paired t-test was performed for each population between BL and 6M HRT samples.

Similar trends were observed in the CD8+ T cell population. Thus, percentages of central memory and naïve CD8+ cells were not significantly changed after 6 months of HRT (Fig. 19B, C, F, G) and the percentages, though not the absolute numbers, of effector memory CD8+ T cells were decreased (Fig. 19A, E). Just as in CD4+ T cells, the percentages and absolute numbers of TEMRA CD8+ T cells were significantly increased (Fig. 19D, H).

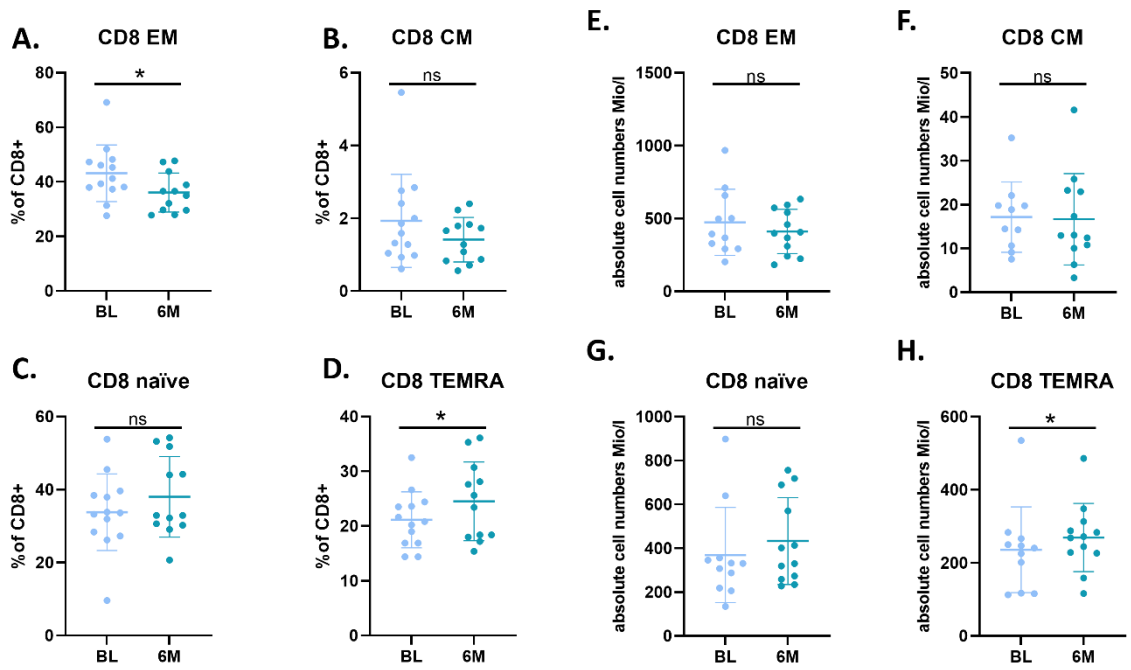

Figure 19. Effector and memory state of CD8+ T cells changes upon testosterone treatment. The percentage of effector memory (**A**), central memory (**B**), naïve (**C**) and TEMRA CD8+ (**D**) T cells. The absolute cell numbers of effector memory (**E**), central memory (**F**), naïve (**G**) and TEMRA (**H**) cells of CD8+ T cells. A subject paired t-test was performed for each population between BL and 6M HRT samples.

To shed additional light on the influence of testosterone on T cells, we not only examined the effector and memory state of the FTM samples (Fig. 18 and 19) but also the frequencies of specific T cell subpopulations. Regulatory T cells are one of the important T cell populations presumably involved in autoimmune diseases (see Introduction). In FTM samples, an increase in the frequencies and absolute number of Tregs 6M after testosterone treatment compared to BL was observed (Fig. 20A, B). Furthermore, we found that Tregs expressing CD73 increased in frequency and absolute numbers in the 6M samples (Fig. 20C, D). CD73 and CD39 are thought to play a role in the immune suppressive function of Tregs due to their ability to degrade proinflammatory ATP. Interestingly, CD73- CD39- Tregs also increased in frequency and absolute numbers in the 6M samples (Fig. 20E, F). CD39 positive and CD39+ CD73+ double positive Tregs were not significantly altered (not shown). Regarding the effector and memory state of the Tregs, we identified that there was a significant increase in both naïve-like (defined as CD45Ra+) and effector-like (defined as HLA-DR+) Tregs in frequency and absolute numbers (Fig. 20G–J).

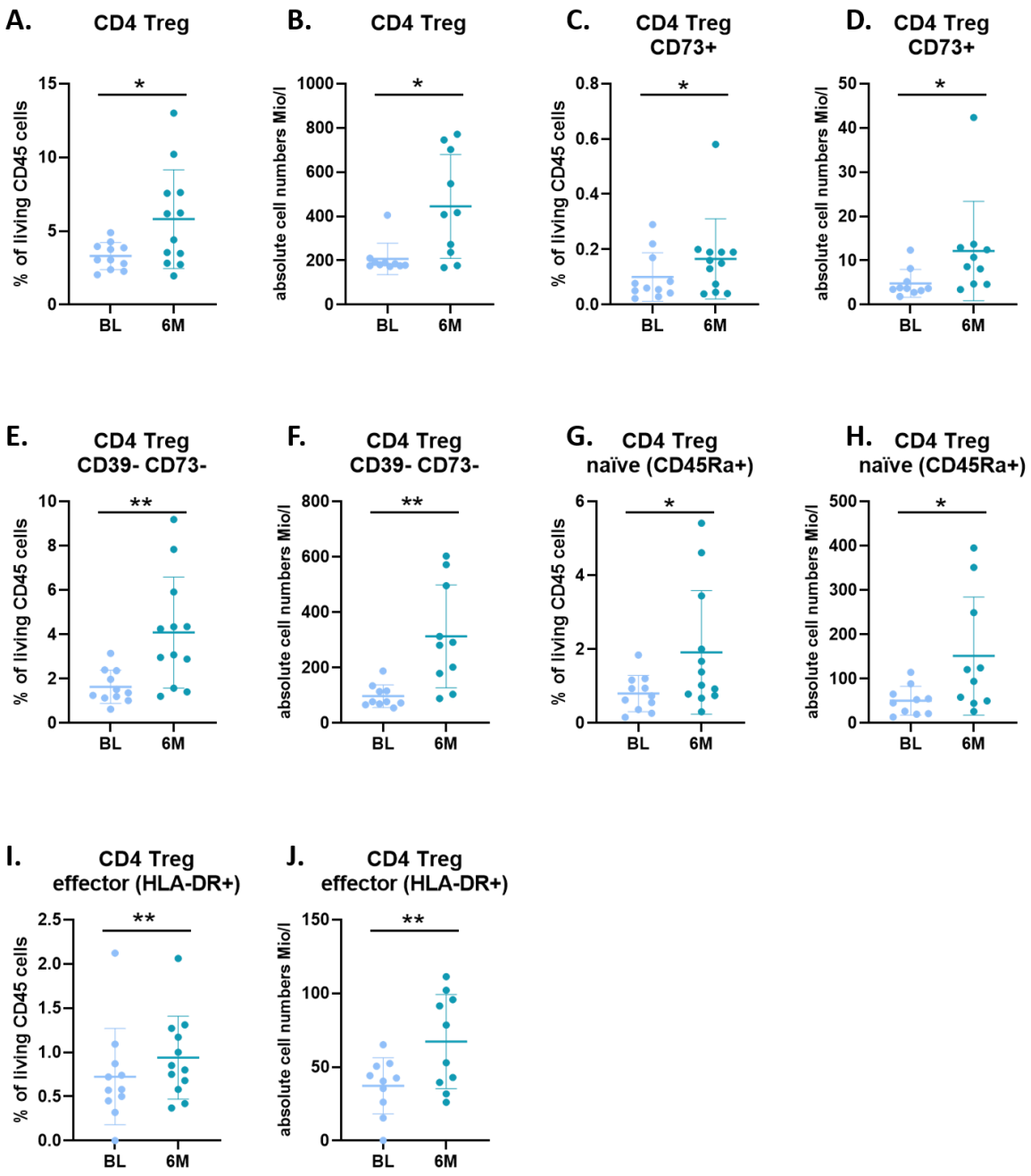

Figure 20. Frequencies and absolute numbers of Tregs and Treg subtypes are altered upon testosterone treatment. Frequencies (**A**) and absolute cell numbers (**B**) of Tregs in FTM samples at BL and 6M timepoints. Frequencies (**C**) and absolute cell numbers (**D**) of CD73+ Tregs. Frequencies (**E**) and absolute cell numbers (**F**) of CD739 and CD73 double negative Tregs. Frequencies (**G**) and absolute cell numbers (**H**) of naïve-like (CD45Ra+) Tregs. Frequencies (**I**) and absolute cell numbers (**J**) of effector-like (HLA-DR+) Tregs. A subject paired t-test was performed for each population between BL and 6M HRT samples.

In contrast to the findings on Tregs, the expression of CD39- CD73- and CD73+ was not significantly altered across the total CD4+ T cells and even a slight decrease in the frequencies of CD39+ single positive and CD39+ CD73+ double positive CD4 +T cells was observed, which was not significant in a subject paired analysis (not shown, p = 0.0594, p = 0.0691). Similarly, in CD8+ T cells, CD73+, CD39- CD73- and CD39+ CD73+ cells were not significantly altered in frequency or absolute numbers (not shown). However, the frequencies of CD39+ expression on CD8+ T cells was significantly decreased after 6M of testosterone therapy (Fig. 21A–D).

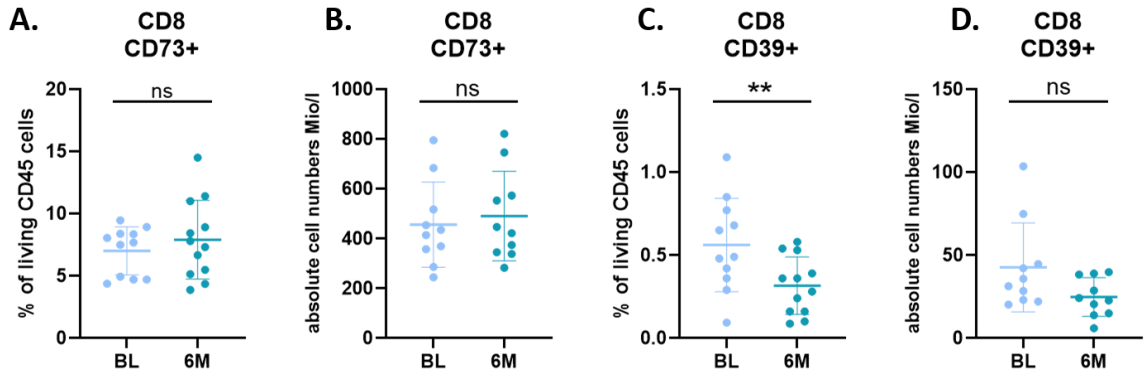

Figure 21. CD39 expression on CD8+ T cells decreases after testosterone therapy. Frequencies (**A**) and absolute cell numbers (**B**) of CD73 positive CD8+ T cells. Frequencies (**A**) and absolute cell numbers (**B**) of CD39 positive CD8+ T cells. A subject paired t-test was performed for each population between BL and 6M HRT samples.

In addition to Tregs, other CD4 subpopulations and T cell effector functions are important for a balanced and functional immune system (see Introduction 1.1.1.). TH1- and TH2-like CD4+ T cells frequencies and absolute numbers were slightly reduced upon testosterone treatment but not significantly altered (Fig. 22C–E; absolute numbers not shown). Moreover, similar NKT cell frequencies (CD3+ CD56+) before and after testosterone treatment were observed (Fig. 22F), while NK cells (CD3-CD56+) were significantly increased (not shown). Interestingly, the frequencies and absolute numbers of TH17-like CD4+ T cells and real TH17 cells (with additional CD161+ expression and gating, see Fig. 45) were highly significantly reduced (Fig. 22A–B).

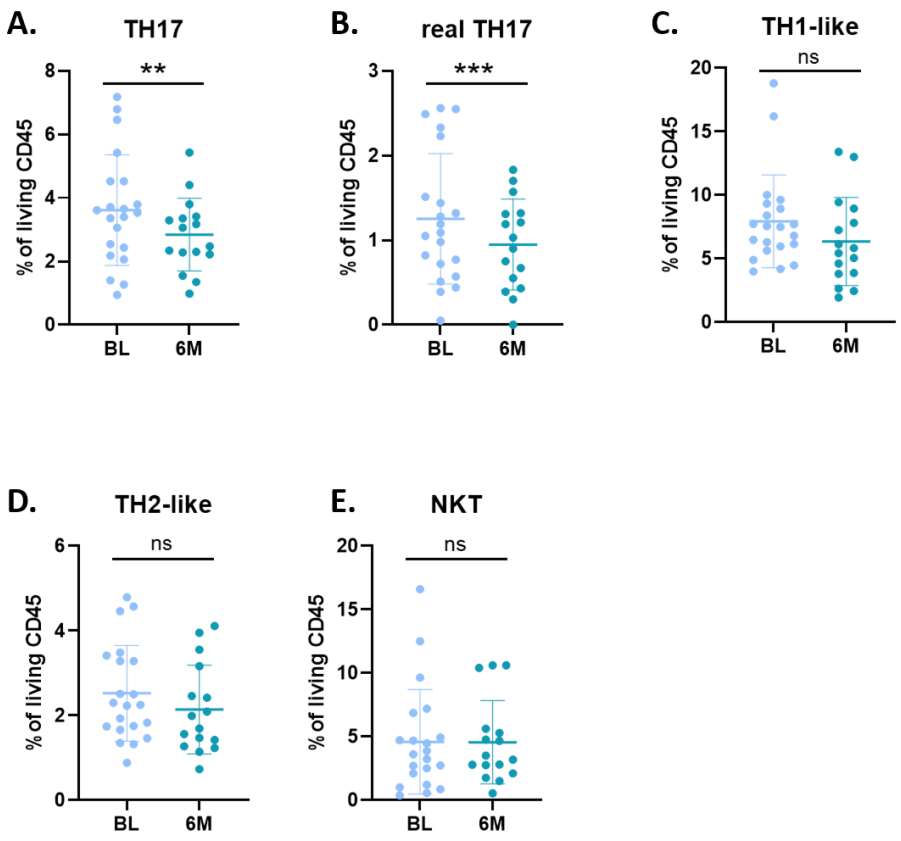

Figure 22. Frequencies of the CD4+ T helper subset are reduced upon testosterone treatment. The frequencies of TH17-like (**A**), real TH17 with additional CD161 expression (**B**), TH1-like (**C**), TH2-like (**D**) and NKT cells (**E**). A subject paired t-test was performed for each population between BL and 6M HRT samples.

A balance between proinflammatory and regulatory T cells is very important for immune cell homeostasis. Therefore, we calculated the ratio of TH17/Treg, Th1/Treg, TH17/TH1 and TH1/TH2 cells. The immune ratios of TH17/TH1 and TH1/TH2 cells were not significantly altered (Fig. 23B–C, F–G). However, we observed a significantly reduced TH17/Treg ratio in frequencies and absolute cell numbers (Fig. 23A, E). Additional TH1/Treg ratios were significantly reduced (Fig. 23B, F). Both of these findings indicate a shift towards a more anti-inflammatory CD4 phenotype.

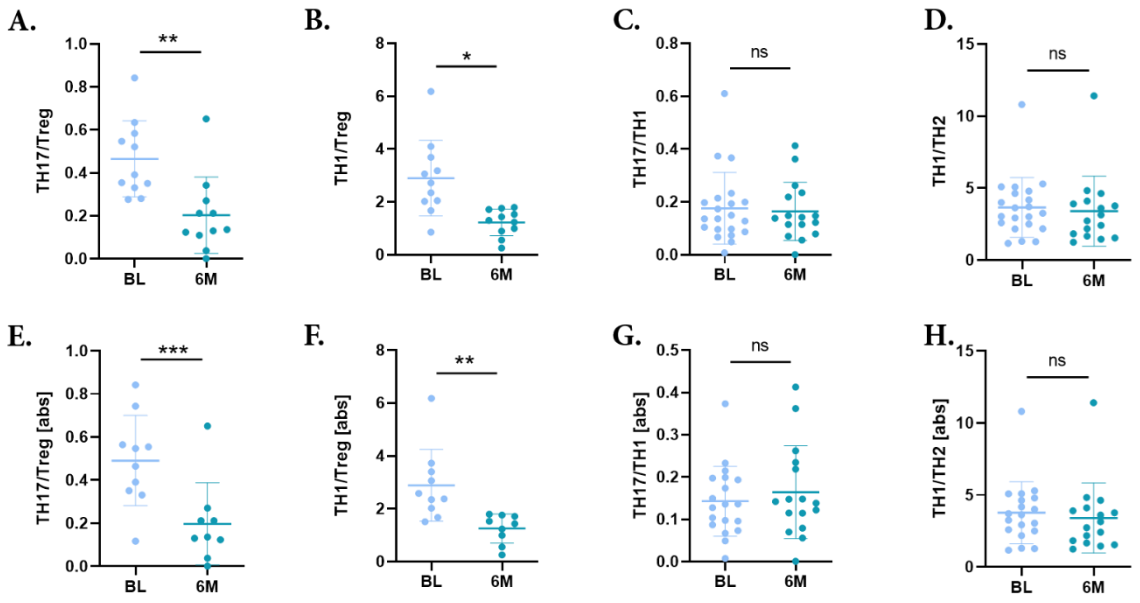

Figure 23. The immune balance ratios of CD4+ subsets are altered upon testosterone treatment. The ratios of TH17/Treg (**A**), TH1/Treg (**B**), TH17/TH1 (**C**) and TH1/TH2 (**D**) cells based on their frequencies. The ratio of TH17/Treg (**E**), TH1/Treg (**F**), TH17/TH1 (**G**) and TH1/TH2 (**H**) cells based on their absolute cell numbers. A subject paired t-test was performed for each population between BL and 6M HRT samples.

In addition to the classic gating strategies described in section 5.1.16, an unbiased approach was used for the Treg, T cell I and T cell II panel (for definitions, see 5.1.6) to identify populations that were not examined via classic gating and to confirm that populations were significantly different following testosterone treatment in an unbiased manner. This unbiased approach was done with the creation of a SPADE/VizR cluster tree and tested for differential abundant clusters between BL and 6M samples (see 5.1.16 for methods). The statistical significance of the relevant populations was confirmed by manual gating and tested for confirmation.

The SPADE Tree of the Treg panel did not reveal any significant populations that had not already been detected by manual gates within the T cells (not shown). Furthermore, we created a SPADE tree with our T cell panel I (Fig. 24A), and differential abundant clusters were identified (Fig. 24B). One cluster (cluster 13) was significantly enriched after 6 months of testosterone treatment, while 10 (4, 35, 40, 62, 90, 102, 147, 151, 173, 181) were significantly reduced after 6 months of testosterone treatment (Fig. 24B). We characterized these clusters with a phenotypic heatmap and cluster marker expression phenographs (Fig. 24C–E). Clusters 40, 62, 102 and 151 were characterized by negative or medium CD3 expression and were excluded due to their lack of a non-T cell defining

population marker (Fig. 24A, C). Clusters 90 and 181 showed no clear phenotype across all of the samples and were therefore also excluded from further analysis.

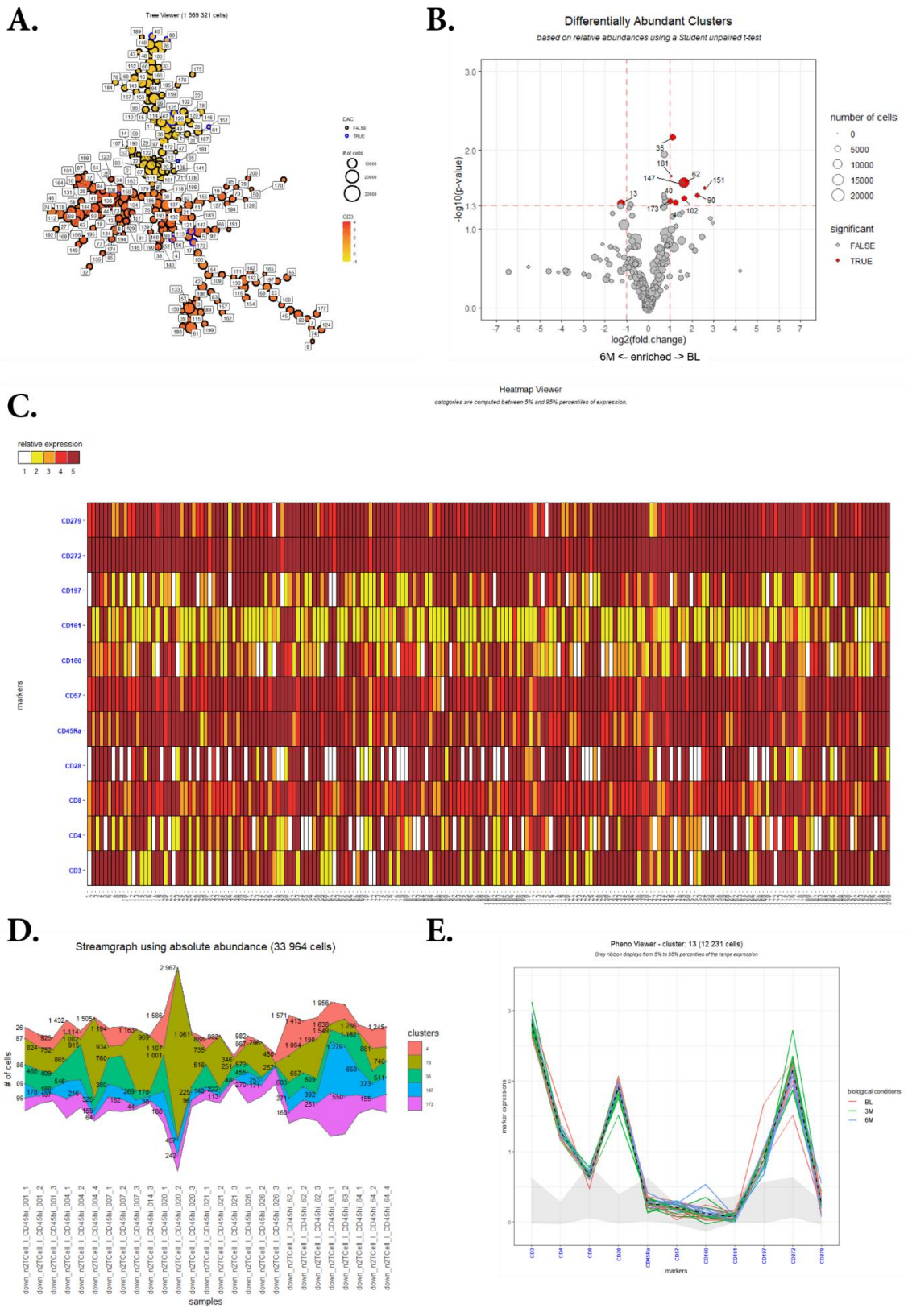

Figure 24. The SPADE/VizR analysis of T cell I panel reveals altered T cell populations after testosterone treatment. Live CD45high cells were used to perform SPADE and SPADEVizR analyses **A.** Clustering tree

from the SPADE analysis of FTM samples from panel I of the live CD45high cells. CD3 expression is marked from low (yellow) to high (red) and differentially abundant clusters (DAC) from B are marked in blue. **B.** DAC analysis of samples before testosterone therapy and 6 months after the start of testosterone therapy (6M). Significantly different clusters are marked in red. **C.** Heatmap of marker expression in all clusters from no (white) to high (deep red) expression. **D.** Absolute cell numbers for clusters 4, 13, 35, 147 and 173 in all included samples. **E.** Phenograph of marker expression in cluster 13 compared to all other clusters for the definition of cluster marker expression. FTM samples from before testosterone therapy (BL) are marked in red, 3 months of testosterone therapy (3M) in green and 6 months of testosterone therapy (6M) in blue. The grey area indicates 5 to 95% of marker expression across all clusters.

The remaining clusters were confirmed by manual gating and clusters 147 and 173 were combined due to their similar expression patterns. The statistical analysis of these clusters confirmed three relevant clusters. The frequencies and absolute numbers of cluster 13 increased after testosterone treatment, while the frequencies but not the absolute numbers of cluster 4 and cluster 147/173 were significantly decreased. Cluster 13 was comprised of CD4+ T cells expressing CD28+, CD197^{med} and CD272+, while cluster 4 contained CD4+ T cells expressing CD28 and CD161, and cluster 147/173 consisted of CD8+ T cells expressing CD28, CD57 and CD161 (Fig. 25).

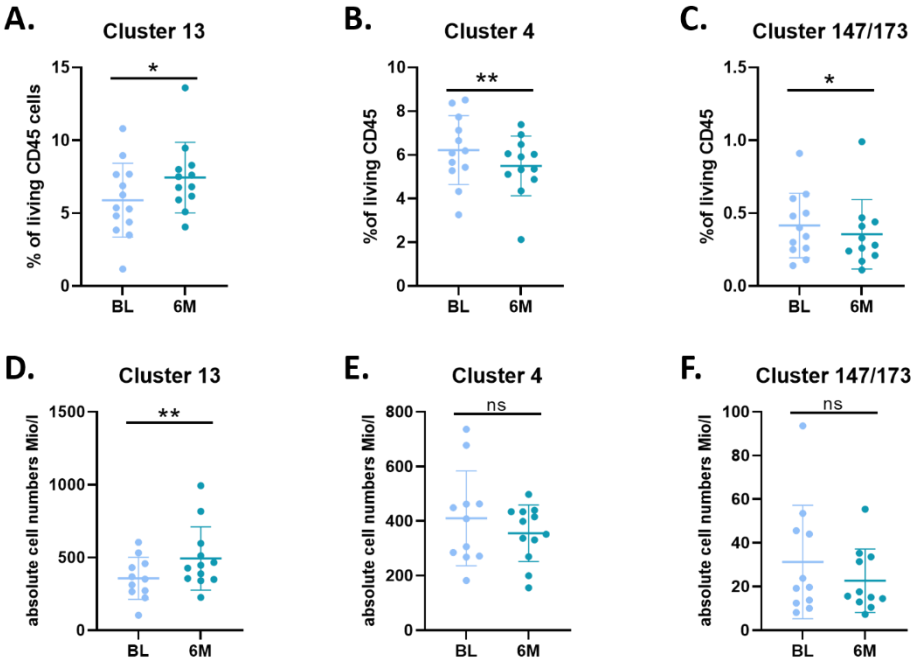

Figure 25. Cluster 13 of the SPADE/VizR T cell panel I analysis increased after testosterone therapy. A–C. Frequencies of clusters of living CD45 cells in FTM samples from before testosterone therapy (BL) and 6 months after testosterone therapy (6M). **D–F.** Absolute cell numbers of FTM samples from before testosterone therapy (BL) and 6 months after testosterone therapy (6M). **A, D.** Cluster 13 are CD4+ T cells, which express CD28+, CD197med and CD272+. **B, E.** Cluster 4 are CD4+ T cells expressing CD28 and CD161. **C, F.** Cluster 147/173 are CD8+ T cells expressing CD28, CD57 and CD161. A subject paired t-test was performed for each population between BL and 6M samples.

In a second T cell panel (T cell II), the SPADE-VizR analysis revealed only one population, which proved to be significantly different between BL and 6M. This cluster consisted of CD4+ CD8+ double positive T cells and was significantly reduced upon testosterone treatment (cluster 58; SPADE analysis not shown). This cluster was not only double positive for CD4 and CD8 but also expressed CD25, CD44, CD45Ra and CD62L (Fig. 26G). Applying the SPADE analysis to T cells only (CD3+; Fig. 26A–E) led to the identification of cluster 126, which was significantly reduced in frequency (not shown) and in absolute cell numbers (Fig. 26F). Cells from cluster 126 were characterized as CD4+ T cells, expressing CD25, CD45Ra, CD49a, CD49b, CD62L and CD44 (Fig. 26E).

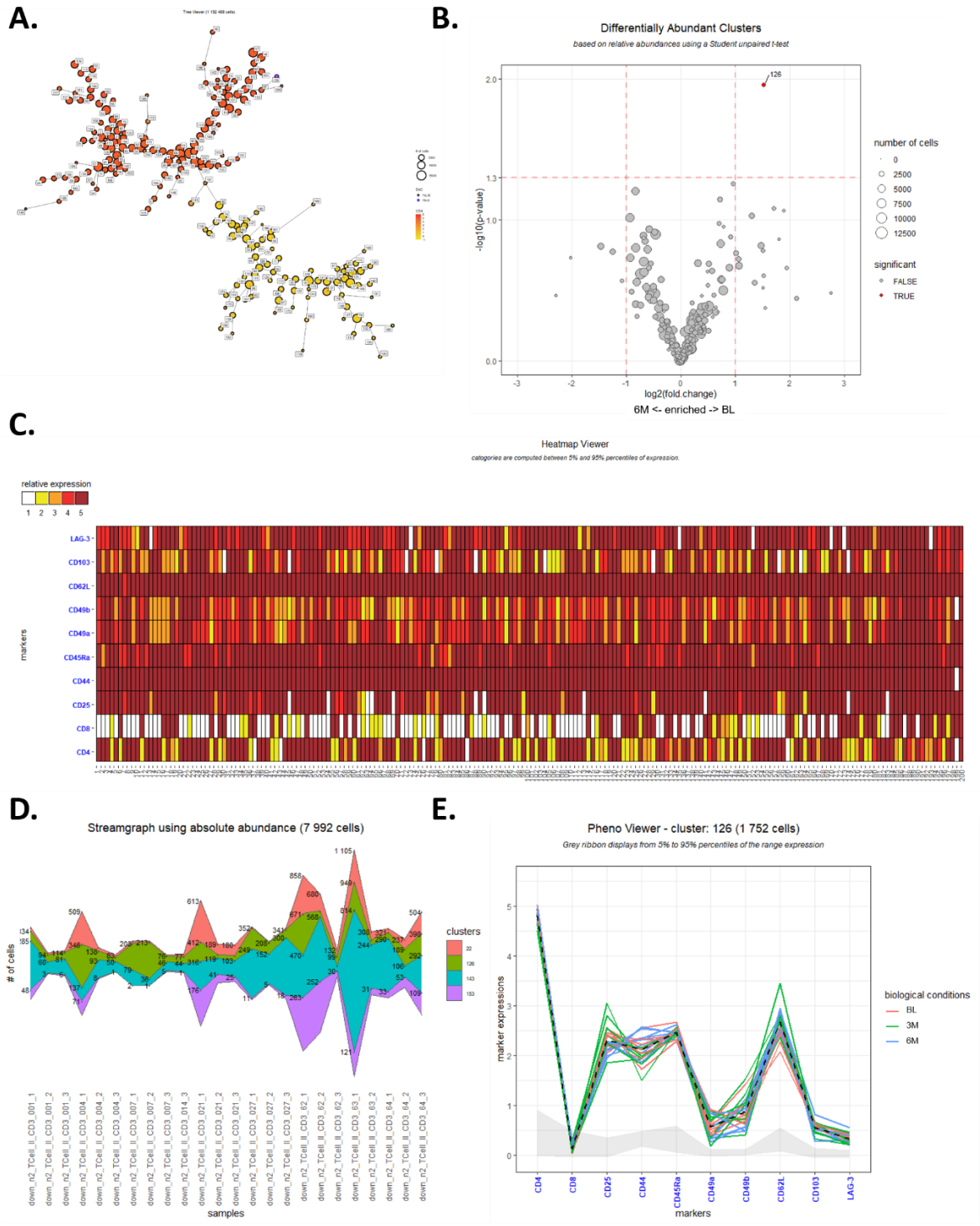
A.
B.
Differentially Abundant Clusters
based on relative abundances using a Student unpaired t-test
-log10(p-value)
log2(fold.change)
6M <- enriched -> BL
number of cells
significant
FALSE
TRUE
C.
Heatmap Viewer
catogories are computed between 5% and 95% percentiles of expression.
relative expression
markers
LAG-3
CD103
CD62L
CD49b
CD49a
CD45Ra
CD44
CD25
CD8
CD4
D.
Streamgraph using absolute abundance (7 992 cells)
# of cells
samples
clusters
E.
Pheno Viewer - cluster: 126 (1 752 cells)
Grey ribbon displays from 5% to 95% percentiles of the range expression
marker expressions
markers
biological conditions
BL
3M
6M
F.
cluster 126
absolute cell numbers Mio/l
BL
6M
G.
cluster 58
absolute cell numbers Mio/l
BL
6M

Figure 26. The SPADE/VizR T cell II panel analysis revealed reductions in two T cell populations upon testosterone treatment. CD3+ cells were used to perform SPADE and SPADEVizR analyses. **A.** Clustering tree from the SPADE analysis of FTM samples from panel II. CD4 expression is marked from low (yellow) to high (red) and differentially abundant clusters (DAC) from B are marked in blue. **B.** DAC analysis of samples before testosterone therapy and 6 months after the start of testosterone therapy (6M). Significantly different clusters are marked in red. **C.** Heatmap of marker expression in all clusters from no (white) to high (deep red) expression. **D.** Absolute cell numbers in clusters 22, 126, 143 and 153 for each sample. **E.** Phenograph of marker expression in cluster 126 compared to all other clusters for the definition of cluster marker expression. FTM samples from before testosterone therapy (BL) are marked in red, 3 months with testosterone (3M) in green and 6 months with testosterone (6M) in blue. The grey area indicates 5 to 95% of marker expression across all clusters. **F, G.** GraphPad analysis of absolute numbers of clusters 126 and 58; due to a lower number of matched pairs, an unpaired t-test was used.

To further characterize the influence of testosterone on T cell functions, we next analyzed the expression of T cell-secreted cytokines. Fresh whole blood FTM samples were stimulated with PMA/ionomycin and T cell cytokine production was analyzed. Even though this stimulation revealed a high degree of variance, some interesting tendencies were found and are highlighted in Figure 27. A reduction in the frequency and absolute numbers of TNFα/IFNγ production from CD4, CD8, and double negative T cells were observed but were not statistically significant.

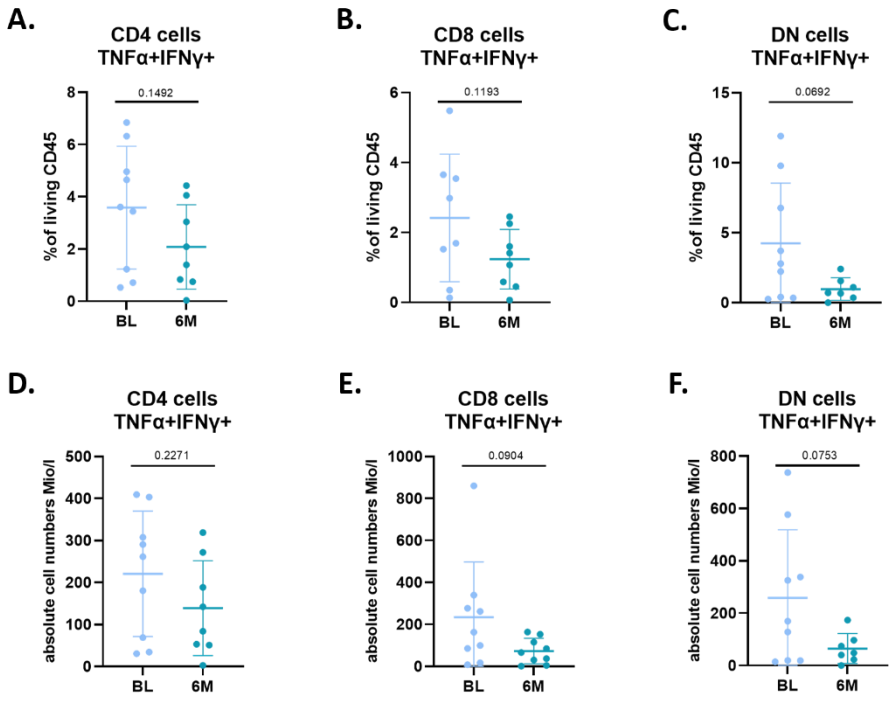

Figure 27. A tendency for decreased TNFα/IFNγ cytokine production by T cells after PMA/ionomycin stimulation in the FTM samples. A–C. Frequencies of TNFα+ and IFNγ+ populations of living CD45 cells in FTM samples before testosterone therapy (BL) and 6 months of testosterone therapy (6M). **D–F.** Absolute cell numbers of A–C. **A, D.** CD4+ T cells. **B, E.** CD8+ T cells. **C, F.** CD4 and CD8 negative T cells. An unpaired t-test was performed for each population between BL and 6M samples.

Since testosterone treatment altered some of the T cell markers and the effector memory state, we examined whether we could specify the altered effector and memory state of the changed T cell subsets.

In the Treg panel, the typical CD62L, CD197 (CCR7) and CD45Ra gating could not be used since CD62L and CD197(CCR7) were not included in the FACS panel. Here, naïve cells were defined as CD45Ra+ and HLA-DR-, while effector Tregs were defined as HLA-DR+ and CD45Ra-. In the Treg population, both increased, as Figure 20 shows. Of the CD8+ CD39+ cells, which decreased under testosterone (Fig. 28A), approximately 35% belonged to TEMRA cells and about 16% to the naïve cell type (Fig. 28B). Therefore, the CD8+ CD39+ T cells cannot be clearly assigned to one effector or memory cell type. In contrast, CD4+ T cells positive for CD161, which decreased under testosterone (Fig. 28C and cluster 4 from Fig. 25), were primarily effector memory T cells (~ 77%), though some were central memory T cells (~18%) and a very few were TEMRA or naïve T cells (<4%). Similarly, CD8+ T cells, which are CD161, CD28 and CD57 positive, decreased under testosterone (Fig. 28E and cluster 147/173 from Fig. 25). The effector and memory state of these cells were similar to the CD4+ population. Most were effector memory T cells (53%); however, the rest were primarily TEMRA (43%) instead of memory cells or naïve cells (<4%) (Fig. 25F). The fold change of CD8+ T cells expressing CD69 increased under testosterone (Fig. 16 and 17). These increased cells were a mix of TEMRA (38%), effector memory (36%), naïve (18%) and central memory (8%) T cells (Fig. 29H). Another increased CD8 population was CD44high (Fig. 28I), which was mainly composed of effector memory (40%) and central memory (38%) T cells, though some were naïve (16%) and a few were TEMRA (6%) T cells (Fig. 29J). Lastly, a CD4+ T cell subpopulation, which increased after 6 months of testosterone therapy, were CD28, CD272 (BTLA) positive and CD197 medium (Fig. 29K). These cells were mainly naïve (44%) and central memory (30%) T cells, with the remaining composed of effector memory (20%) and TEMRA (5%) T cells (Fig. 28L).

Furthermore, two populations found through SPADE decreased: one naïve CD4+ and one naïve DP T cells (cluster 126, Cluster 58) (Fig. 28). Cluster 13, which increased upon testosterone therapy, were CD4+ memory T cells (Fig. 25). Even in the effector and memory mixed phenotype populations, a shift towards more TEMRA and fewer effector memory (EM) cells within these cell populations can be observed. This shift can be seen in decreasing populations such as CD8+ CD28+ CD57+ CD161+, where TEMRA cells

increased and EM cells decreased within this population (Fig. 28Fa). However, in increasing populations such as CD4+ CD28+ CD197^{med} CD272+, the memory cells EM and CM strongly decreased, while naïve cells increased (Fig. 28La). This finding underlines the overall shift that occurs in the memory and effector phenotype across different T cell populations upon testosterone therapy.

Overall, CD4+ and CD8+ TEMRA T cells increased upon testosterone treatment, and CD4+ and CD8+ T cells with a mixed effector and memory state seemed to be enhanced. In contrast, two subsets of T cells with a predominant effector memory phenotype, CD4+ EM cells and two subsets with a clear naïve phenotype decreased upon 6 months of testosterone treatment.

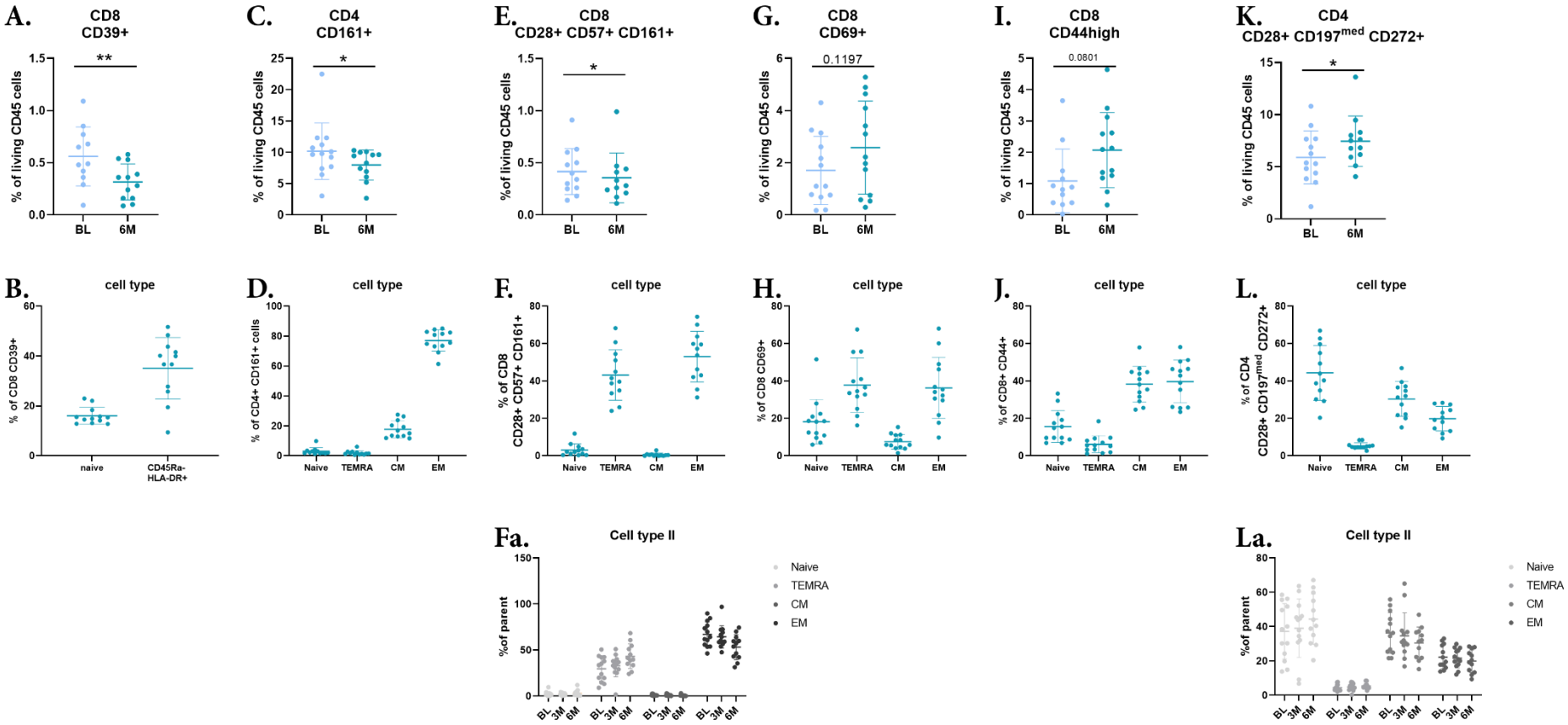

Figure 28. T cell subpopulations showed a changed effector and memory state under testosterone. Upper panel: Frequencies of the populations of living CD45 cells in FTM samples from before testosterone therapy (BL) and 6 months after testosterone therapy (6M). A subject paired t-test was performed for each population between BL and 6M samples. **Lower panel:** Effector memory state of the populations from upper panel of FTM samples 6 months after testosterone therapy (6M). **A, B.** CD8+ T cells expressing CD39. **C, D.** CD4+ T cells expressing CD161. **E, F.** CD8+ T cells expressing CD28, CD57 and CD161. **G, H.** CD8+ T cells expressing CD69. **I, J.** CD8+ T cells, which were CD44high. **K, L.** CD4+ T cells expressing CD28, CD272 and CD197 medium. **Fa.** Effector memory state of cells from E and F at all three timepoints: BL, 3M and 6M. **La.** Effector memory state of cells from K and L at all three timepoints: BL, 3M and 6M.

In summary, our flow cytometry-based deep immunophenotyping revealed that *in vivo* treatment with testosterone did not change the frequencies or absolute numbers of CD4+, CD8+, double positive and double negative T cells. However, we observed significant alterations in important subpopulations of CD4+ and CD8+ T cells, such as Tregs, TH17 cells and CD4+ and CD8+ TEMRA cells. The T cells with either significantly different frequencies or absolute cell numbers after 6 months of testosterone treatment are summarized in Figure 29. For comparison, the mean of the fold change from BL to 3M and 6M are displayed in a heatmap, but in all of the populations shown, only the 6M samples were significantly different from BL. The categorization of the populations in an effector memory state is indicated on the left side of the heatmap, where it was possible to gate in the corresponding flow cytometer panel (see section 5.1.6). We found increased TEMRA T cells and decreased effector and central memory cell subpopulations upon testosterone treatment. Some subpopulations of naïve T cells decreased, but within mixed populations, the proportion of naïve cells increased. These changes might help maintain a diverse repertoire of naïve T cells. In general, high testosterone leads to diverse changes in the T cell atlas, with important parameters involved in autoimmunity, such as high TH1, high TH17 and low Tregs, indicating a shift towards a more anti-inflammatory phenotype. On the other hand, TEMRA-like T cells, long thought to be proinflammatory, increased. However, the overall T cell atlas in the peripheral blood seems more balanced, with a slight tendency for anti-inflammatory processes under high testosterone conditions.

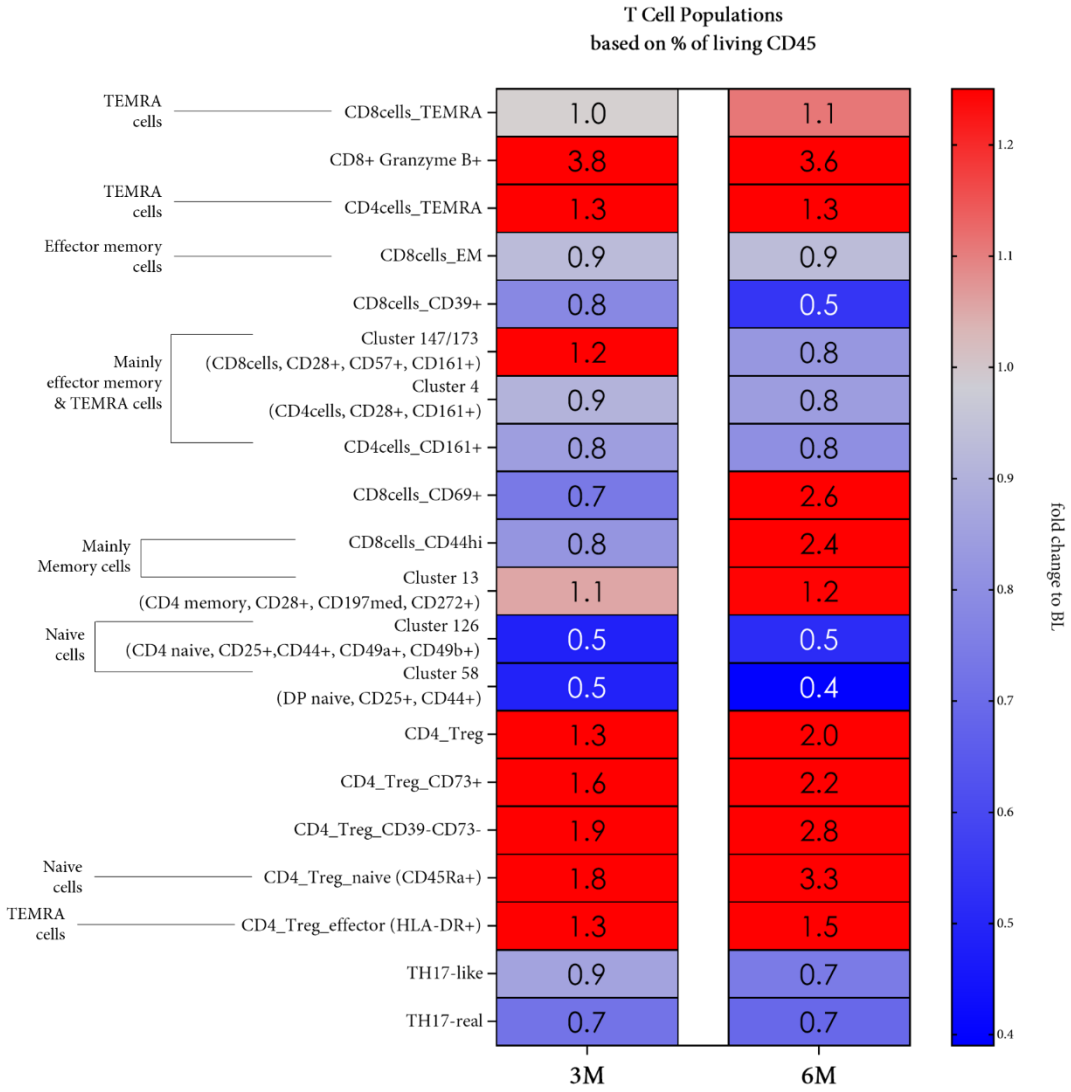

Figure 29. T cell populations were significantly different at 6 months of testosterone treatment. Summary heatmap of fold change between FTM samples before testosterone therapy started and upon 3 or 6 months of therapy with testosterone (3M or 6M) based on the frequencies of living CD45 cells. Grey (1.0) signals no fold change, while red indicates the populations that increased under testosterone and blue marks those that decreased. Only populations that were individually significantly different in either frequencies or absolute numbers after 6M compared to baseline (BL) are displayed. Mean fold changes of BL to 3M for the same populations are shown for comparison, despite not being significant. Left legend: Cells were categorized in an effector memory state, if possible.

3.7. CD4 and CD8 T cell subpopulations shift and invariant T cells change their expression profile under testosterone

To confirm and deepen our understanding of the findings, we performed single-cell sequencing with a parallel analysis of surface proteins and the TCRαβ repertoire (see the methods in 5.1.15). We analyzed sorted CD3+ positive T cells from 4 different subjects of our FTM cohort with samples from BL and 6M after the start of hormone treatment. For comparison, the same number of sequenced cells from each sample was used for analysis (4,400 cells each, 35,200 cells total).

We identified 12 distinct T cell populations in the peripheral blood of the eight samples (Fig. 30A). The identification of these populations was made according to their RNA expression and their surface protein expression via CITE-Seq antibodies (Fig. 30B, C). The identified clusters (0–11) were naïve CD4 T1 cells, TH17-like CD4 cells, naïve-like CD4 cells, TC1/naïve-like CD8 cells, CD57+ γδ T cells, MAIT/TC17 CD8 cells, naïve-transition CD4 cells, TC2/TC1-like CD8 cells, Tregs, CD28+ γδ T cells, GZMB+/CD57+ TEMRA-like CD8 cells and naïve-like CD4 T3 cells (Fig. 30A).

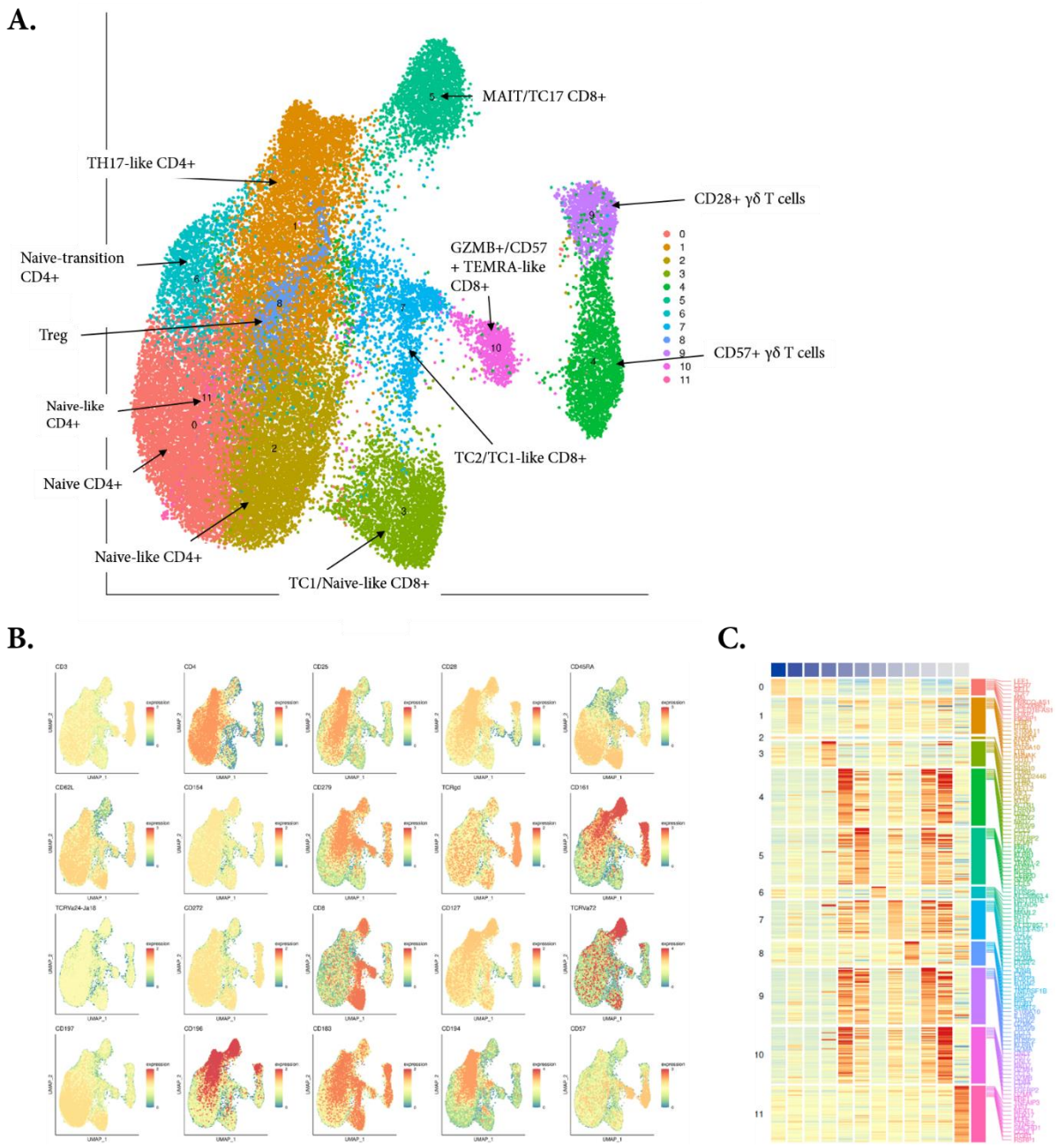

Figure 30. Single-cell CITE sequencing of eight FTM samples revealed different T cell subsets. A. UMAP clustering of FTM samples according to their RNA expression. The resulting clusters were categorized into T cell subpopulations according to their most expressed genes (C) and their surface marker expression (B). **B.** Expression of surface proteins from each cell. **C.** Heatmap of the dominant differential expressed genes in each cluster compared to all other clusters.

Next, we aimed to analyze changes in *in vivo* T cell activation and differentiation and compared the density of the clusters between BL and 6M of testosterone treatment. Upon 6M of testosterone treatment, we detected a decreased density in the MAIT cell population compared to the BL control. In contrast, γδ T cells and the TEMRA CD8+ cluster seemed to increase (Fig. 31A). To characterize these findings in detail and to

confirm the changes in the amount and frequencies for all four of the subjects, we analyzed the fold change of cells per cluster at 6M compared to BL. The naïve-like CD4 cluster (cluster 2) and the TEMRA-like CD8 cluster (cluster 10) consistently increased after testosterone treatment in all of the samples. In regard to CD57+ γδ T cells (cluster 4), only three out of four subjects showed the same tendency, and the MAITs (cluster 5) revealed a similar pattern (Fig. 31B).

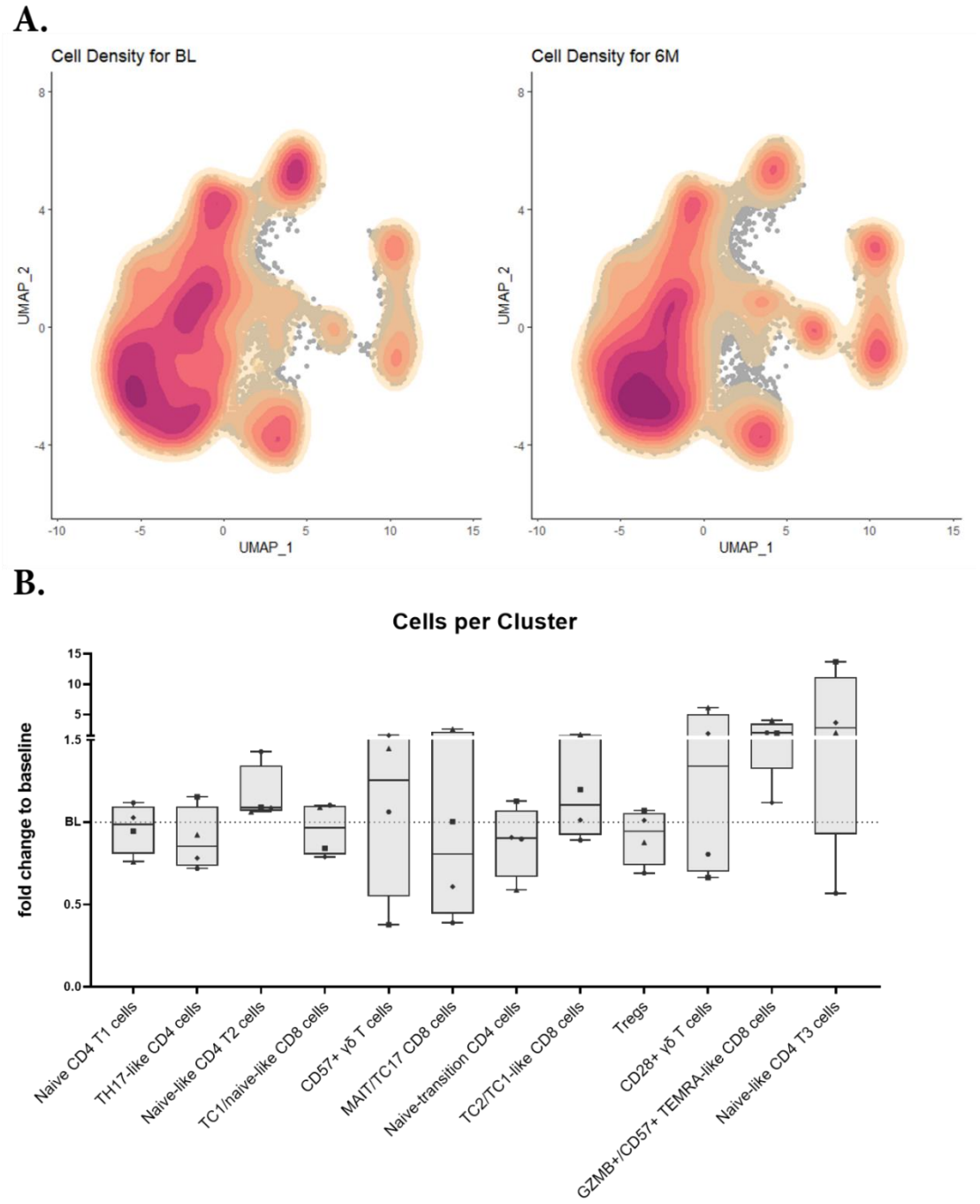

Figure 31. Sequencing cluster abundancy was altered upon 6-month testosterone treatment. A. Density UMAP from before testosterone therapy (BL) and 6 months with testosterone (6M). **B.** Fold change of cell numbers between BL and 6M in all 12 clusters. Each subject is marked with different symbol.

In order to gain more functional insights, we next analyzed the changes in gene expression upon testosterone treatment in our cohort. We analyzed the gene expression in all of the cells without considering clusters and single cells (bulk analysis). The overall differential expressed genes after 6M of testosterone treatment were visualized through a heatmap (Fig. 32).

We identified some genes that are known to modulate T cell interactions, including the expression of CXCR4 and IL21R, while the role of other genes such as GIMAPs is still unclear. To understand whether the alterations in gene expression could lead to functional changes, we performed a pathway analysis of all upregulated genes (80 genes). To date, this method has not uncovered any relevant known mechanisms and needs to be further analyzed (not shown).

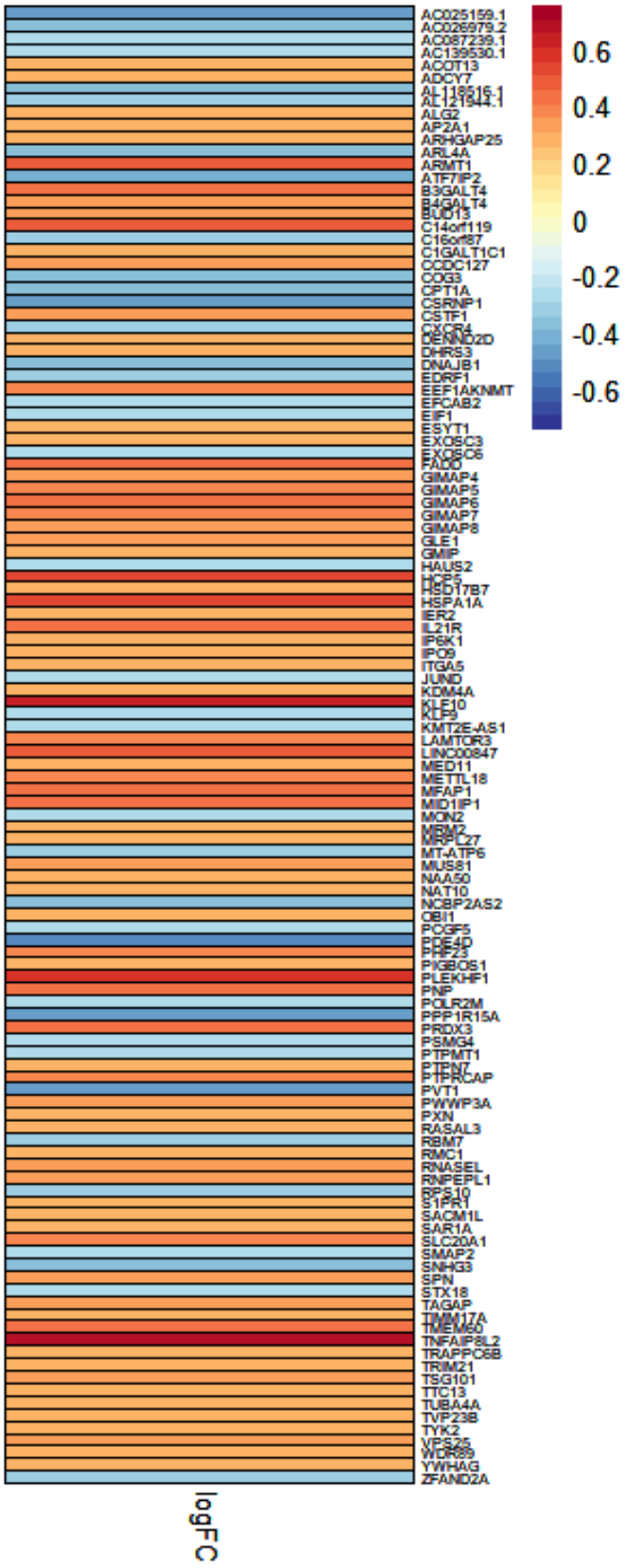

Figure 32. Analysis of sequenced bulk T cell RNA reveals significant changes upon testosterone treatment. Heatmap of logFC (red = upregulated in 6M) of differential expressed genes before (BL) and 6 months of testosterone treatment (6M). Genes are ordered alphabetically.

To perform a more specific T cell subset analysis and detect genes affected by testosterone in each T cell subset, we investigated the differential gene expression (DGE) in our previously identified clusters.

Most T cell subsets had two to three genes changed upon testosterone treatment (Fig. 33A). Interestingly, some of these differentially expressed genes were found in many clusters. *GIMAP7* was upregulated upon testosterone treatment in naïve CD4 T cells (cluster 0, 2), naïve-transition CD4 T cells (cluster 6), TH17-like CD4 T cells (cluster 1), Tregs (cluster 8), CD57+ γδ T cells (cluster 4), MAITs (cluster 5), TC2/TC1-like CD8 T cells (cluster 7) and TEMRA-like CD8 T cells (cluster 10) (Fig. 33B). *CCR7* was upregulated in the naïve and naïve-like CD4 T cells clusters (cluster 0, 2, 6), while *JUNB* was upregulated in naïve-like CD4 and CD8 T cells (cluster 2, 3). However, T cells belonging to the invariant phenotype showed the greatest differential gene expression. This group was also the only subset with up- and downregulated DGE genes. The CD57+ γδ T subset exhibited the greatest differential gene expression upon testosterone treatment, while the MAITs exhibited the second greatest (Fig. 33A). The three most predominant up- and downregulated genes after 6M of testosterone in all T cell subsets are summarized in a heatmap in Figure 34B.

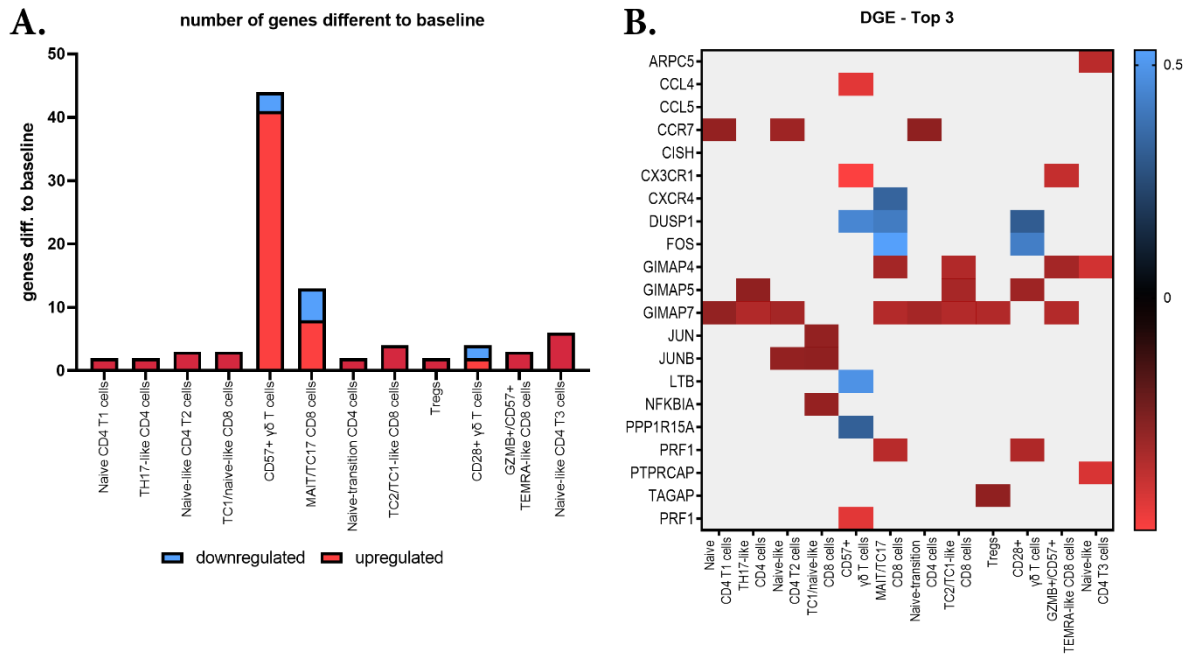

Figure 33. Differentially expressed genes between BL and 6M showed similarities and differences according to T cell subtype. A. Number of genes differentially expressed (DGE) in FTM samples after 6 months of testosterone compared to baseline per cluster. Upregulated genes are marked in red and downregulated genes in blue. **B.** Heatmap of fold changes of the top 3 up- (red) and down- (blue) regulated genes in each cluster after 6 months of testosterone.

Since some genes were differentially expressed upon testosterone treatment in more than one T cell subset, we took a closer look at the gene expression at BL and 6M in all of the clusters (Fig. 34A). This analysis confirmed that *GIMAP7* was significantly upregulated in many clusters. Interestingly, *GIMAP7* was also differentially expressed in the bulk analysis (Fig. 32). However, other genes such as *DUSP1* and *FOS* were only downregulated in the subset detected by the previous DGE analysis (Fig. 34B), and *JUNB* showed a tendency for downregulation in some subsets, in contrast to its significant upregulation in the naïve-like T cells found in the DGE analysis (Fig. 34A). Thus, testosterone has different effects on T cell gene expression depending on the T cell subtype.

The CD57+ γδ T cell subset contained the most differentially expressed genes upon testosterone treatment and we therefore analyzed them in more detail. We performed a pathway analysis of all upregulated genes after testosterone treatment in these CD57+ γδ T cells. This analysis revealed that testosterone upregulates the pathways of cell-cell adhesion, cytolysis, cytotoxicity, migration and activation in γδ T cells (Fig. 34B).

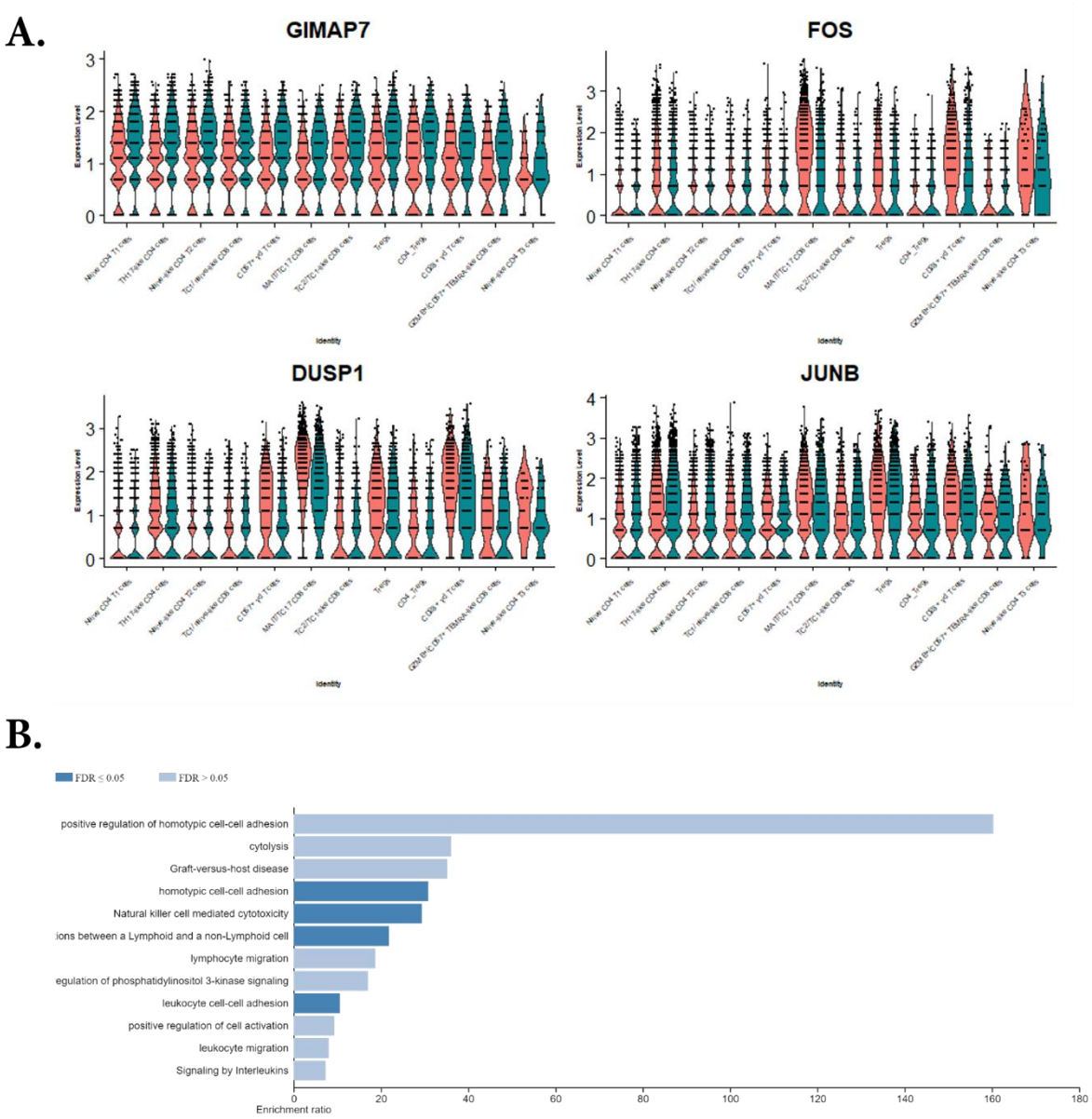

Figure 34. ***GIMAP7*** **expression was reduced upon testosterone therapy in almost all T cell clusters. A.** Expression of *GIMAP7*, *FOS* and *DUSP1* across clusters split in samples before (BL) and after testosterone therapy (6M). **B.** Pathway analysis of upregulated genes in CD57+ γδ T cells (cluster 4).

In general, the differential gene expression analysis of samples taken at BL and 6M revealed that testosterone not only upregulates *GIMAP7* in bulk T cells but also in different distinct T cell subsets, such as naïve and TH17-like T cells. The consequence of this *GIMAP7* upregulation is as yet unknown (see Discussion). Furthermore, the analysis revealed that testosterone upregulates different pathways in a subset of γδ T cells, including pathways of cytotoxicity.

Next, we aimed to confirm this *ex vivo* DGE upon testosterone treatment in our *in vitro* T cell experiment, where we saw the influence of proinflammatory cytokines (Fig. 9). Therefore, we analyzed the gene expression of *GIMAP7*, *JUNB* and *CCR7* in T cells stimulated *in vitro* and cultured in the presence of testosterone. We observed significantly increased *GIMAP7* gene expression in testosterone-treated T cells compared to untreated controls. This upregulation was mainly observed in T cells derived from female donors (orange) (Fig. 35). The expression of *CCR7* was not altered in bulk T cells (not shown). In the CITE-Seq analysis, testosterone treatment had mixed effects on *JUNB* expression; however, in the bulk T cells treated *in vitro*, a significant downregulation was observed (Fig. 35). Overall, the strong upregulation of *GIMAP7* in different T cell subsets from the trans men cohort was confirmed with cells from healthy female donors treated *in vitro* with testosterone.

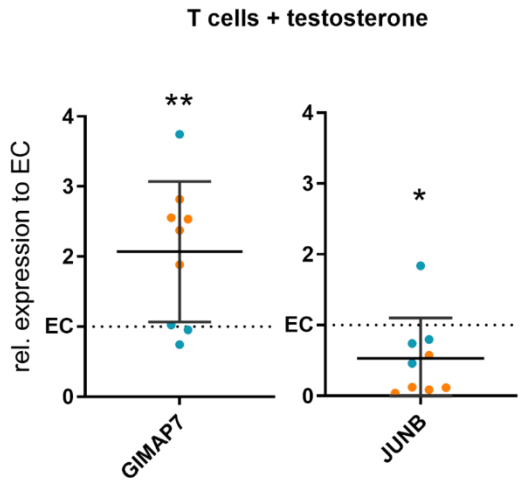

Figure 35. T cells treated with testosterone *in vitro* showed increased *GIMAP7* and decreased *JUNB* expression. T cells were treated with 150 ng/ml testosterone and aCD3/CD28 for 24 hours. Relative gene expression to dilution control (EC = 1). Left = *GIMAP7*; right = *JUNB*; orange dots = female; blue dots = male. Statistical significance was tested with an unpaired t-test for each gene.

Overall, our flow cytometry data and sequencing data could link sex-specific differences in gene regulation and responsiveness upon stimulation with testosterone.

3.8. Transferring this knowledge to autoimmune liver diseases

The autoimmune liver diseases autoimmune hepatitis (AIH) and primary biliary cholangitis (PBC) are among the autoimmune diseases with the highest female bias. The mechanisms behind the sex differences observed in these diseases remain largely unknown. The incidence of most autoimmune liver diseases peaks around menopause, while AIH peaks around puberty, indeed pointing to the contribution of sex hormones. In addition, pathogenesis in AILD patients is associated with dysfunctional immune cell responses. We therefore aimed to investigate whether we could transfer our knowledge of the impact of testosterone on immune cells gained from our transgender cohort to patients with AIH and PBC.

We first investigated the sex hormone levels in patients with PBC and AIH and compared them to sex- and age-matched healthy controls. The sample included a total of 55 patients and controls, as summarized in Table 4.

We found a significant reduction in free and bioavailable testosterone levels in serum samples from female PBC and AIH patients as compared to the controls (Fig. 36A). Importantly, differences in BMI (Fig. 36B) and medication did not seem to cause the observed changes in testosterone levels. Of note, female AIH and PBC patients without immunosuppressive medication still showed significant lower bioavailable testosterone levels compared to aged-matched healthy controls (Fig. 36C).

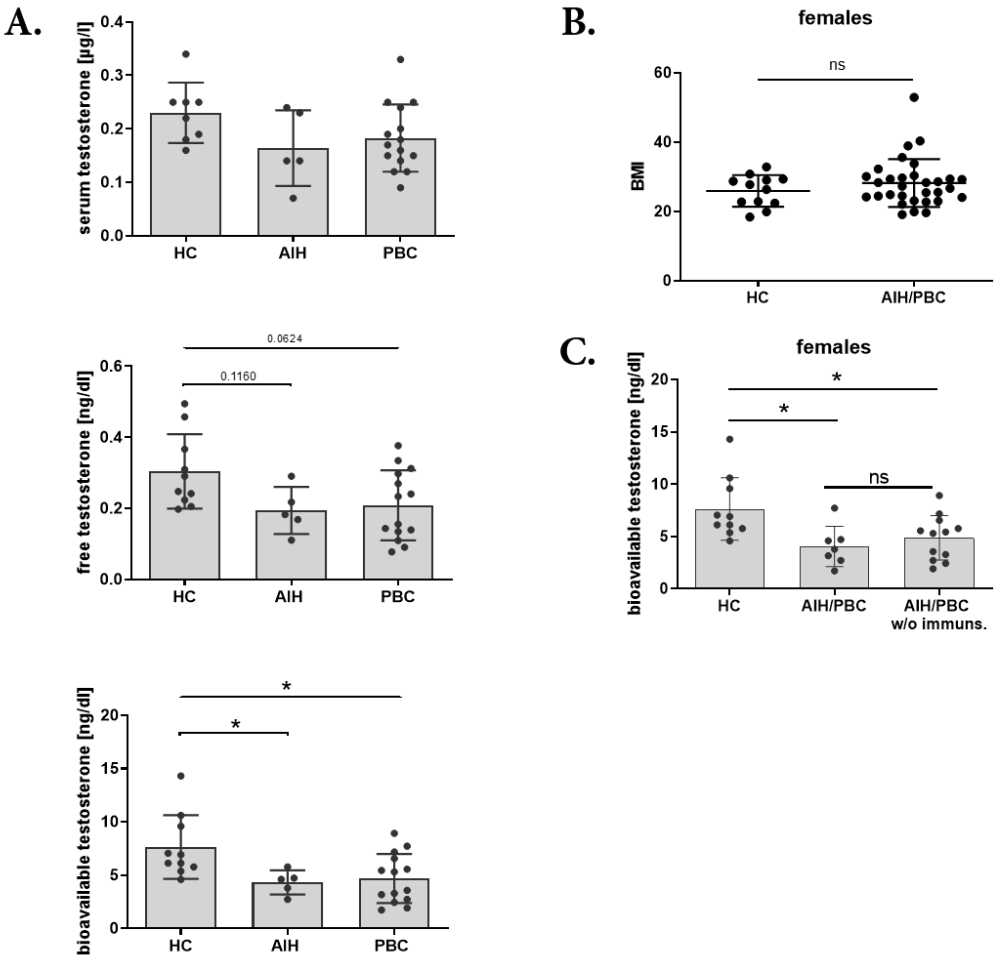

Figure 36. Bioavailable testosterone levels of female AIH and PBC patients were lower than healthy female controls. A. Serum levels of total, free and bioavailable testosterone in healthy female controls (HC), AIH and PBC patients (from top to bottom). An ordinary one-way ANOVA test was performed. **B.** Body mass index (BMI) of healthy female controls vs. AIH and PBC patients. An unpaired t-test was performed. **C.** Bioavailable testosterone levels in healthy controls (HC) and AIH and PBC patients with and without (w/o) immunosuppressive medication. An ordinary one-way ANOVA was performed.

Men with AIH and PBC showed no significant difference in testosterone levels compared to healthy males, as Figure 37A demonstrates. However, in this cohort, the decline of testosterone due to age was very clear and could be correlated with age (Fig. 37B, $p = 0.007$). Due to the low number of male patients, we could not make cutoffs regarding age and disease severity to homogenize the cohort as we did for the female patients. A larger cohort consisting of groups with smaller age ranges could help clarify if there is in fact no difference in hormone levels in males with AIH and PBC.

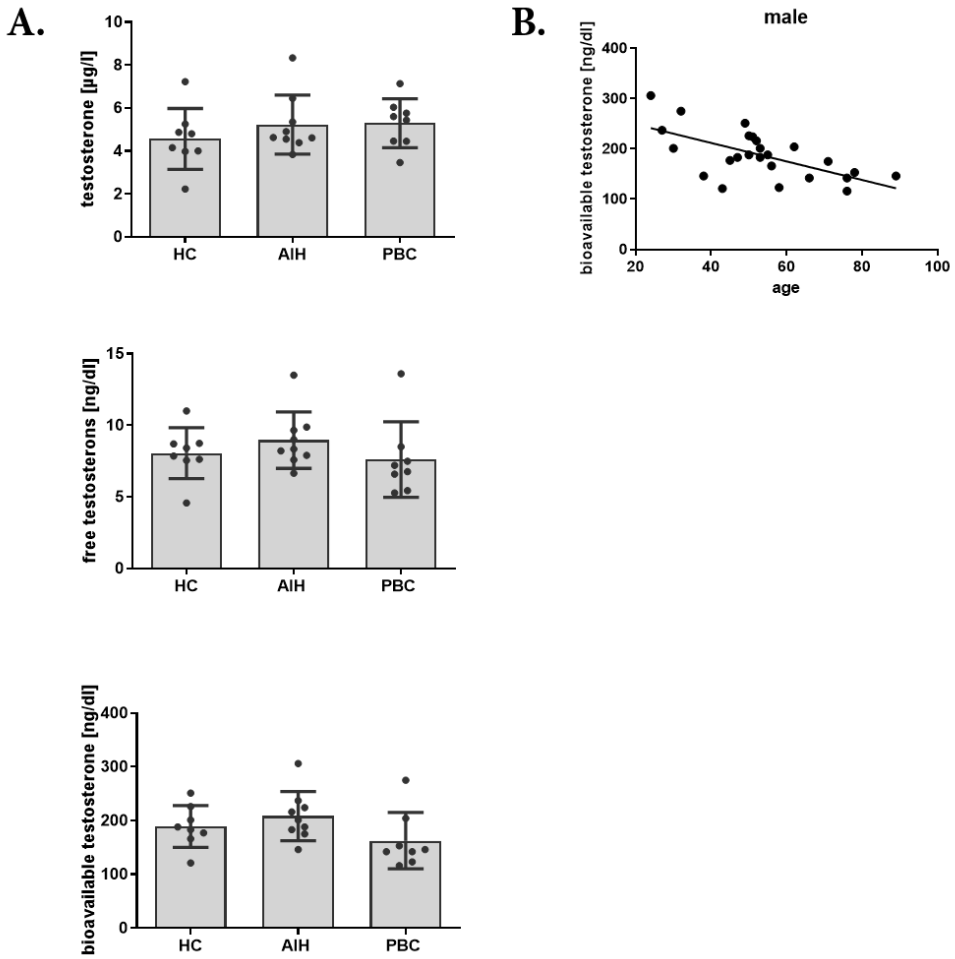

Figure 37. Testosterone levels of male AIH and PBC patients were unchanged compared to healthy male controls. A. Serum levels of total, free and bioavailable testosterone in healthy male controls (HC), AIH and PBC patients (from top to bottom). An ordinary one-way ANOVA test was performed. **B.** Regression analysis of bioavailable testosterone versus age in years in all males from A. A significant linear regression line is shown.

The amount of ß-estradiol was not different between patients with AILDs and healthy controls (not shown). Of note, in our cohort, no significant difference in ß-estradiol was observed between women 37 to 65 years old and men 20 to 89 years old, but there was a highly significant difference in testosterone levels (Fig. 38).

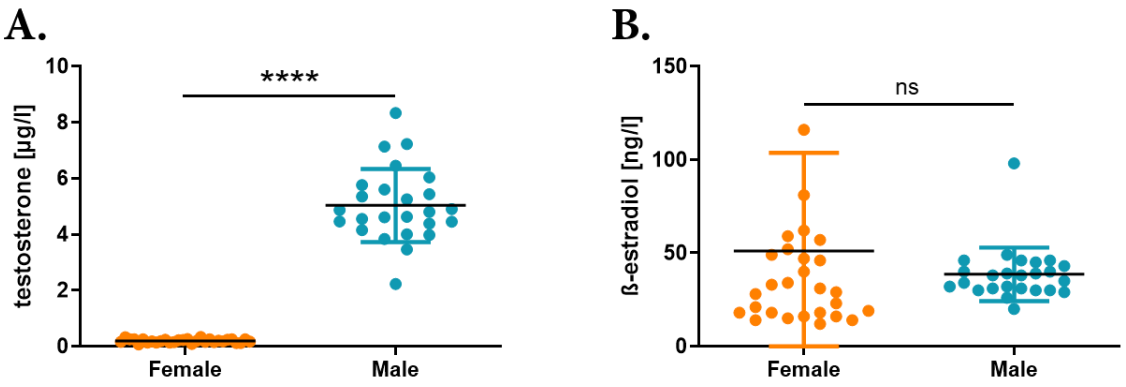

Figure 38. Testosterone levels between healthy males and females differ. A. Total serum testosterone in females and males. **B.** Serum ß-estradiol levels in females and males. An unpaired t-test was performed between males and females.

Female patients with PBC and AIH showed reduced levels of bioavailable testosterone compared to healthy controls. Moreover, in the *ex vivo* transgender samples, we found testosterone had an effect on T cells, which are thought to be involved in autoimmune liver diseases. Therefore, we investigated whether we could find altered TH1, TH17 and Treg frequencies and immune ratios in female AILD patients compared to healthy female age-matched controls. We found that female patients with PBC, AIH or an overlap of both showed a tendency for increased TH17 cells (Fig. 39B). Furthermore, these patients exhibited significantly increased TH1 cells (Fig. 39C). Thus, AILD patients had a tendency of increased ratios of TH1/Treg ($p = 0.19$) and TH17/Treg ($p = 0.15$) compared to healthy controls (Fig. 39D, E).

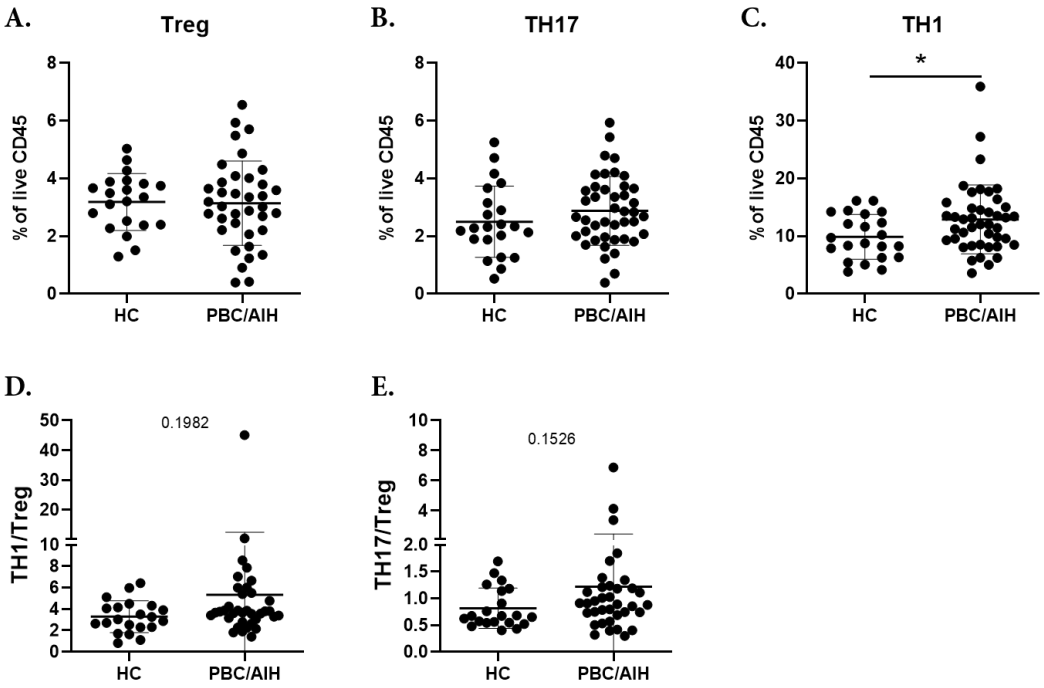

Figure 39. Immune ratios in female PBC and AIH patients tended to be elevated compared to healthy women. Frequencies of (**A**) Tregs, (**B**) TH17 cells, (**C**) TH1 cells from CD45 living cells in healthy female controls (HC) and female patients with PBC and AIH (PBC/AIH). **D.** TH1/Treg ratio based on the frequencies of TH1 and Treg cells of healthy female controls (HC) and patients with PBC or AIH (PBC/AIH). **E.** Same as in D but based on frequencies of TH17 and Treg cells. An unpaired t-test was performed between HC and PBC/AIH.

In general, we observed that female patients with AIH and PBC showed reduced levels of bioavailable testosterone compared to healthy controls. Furthermore, they showed tendencies of increased TH1/Treg and TH17/Treg ratios. We also found that after 6 months of a high dose testosterone treatment, patients from our trans men cohort had decreased TH1/Treg and Th17/Treg ratios. Therefore, higher testosterone levels could contribute to the protection of females from an increase in the proinflammatory TH1/Treg and Th17/Treg ratios observed in autoimmune diseases. Interestingly, cholangiocyte activation was diminished with supernatant from testosterone-treated T cells (not shown). This finding suggests that altered cholangiocyte activation could further contributes to the sex differences observed in autoimmune liver diseases, especially in PBC patients.

However, the lower testosterone levels found in PBC and AIH patients should be confirmed with a larger cohort. Moreover, studies should investigate whether these lower testosterone levels make women more vulnerable to autoimmunity or if they are a consequence of the disease. This could be achieved by including patients at the onset of the disease or at least after receiving the first diagnosis. In addition, other T cell subsets

affected by testosterone, such as CD8+ TEMRA cells, and their role in autoimmunity should be examined. The role of *GIMAP7* in autoimmunity and autoimmune liver diseases should also be investigated in future research.

4. Discussion

Autoimmune diseases are defined as diseases with immune responses directed against self-antigens in organs or tissues. The origin of many autoimmune diseases is not completely clear, but most are associated with alterations in genetic, epigenetic, environmental, or microbiota-related factors. In addition, many AIDs, including the autoimmune liver diseases AIH and PBC, are characterized by sex bias, with more females than males affected. The underlying mechanisms are unknown, but there is increasing evidence that androgens, especially testosterone, are an important modulator of immune cell differentiation and activation. However, most of the studies describing the effects of testosterone on T cells are not very thorough, and a deeper understanding of the *in vivo* effects of testosterone is lacking. In this thesis, we therefore aimed to investigate the effects of testosterone on T cell phenotypes and functions *in vivo* and *in vitro* and how these effects contribute to the pathogenesis of autoimmune liver diseases. Using our unique cohort from patients undergoing high doses of testosterone treatment, we defined T cell subsets and changes caused by testosterone through an in-depth analysis.

Androgens act by binding cytoplasmatic or membrane bound ARs, and the expression of different hormone receptors on immune cells and the cells that directly interact with them has been described previously[90-92,124,144]. However, detailed knowledge of specific immune cell types or of the expression of newly discovered membrane bound receptors such as ZIP9 in immune cells is lacking[145]. In this study, we were able to determine the expression of AR and ZIP9, currently known as the two most relevant androgen receptors, in all of our analyzed immune cell populations, including T cells, DCs and innate immune cells and cholangiocytes (Fig. 6; cholangiocytes not shown). Therefore, we confirmed that immune cells are inherently able to respond to testosterone. To investigate the effects of testosterone on immune cell activation, we analyzed the proliferative capacity of T cells upon stimulation in the presence of testosterone and did not find a clear effect on human PBMC and T cell proliferation upon testosterone treatment (see Fig. 7). These data are in contrast to several older studies that assumed androgens impact the proliferation of immune cells[146-148]. These studies have reported that androgens could impact immune cell activation and survival by androgen-dependent signaling during cell proliferation and apoptosis [149-152].

However, by combining deep flow cytometry-based immunophenotyping with an analysis of single cell levels in our unique cohort, we found that testosterone has an impact on anti- and proinflammatory immune cell subsets *in vivo*.

Using deep immunophenotyping, we observed an increase in immune regulatory cell subsets in trans men at 6 months of testosterone treatment compared to the baseline controls. Briefly, we observed an increase in Treg cells and identified an increase in different subsets of Tregs, such as CD73+ Tregs (Fig. 20). Regulatory T cells have been described as essential for immune cell homeostasis[15]. They mediate immune balance by suppressing effector T cell functions, a mechanism that is also mediated by the function of CD73[211]. The lack or insufficient functionality of regulatory T cells has been associated with the development of AID in humans and mice, highlighting the importance of these cell subsets. Thus, decreased levels of CD4+ CD25hi T cells associated with lower levels of Foxp3 and a decreased ability to inhibit cell proliferation *in vitro* have been found in patients with active AIH[153,154]. Similarly, reduced Tregs numbers, IL-10 levels and disrupted co-stimulation have been reported for PBC[155,156]. Our study revealed in increase in the Treg population and the upregulation of CD73, suggesting that treatment with testosterone directly or indirectly enhances Tregs and thereby leads to a more balanced immune environment. Importantly, these data are in accordance with other reports that have shown that androgens increased Treg numbers in mice[157] and humans[126]. Moreover, some studies have found differences in Treg frequencies between males and females *in vivo*[125,138].

The increase and stability of Tregs upon testosterone treatment could also be provided by other immune cell subsets. We found a significant reduction in BAFF expression on B cells (not shown), and it has been shown that the expression of BAFF on B cells is an important mediator of Treg apoptosis[158]. Of note, this downregulation was the only significant change we found in the B cell subsets. Interestingly, CD39+ expression on CD8+ T cells decreased after testosterone treatment (Fig. 29). In cancer studies, CD8+ T cells expressing CD39 have been identified as exhausted T cells[159].

In addition to affecting regulatory T cells, testosterone also had an impact on other T cell subsets. Other cells that were lower in the trans men at 6M belonged to the effector memory cells or were primarily a mixture of effector memory and TEMRA cells. The reduced T cells subsets were TH17, CD4+ CD161+ CD28+/-, CD8+ CD28+ CD57+

CD161+ and CD8+ CD39+ cells (Fig. 30). These cells probably show more of the classical proinflammatory phenotype due to their CD161, CD57 and CD28 expression[8]. TH17 cells, classified according to surface markers, were significantly reduced after 6 months of testosterone treatment (Fig. 22B*). In* vivo studies in mice have shown that testosterone attenuated IL-17 in the lung and liver[141,160]. Moreover, TH17 cells have been implicated in multiple human autoimmune diseases, such as rheumatoid arthritis and primary biliary cholangitis[161,162].

Some of the other proinflammatory populations, including TH1 cells, only showed a tendency to decrease (Fig. 22C). We calculated the ratios of TH1/Treg and Th17/Treg cells and found significantly reduced ratios in both groups upon testosterone treatment. This finding is important since TH1 cells have been strongly associated with the pathogenesis of AIDs. The hallmark cytokines of TH1 cells are TNFα and IFNγ. Both cytokines have been described as important mediators in autoimmune diseases. Bovensiepen et al. described increased frequencies of TNF and TNF/IFN double positive cells compared to age- and sex-matched healthy controls in patients with AIH[70]. In addition, increased expression of IFN in other autoimmune diseases such as MS has been suggested[163-165]. Interestingly, it has been shown that androgen stimulation reduces the expression of TH1 cytokines in murine-derived T cells[123,137]. These findings nicely link to our observation of *in vitro* assays, where we detected a reduction in TNFα secretion of whole PBMCs upon stimulation and testosterone treatment (Fig. 8). T cells are the most abundant cells in PBMCs[166] and are strong producers of TNFα, and we observed reduced secretion of TNFα and IFNγ from human-derived T cells upon testosterone treatment *in vitro* (Fig. 9). However, we cannot exclude the effects of testosterone in PBMCs on other cells such as monocytes or macrophages[167], which need to be further examined[92,148,168].

Importantly, the striking difference in T cell responsiveness upon testosterone treatment occurs between male- and female-derived T cells. Here, only female-derived T cells showed a significantly reduced release of TNFα and IFNγ upon T cell receptor specific stimulation in the presence of testosterone (Fig. 9). This result could be due to the slightly higher expression of TNFα and IFNγ in female-derived cells or because male-derived cells are more acclimated to higher testosterone levels *in vivo* and therefore less susceptible *in vitro*. Moreover, this finding underlines the importance of further investigating the influence of testosterone on the immune system and autoimmunity in regard to sex chromosomes. In this thesis, we focused on the influence of testosterone on females with

XX chromosomes and can therefore conclude that our findings do not come from XX/XY differences. However, factors such as X chromosome inactivation probably play a role in autoimmune diseases (see Introduction).

In addition to considering X chromosomal effects, the effect of testosterone conversion to estrogen *in vitro* has to be investigated. We therefore analyzed the expression of the aromatase enzyme, which is responsible for converting testosterone to estrogen. We did not detect an increase upon *in vitro* testosterone stimulation, and we therefore exclude the possibility that conversion to estrogen is responsible for the observed effects. A treatment of DHT instead of testosterone could further confirm these data since this derivate cannot be further converted. However, *in vitro* treatment with DHT is known to be difficult since efficiency and stability are strongly affected upon storage, leading to a quick loss of function.

Our deep immunophenotyping analysis revealed that other T cells were changed upon testosterone treatment. Some memory cells were enhanced, including CD8+ CD44high and CD4 memory CD28+ CD272+ (Fig. 29I, K). The glycoprotein CD44 is thought to be involved in T cell migration, adhesion and proliferation[169]. CD8+ CD44high T cells are mainly memory T cells, while gradient-like lower CD44 expression can be found on effector or naïve T cells[17]. They are often associated with tissue residency and can function as a receptor for HUA, found on endothelial cells, and other components of the extracellular matrix[17]. Interestingly, *in vitro* TCR-stimulated CD44high CD8+ mice T cells have been found to express lower levels of T-bet and higher levels of IFNγ than CD44low CD8+ cells[170]. CD272 (BTLA) is a co-inhibitory receptor on T cells belonging to the CD28 immunoglobulin superfamily[171]. Its expression decreases with T cell activation, and its activation reduced IFNγ and IL-10 production in T cells *in vitro*[171]. BTLA signaling has been shown to be altered in the autoimmune disease systemic lupus erythematosus[172,173]. Apart from these findings, it is unclear what role these cells play in autoimmune diseases, especially in autoimmune liver diseases, and what consequences the enhancement of such cells has. Based on the current literature, a more proinflammatory milieu would be expected from an increase of these cells. To date, no connection between CD44 or CD272 (BTLA) and testosterone in T cells has been found. In regard to CD44, some connections between androgens and breast cancer cells have been observed[174,175].

In addition to noting changes in memory T cells, we identified two T cell subsets, one naïve CD4+, CD25+, CD44+, CD49a+, CD49b+ and one naïve CD4, CD8 double positive, CD25+ CD44+ T cell subsets that were suppressed by testosterone (Fig. 26F, G). CD44 is often seen in connection with tissue residency within this CD4+ naïve population. This tissue-resident phenotype is strengthened by the expression of CD49a and CD49b (Table 1). Thus, naïve cells with homing markers seem to manifest in a tissue niche. The role of naïve tissue resident cells in autoimmune diseases is largely unknown. However, Poch et al. recently found naïve-like T cells with a tissue-resident phenotype in livers with PSC, which were more prone to TH17 cells[176]. A reduction of such cells could therefore be beneficial for autoimmunity. How testosterone might influence naïve-like T cells and tissue residency should be further investigated.

In addition to CD4+ T cells, CD8+ T cells and invariant T cells are thought to play a role in AILDs such as AIH[177]. We observed higher frequencies of TEMRA cells after testosterone treatment, which were mainly CD8+ T cells, though some CD4+ cells were present (Fig. 18, 19). Moreover, with the addition of single-cell sequencing (CITE-Seq), we could further specify that a distinct CD8 TEMRA cluster was increased (Fig. 32B). Interestingly, this population is CD57+ and CD28- (Fig. 31). CD8+ TEMRA T cells have been described as mainly CD27 and CD28 negative, which are often connected with the impairment of T cell functioning. The loss of CD28 expression in particular has been linked with telomere loss, reduced proliferative capacity and increased senescence[178,179]. Furthermore, TEMRA cells are often described as KLRG1 and CD57 positive, and together with PD-1, they are implicated in replicative senescence[178,180-182]. TEMRA cells have also been associated with strong cytokine production (Granzyme B, IFNγ, and TNFα) and a high cytotoxicity[183,184]. Similar findings have been reported on CD4+ TEMRA cells, though the authors suggested that senescence was reversible in these cells[185]. Others have described subpopulations of CD4+ TEMRA cells with different functions[186]. Compared to CD8+ TEMRA cells, the CD4+ subset is low in the peripheral blood, which might prevent a clear separation in the CITE-Seq data (Fig. 31).

Research has primarily described the phenotype of TEMRA cells as highly cytotoxic, which is contrary to the immune suppressive effects of testosterone described to date. However, studies have also indicated that TERMA cells have immunoprotective and regulatory roles[178,187]. It is also likely that there are subpopulations of TEMRA cells, and their function *in vivo* remains to be determined. Moreover, the simplistic view that the immune

system contains several proinflammatory T cells, such as TH17 cells, and fewer anti-inflammatory T cells, such as Tregs, might be too narrow. A balanced immune system that also contains cytotoxic T cells to keep the immune system in check is probably required for the long-term prevention of autoimmune diseases. In addition to the classic TH17, TH1 and Tregs, TEMRA cells could play an important role in autoimmunity.

Of note, anti-TNF immunotherapy has been shown to reduce CD8+ TEMRA cells; this TNF therapy has recently been explored in multiple studies on autoimmune diseases[188]. However, a successful therapy for MS with the immunomodulator FTY720 led to a relative increase of TEMRA cells, suggesting the beneficial role of TEMRA cells in this disease[189].

The analysis of gene expression on a single cell level (CITE-Seq data) confirmed some of our findings from our *in vitro* and *ex vivo* data, and we identified several other markers. The advantage of the Seq data is that it allows for a deeper analysis and classification of the T cell subsets due to the additional RNA information it provides, and changes in RNA expression across different subsets can be investigated. Moreover, further analyses, such as analyzing the interactome by examining the receptor ligand expression in the clusters, would be possible with this sequencing data[190]. The differences between the deep flow cytometry-based immunophenotyping and CITE-Seq data could be related to differences in group sizes and the time of data acquisition. Flow cytometry data are based on at least 10 different subjects, while four individuals were chosen for the CITE-Seq analysis. There are intra-individual differences in human cohorts that can only be limited by increasing the number of subjects.

Overall, we found that two T cell subsets increased in all four individuals after testosterone treatment: a CD4 naïve cluster and the previously discussed CD8 TEMRA cluster (Fig. 32B). The naïve CD4 cells did not increase in general, but through the addition of RNA sequencing, the naïve CD4 T cells could be split into further subsets, one of which increased. In the flow cytometry data, the naïve CD4 T cells were not significantly enhanced through testosterone treatment. However, the deeper classification of the naïve subcluster through their RNA profiles, as in the CITE-Seq experiment, was not possible. Our data showed an increase in one naïve CD4 T cell cluster and a decrease in another. Though the flow cytometry data revealed only a significantly decreased subset of naïve CD4+ T cells, overall, the naïve CD4 T cells showed a tendency to increase (Fig. 18G; $p = 0.0869$). Therefore, it is likely that with additional markers, the flow cytometry could also

detect an increase in one naïve population. Furthermore, the expression of CCR7, a naïve and CM marker, increased upon testosterone treatment in the naïve and naïve-like CD4 clusters (Fig. 34B). This increase could ensure that the cells remain in the naïve state. Since the simultaneous sequencing of surface protein expression and RNA expression allowed us to define these T cells subsets, we were able to find altered gene expression not only in naïve T cells but in all of the clusters.

Most strikingly, we found a significant upregulation of *GIMAP7* in almost all T cell subsets after testosterone treatment (Fig. 35A). GIMAP7 is a small GTPase belonging to the immune-associated nucleotide family[191]. Members of the GIMAP family, such as GIMAP3, 5 and 1, have been found to be involved in the development and proliferation of mature and immature T cells and have been further linked to normal liver functions[192-197]. The role of GIMAP7 in T cells is largely unknown, and to date, research has only described a higher *GIMAP7* expression in T lymphocytes than in B lymphocytes in mice[198]. However, we confirmed *GIMPA7* upregulation in our *in vitro* stimulated T cells (Fig. 36), a finding that supports the essential functional role of GIMAP7 in T cells upon testosterone treatment.

In addition to *GIMAP7*, also other genes were differentially regulated after testosterone treatment in more than one cluster. We observed the downregulation of *FOS* and *DUSP1*, and *JUNB* was upregulated in some clusters (Fig. 34). Interestingly, in *in vitro* bulk T cells, *JUNB* was downregulated after testosterone treatment (Fig. 36). The role of JUNB activation on T cell activation and function has been previously described. An increased JUNB activation upon the TCR stimulation of T cells has been associated with the differentiation of T cells into TH2 and TH17 cells[199-203]. In addition, JUNB has been reported to be involved in Treg activation and its ability to suppress effector T cells[204]. Notably, JUNB-deficient mice are resistant to the induction of EAE, but mice lacking JUNB in T cells have been shown to display a disrupted Treg development and a higher susceptibility to colitis[205,206]. Mechanistically, JUNB can form a heterodimer with FOS to produce the AP-1 transcription factor, which is involved in various T cell functions and differentiations[207,208]. Dual-specificity phosphatases (DUSPs) are involved in different T cells signaling mechanisms, and mice lacking DUSP1 also display resistance to EAE induction and a disrupted T cell immune response[209]. To date, there are no clear data on the effects of testosterone on JUNB, FOS or DUSP1 activation in human-derived T cells. However, there is one study from the breast tissue of FTM individuals that showed an

increased expression of *JUNB* and *FOS* upon testosterone treatment[210]. Therefore, the consequences of changes in the expression of *JUNB*, *FOS* and *DUSP1* in specific T cell subsets should be investigated. However, more importantly, the consequences of enhanced *GIMAP7* expression due to the effects of testosterone treatment on different T cell subsets and T cells overall should be examined. A knockout or knockdown of *GIMAP7* in different T cell populations could help decipher the mechanistic outcomes for T cell function and differentiation.

We also observed differences in the abundancy of the TEMRA CD8+ subcluster upon testosterone treatment. Therefore, we recommend a further analysis to determine the effects of this subcluster and its contribution to the overall inhibitory effects of testosterone or whether it functions as a counter mechanism.

While only a few genes were affected in the TH and TC subsets, invariant γδ T cells and MAITs showed a high number of altered genes upon testosterone treatment (Fig. 34A), even though we only detected tendencies for frequency changes (Fig. 32B). MAITs and γδ T cells have been implicated in autoimmunity and especially in autoimmune liver diseases. In patients with PBC, circulating MAITs were decreased but showed a higher activation status, and hepatic MAITs were increased compared to healthy controls[211]. Ursodeoxycholic acid treatment reduced the differences in circulating MAITs[211]. In liver tissues from metastatic liver tumors reduced MAIT frequencies compared to controls with no chronic liver diseases were found[212]. Another study found reduced frequencies of MAITs in the peripheral blood and liver tissue of patients with autoimmune liver diseases (AIH, PBC, PSC) compared to controls[213]. Furthermore, AILD MAITs showed signs of exhaustion[213]. A study investigating Vδ1 T cells of the γδ T cells found higher numbers than in age-matched controls[214]. An older study also found increased γδ T cells in the peripheral blood and portal areas of the liver in patients with AILDs compared to controls[215]. The problem with these data is that they mostly originate from patients with AILDs that have already manifested; therefore, researchers can only speculate on the initial state of T cells at disease onset. Moreover, the effects of these increased and decreased subsets are unknown. It has been speculated that γδ T cells have pathogenic as well as protective functions depending on the subset of γδ T cells[216,217]. Currently, there is no clear data on the effects of testosterone on human MAIT or γδ T cells. One older study using a B1.Tg.Ealpa mice model with a coxsackievirus B3 infection showed increased γδ T cells after testosterone application[218], and some sex differences in human MAIT cells

were found. For example, the researchers observed reduced MAITs in the livers of male but not female obese mice[219]. Interestingly, a recent preprint study on COVID-19 patients showed a female-specific protective MAIT profile[220]. Therefore, it is possible that the increased activity of MAITs or γδ T cells through testosterone treatment are beneficial to autoimmunity.

In summary, we propose that testosterone does not lead to an overall suppression of T cells nor to the differentiation of a more proinflammatory phenotype. Testosterone seems to balance immune system functions, shielding men from autoimmunity and making them more susceptible to infections. Testosterone influences different T cell subsets to create a balanced microenvironment in favor of immune tolerance. In keeping with this finding, testosterone leads to a reduction of proinflammatory T cells, such as effector memory CD161+ T cells and TH17 cells, and proinflammatory cytokines from T cells including TNFα and IFNγ. In addition, regulatory cells such as Tregs were enhanced, and ratios of TH1/Treg and Th17/Treg were significantly lower after 6 months of testosterone treatment. However, our data also suggest that excessive testosterone could cause contradictory outcomes. TEMRA T cells, which are thought to be proinflammatory, were also upregulated. Moreover, the RNA activity of invariant γδ T cells and MAITs was greatly changed upon testosterone treatment, probably leading to a higher activity. In addition, the effects of testosterone on T cells are likely altered by inflamed tissue. Overall, the combination of single-cell flow cytometry and RNA sequencing allowed us to identify various changes in T cells subsets upon testosterone treatment, as Figure 40 illustrates.

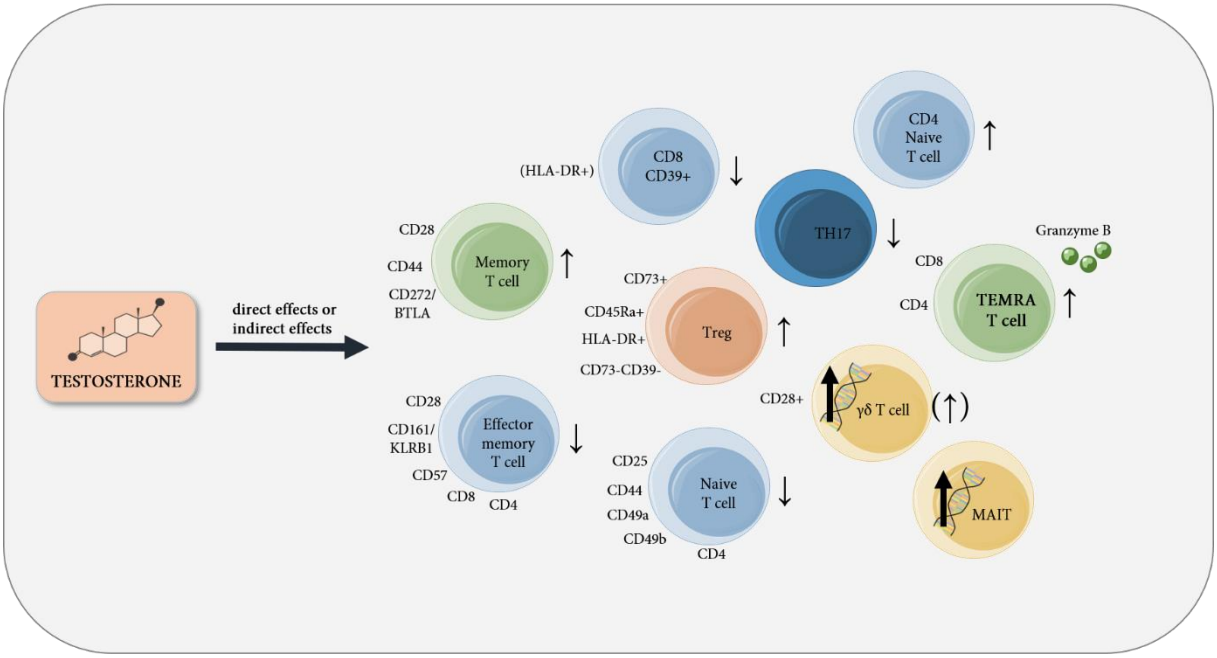

Figure 40. Schematic summary of changes in peripheral female T cells subsets upon 6 months of testosterone treatment.

In a translational approach to studying the impact of testosterone on autoimmunity, we investigated patients with the autoimmune liver diseases PBC and AIH. Notably, we found that in women with PBC and AIH, the serum bioavailable testosterone levels were lower than in healthy age-matched controls (Fig. 37A). This finding further supports the idea that testosterone plays a protective role in the context of autoimmunity. In addition, this finding suggests that the level of testosterone is likely crucial, and a specific beneficial range of testosterone in women and men exists in regard to autoimmunity. This balance is very important, as amounts that are too high likely make the immune system more vulnerable to outside attacks, such as infection, which is possibly exemplified by higher mortality rates of males with COVID-19[221,222]. We did not find different levels of testosterone in men with PBC and AIH compared to healthy controls (Fig. 38A). However, we also faced the difficulties associated with analyzing a diverse male patient group regarding age and medication. To better evaluate whether hormone levels differ between male AILD patients and controls, we would need a larger number of patients divided into subgroups based on age to correct for this limitation.

Both TH1 and TH17 cells have been implicated in several autoimmune diseases. Moreover, in our data of female patients with the autoimmune liver diseases PBC and AIH, we found a significant increase of TH1 cells, which supports the data previously described

from Bovensiepen et al.'s study[70]. In addition, AIH and PBC patients showed a tendency for increased immune balance TH1/Treg and TH17/Treg ratios compared to healthy controls (Fig. 40).

Since we found decreases of these parameters upon testosterone treatment in our transgender cohort, we suggest that testosterone plays a part in the pathogenesis of the autoimmune liver diseases AIH and PBC. Whether the observed low levels of testosterone and the increase in TH17/Treg and TH1/Treg ratios in female AILDs patients contribute to the cause of these diseases or only their progression should be evaluated. The results of these peripheral T cell changes should be compared to changes in the local liver niche, which could be possible with the use of rare liver biopsies. To further strengthen the overall link between the transgender patient data and autoimmune diseases, additional research is needed. For example, the investigation of liver tissue T cells from the transgender cohort would be interesting, though it is not possible. However, the measurement of hormones in autoimmune liver diseases should be repeated with a second cohort, and the role of other immune cells found in the trans men cohort, such as TEMRA, MAIT and γδ T cells, should be investigated in relation to these diseases. Additionally, other know aspects of autoimmune liver diseases such as the microbiome should be explored since it is already known that the AILD microbiome differs from the healthy microbiome and can influence T cells[223,224]. Interestingly, it has been reported that testosterone levels can be influenced by the microbiome[40], and therefore examining the interaction of the microbiome, testosterone and T cells would add another layer to our understanding of sex differences in autoimmunity.

Overall, the knowledge we obtained in this thesis will help us further understand the differences in immune cell responses between men and women and why women are more prone to develop autoimmune diseases.

4.1. Final conclusion

In summary, testosterone enhances and suppresses different types of T cell subsets. Testosterone treatment led to increased CD8+ TEMRA and Treg cell numbers and suppressed effector memory T cells such as TH17 cells. These effects might lead to a more balanced immune system that promotes anti-inflammation, which is less likely to drive autoimmune responses and could be part of the reason why males are less likely to develop autoimmune diseases. In combination with local niches such as the liver, which have cells especially sensitive to this altered T cell milieu, including cholangiocytes, this could lead to an even higher female predominance in autoimmune liver diseases such as PBC. Moreover, the hormone measurements of autoimmune liver disease patients showed lower testosterone levels in female patients compared to age-matched controls, which could suggest that these women are even more vulnerable to autoimmune attack and manifestation than other women with higher testosterone levels. If this is part of the cause or evolves during disease progression should be further investigated.

5. Material and Methods

5.1. Methods

5.1.1. Patient selection and sample collection

Blood, serum and PAXgene samples of female-to-male (FTM) patients and AIH, PBC and healthy controls were collected and tested in this study. Liver explant tissue from transplantation was used to isolate primary cholangiocytes. Disease diagnosis and other relevant parameters are summarized in Tables 3 and 4. FTM samples were collected before the start of hormone replacement therapy (HRT) and 3 and 6 months after treatment began. The deviations and specific time points of blood collection are shown in Table 3. To meet the inclusion criteria for recruitment, female AIH and PBC patients ages 40–65 had to have non-cirrhotic livers and normal bilirubin levels and receive treatment with less than 7.5 mg prednisolone per day. Male AIH and PBC patients were recruited independently of their age, disease severity and medication state due to the low number of patients. Additional parameters that could be relevant for hormone status were evaluated and are summarized in Table 4. All AIH and PBC patients were recruited from the specialized outpatient clinic of the I. Department of Medicine at the UKE (University Medical Centre Hamburg Eppendorf). Healthy donors were carefully selected based on age and sex, and additional parameters were evaluated; these details are summarized in Table 4.

All donors included in this study provided written informed consent, the study received local ethics approval (PV5982, PV4081, PV5473).

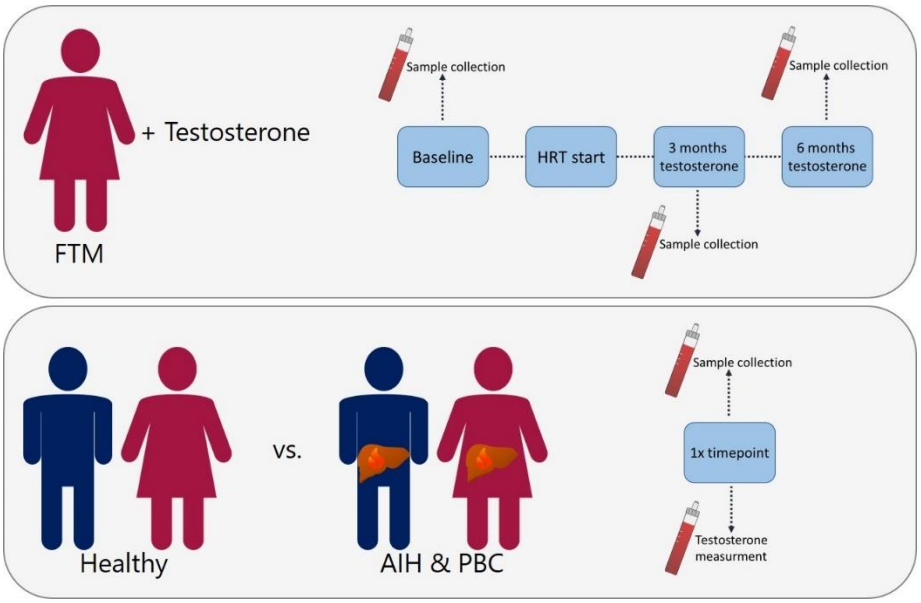

Figure 41. Schematic representation of the sample collection of the FTM probands and the AIH and PBC patient cohort as well as healthy controls.

5.1.2. Cell isolation from whole blood

Peripheral blood mononuclear cells (PBMCs) were isolated from EDTA blood tubes. Blood was diluted with PBS and overlaid on Biocoll solution in order to separate the blood components based on their size and granularity by density gradient centrifugation (20 min, 400 g, acceleration 1, brake 0). The resulting PBMC layer was removed using a Pasteur pipette, and the cells were washed twice with PBS (5 min, 400g, acceleration 9, brakes 9). After counting (using the Neubauer-Zählkammer), cells were ready for further processing. For this study, cells were either frozen in freezing media for long-term storage (6-10x10^6 cells in 1ml 10%DMSO/90% FCS) or used directly for *in vitro* experiments (see sections 5.1.4. and 5.1.5.).

5.1.3. Magnetic activated cell sorting

For the T cell *in vitro* experiments, untouched T cells were isolated from PBMCs using the Pan T Cell Isolation Kit according to the manufacturer's instructions. After separation by magnetic activated cell sorting (MACS), cells were counted and used for *in vitro* experiments (see section 5.1.5.). Additionally, for the RNA analysis of different immune cell populations, the Pan Monocyte Isolation Kit, Pan-DC Enrichment Kit and CD4 and CD8 Microbeads Kits were used according to manufacturer's protocols to isolate respective

populations from PBMCs. For RNA isolation, all cell populations were directly resuspended in lysis buffer from the RNA kit following isolation (see section 5.1.10.).

5.1.4. *In vitro* stimulation of PBMCs and T cells with and without androgens

For unspecific *in vitro* cytokine stimulation assays, PBMCs were stimulated with PMA/ionomycin (50 ng/ml PMA/ 1µg/ml ionomycin) or LPS (100 ng/ml) using 96 uncoated suspension cell culture plates for 4 hours after hormone stimulation for 24 hours. For T cell receptor specific activation (aCD3/CD28), cells were stimulated with coated anti-CD3 (2 µg/ml) (min. 1h, 37°C) and soluble anti-CD28 (2 µg/ml) for 24 hours parallel to hormone stimulation. Then, 300,000 cells/200µl/well were seeded in lymphocyte media (Table 9). To perform the hormone stimulation, we added testosterone in the given amounts (0.5–500 ng/ml). A stock solution of testosterone was dissolved in ethanol and then further diluted in lymphocyte media, not exceeding 0.015 % of the final ethanol concentration. To make the ethanol control (EC), we added an amount of ethanol equal to the highest concentration. Dihydrotestosterone (DHT) stock was dissolved in methanol (MeOH) and diluted in lymphocyte media to achieve the final concentration and added to the cells in the given concentrations (0.3–30 ng/ml). Controls (MC) were given the same amount of MeOH as the highest concentration, equal to 0.0003% of the final MeOH concentration. Cells were incubated for 24 hours in the incubator (37°C, 5% CO2). For the cytokine analysis, the supernatant was harvested and frozen at -20°C. To conduct the RNA analysis, we pooled the remaining cells of at least two wells with the same conditions and then resuspended cell pellets in 350µl of RNA lysis puffer (RA1) and froze them at either -20°C or -80°C.

5.1.5. ELISA

The analysis of cytokines from serum and supernatant was done using a sandwich ELISA for single cytokine analysis (TNFα, IFNγ, IL-6, IL-8, CCL20 and CCL2; see Table 11). The ELISAs were performed according to the manufacturer's instructions, and the supernatant was diluted according to the expected cytokine levels, from undiluted up to

a 1:20 dilution. The absorption was measured on the Tecan microplate reader for the ELISAs.

5.1.6. Flow cytometry staining of whole blood

Fresh heparinized blood was stained the day after blood collection for equal processing across all of the samples. For the analysis of surface markers, we used previously established staining panels for innate cells, B cells and subsets of T cells (T cell I, T cell II and Treg). Antibodies were mixed in staining cocktails, as explained in Table 2. Next, 50 µl of the respective master mix cocktails were added to a 5 ml flow cytometry tube (FACS tube). We then added 100 µl of whole heparinized blood, which was gently vortexed and incubated for 30 min at room temperature (RT) in the dark. Afterwards, 1ml of lysing buffer (RBC lysis 1:10 H_2O) was added, vortexed and incubated for 10 min at RT in the dark. Then, samples were washed twice with PBS (5 min, 400 g) and the supernatant was removed. Finally, samples were resuspended in 180 µl of FACS buffer and stored at 4°C in the dark until they were measured using the flow cytometer BD™ LSR Fortessa.

The stimulation panels were processed as follows (T ICC, Mono ICC). Staining cocktails were prepared (see Table 2), and the master mixes for stimulation contained 50 µL X-vivo, 0.5 µL PMA (final: 250 ng/ml) and 1 µL ionomycin (final: 5µg/ml) for each T ICC tube and 50 µL X-vivo and 1 µL LPS (final: 2.5 µg/ml) for each Mono ICC tube. An unstimulated control for T ICC and Mono ICC was prepared with only 50 µl X-vivo. Master mixes were mixed with 100 µl of whole blood in a FACS tube, gently vortexed and incubated for 30 min at 37°C. Then, inhibition mixes were added, containing 50 µl X-vivo and 0.7µl Brefeldin A, and the Mono ICC tubes additionally contained 0.2 µl Monensin for each sample. Samples were then incubated for 4.5h at 37°C. Afterwards, the staining surface cocktails (only surface antigens) were added, gently vortex and incubated for 30 min at RT in the dark. Then, cells were lysed and fixed with 1ml lysis buffer for 10 min at RT in the dark. Again, they were washed twice with PBS (5 min, 400 g), then resuspended in 50 µl of saponin buffer and incubated for 5 min at RT in the dark. Afterwards, the cytokine staining cocktail (cytokine antigens and CD4) was added, gently vortexed and incubated for 30 min at RT in the dark. Cells were washed once with PBS (400 g, 5 min), resuspended in 180 µl of FACS buffer and stored at 4°C in the dark until the measurements were taken with the BD™ LSR Fortessa.

Table 2. Staining cocktails (antibodies listed in Table 7)

Panel I: Tcell I	
Fluorochrome	antigen
BV421	CD272
BV510	CD8
BV605	CD279
BV650	CD3
BV711	CD45Ra
BV785	CD45
FITC	-
PerCP-Cy5.5	CD160
PE	CD161
PE-Texas	CD57
PE-Cy7	CD28
APC	CD197
AF700	CD4
APC-Cy7	L/D

Panel II: Tcell II	
Fluorochrome	antigen
BV421	CD25
BV510	CD62L
BV605	CD103
BV650	CD3
BV711	CD45Ra
BV785	CD45
FITC	CD49b
PerCP-Cy5.5	CD69
PE	CD44
PE-Texas	CD4
PE-Cy7	CD49a
APC	LAG-3
AF700	CD8a
APC-Cy7	L/D

Panel III: Treg	
Fluorochrome	antigen
BV421	CD25
BV510	CD8
BV605	-
BV650	CD127
BV711	CD45Ra
BV785	CD45
FITC	HLA-DR
PerCP-Cy5.5	CD3
PE	CD73
PE-Texas	-
PE-Cy7	CD39
APC	-
AF700	CD4
APC-Cy7	L/D

Panel IV: T ICC	
Fluorochrome	antigen
BV421	CD56
BV510	L/D
BV605	-
BV650	TNFa
BV711	IL17A
BV785	CD45
FITC	Granzyme B
PerCP-Cy5.5	CD3
PE	IL10
PE-Texas	CD4
PE-Cy7	IL4
APC	FoxP3
AF700	CD8; CD20
APC-Cy7	IFNg

Panel V: Mono ICC	
Fluorochrome	antigen
BV421	IL1ß
BV510	L/D
BV605	-
BV650	TNFa
BV711	CD14
BV785	CD45
FITC	IL8
PerCP-Cy5.5	IL12p40
PE	IL10
PE-Texas	-
PE-Cy7	-
APC	IL6
AF700	-
APC-Cy7	CD16

Panel VI: Bcells	
Fluorochrome	antigen
BV421	CD20
BV510	L/D
BV605	-
BV650	-
BV711	-
BV785	CD45
FITC	CD38
PerCP-Cy5.5	CD24
PE	sIgD
PE-Texas	CD19
PE-Cy7	CD43
APC	CD268
AF700	-
APC-Cy7	CD27

Panel VII: Subsets	
Fluorochrome	antigen
BV421	CD56
BV510	L/D
BV605	CD16
BV650	-
BV711	CD14
BV785	CD45
FITC	HLA-DR
PerCP-Cy5.5	CD3
PE	-
PE-Texas	CD11c
PE-Cy7	CD123
APC	-
AF700	CD20
APC-Cy7	CD1c

Panel VIII: CCRs	
Fluorochrome	antigen
BV421	CD56
BV500	L/D
BV605	CD161
BV650	CD3
BV711	CD183/CXCR3
BV785	CD45
FITC	Integrin-β7
PerCP-Cy5.5	CD196/CCR6
PE	CD49d/Integrin-α4
PE-Texas Red	CD8
PE-Cy7	CD194/CCR4
APC	CD199/CCR9
AF700	CD4
APC-Cy7	CD16

5.1.7. Cell isolation from livers

Liver pieces from explant liver tissue were stored in RPMI with 5% FCS and 1% P/S at 4°C until processing. For cell isolation, liver explant tissue was cut into very small pieces with a scalpel or surgery scissors in a petri dish. Then, the tissue was digested with collagenase. We used approximately 10 ml GBSS with 0.01 g collagenase solution for 20 min in a 50 ml falcon tube in a 37°C water bath. Following digestion, the liver tissue was passed through a 100 µm cell strainer. Afterwards, samples were centrifuged twice for 4 min with 40 g to removed hepatocytes, and the supernatant was transferred into a new 50 ml falcon. The supernatant was then centrifuged for 7 min at 400 g. Next, the supernatant was removed, and the cell pellet was washed twice with PBS (400g, 5min). Cells were resuspended in approximately 500 µl of MACS buffer and stained with 10 µl of EpCAM-APC antibody for 10 min at 4°C in the dark. Afterwards, cells were washed twice with 2 ml of MACS buffer (400 g, 5 min) and resuspended in approximately 80 µl of MACS buffer and 20µl of a-APC microbeads. After incubation for 15 min at 4°C in the dark, cells were washed again and resuspended in 1 ml of MACS buffer. Then, EpCAM positive cells were isolated using an LS MACS column following the manufacturer's protocol but with an additional pre-separation filter (30µm) on the columns. Flow-through and MACS-separated cells were seeded in primary cholangiocyte media (see Table 9) into 24-well plates, which were precoated with collagen (1:2 with H2O) for at least 1 h at 37°C and then washed with PBS.

The media was changed the next day, and cell growth was observed daily until 80% confluency was reached. Next, cells were trypsinized and transferred to a T25 flask for further growth until 80% confluency was reached again and then finally transferred into T75 flask for expansion. Upon reaching confluency, cholangiocyte cells were harvested for long-term storage or to be used in the experiments.

5.1.8. Charcoal stripping of FCS

To avoid hormone enrichment, charcoal stripped FCS (DCC-FCS) was used in *in vitro* experiments instead of normal FCS. Therefore, approximately 2 g of dextran-coated charcoal was added to 100 ml of FCS and mixed gently without a stir bar on a shaker overnight at 4°C. The solution was then centrifuged for 15 min at 2000 rpm, the supernatant was filtered, and the charcoal stripped FCS was aliquoted and stored at -20°C.

5.1.9. RNA isolation, cDNA and qPCR

Total RNA was isolated from tissues or cells using the Nucleospin RNA Kit. Samples were taken according to the manufacturer's protocols. Isolated cells and mechanically disrupted tissue were resuspended with RNA lysis buffer (RA1) with the addition of β-mercaptoethanol. Following RNA isolation, 1 µg cDNA was transcribed using the High Capacity cDNA Reverse Transcription Kit according to the manufacturer's instructions. For the gene expression analysis, qPCRs were performed with TaqMan™ Gene Expression Assays and TaqMan™ Fast Advanced Master Mix. The primer probes and catalogue numbers are summarized in Table 8. Afterwards, the relative expression was calculated using the ΔCt method with the equation:

$$\Delta Ct = Ct\,\text{Hprt} - Ct\,target\,gene$$

$$x - fold\,expression = 2^{-\Delta Ct}$$

To isolated RNA directly from the PAXgene blood collection tubes, the PAXgene Blood RNA Kit was used as described by the manufacturers.

5.1.10. Blood parameter and hormone analysis

To perform the differential blood count of human samples, we analyzed small EDTA-blood collection tubes after blood was drawn at the clinical chemistry department of the UKE.

For the detection of hormone levels (estrogen, testosterone, SHGB and albumin), frozen serum samples were either analyzed via clinical chemistry or alternatively, the total testosterone level was measured with a human testosterone ELISA (Table 11). The instructions of the manufacturers were strictly followed. Free and bioavailable testosterone levels were calculated with the calculator from the University Hospital of Ghent[225] according to the equation of Vermeulen[226].

5.1.11. Proliferation analysis with PrestoBlue™ and CellTrace™

The proliferation of immune and H69 cells were analyzed with the PrestoBlue™ assay. In brief, cells were seeded in 96 well plates and cultured for 24, 48, 72 and 96 hours (see section 5.1.9). The PrestoBlue™ assay was performed following the manufacturer's protocol. Thus, 10 µl of PrestoBlue per 100 µl of medium were added after cell growth and incubated until a visible color change occurred. The absorption of the plates was measured at 560 nm using 600 nm as a reference wavelength.

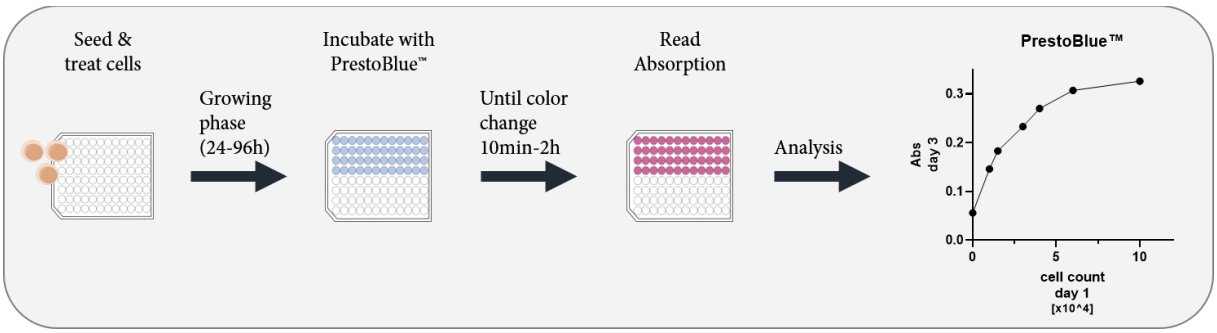

Figure 42. Schematic representation of the proliferation assay with PrestoBlue™.

Additionally, the proliferation of lymphocytes was analyzed with CellTrace™. Lymphocyte proliferation was detected by flow cytometry analysis using intracellular CellTrace™ staining. Before seeding, cells were suspended in PBS at a concentration of $1x10^7$ cells/ml and stained with 1 µl of 1:1000 diluted CellTrace™ per ml. Cells were incubated for 20 min at 37°C. The staining process was stopped by adding 5 times the amount of medium

containing FCS. Cells were incubated for 5 min and washed twice with the medium. Afterwards, cells were seeded and treated as with the T cell receptor specific stimulation described above (2µg/ml aCD3/CD28) and IL-2 (100U/ml) (see section 5.1.4). After the proliferation experiment concluded (4 days), cells were harvested and measured with the BD™ LSR II in the DAPI channel.

5.1.12. Single-cell Cite-Seq experiments

The Cite-Seq experiments used samples from four subjects from the FTM cohort (see Table 3) at both BL and 6M after beginning testosterone therapy (mean age = 23.7; testosterone injection). All materials used for cell thawing and sorting were coated overnight with the MACS buffer. Frozen PBMCs were briefly thawed at 37°C in a water bath and quickly transferred into 10 times the amount of the pre-warmed medium (PRMI Glutamax + 10% FCS) to remove the cell toxic DMSO contained in the freezing medium. From this point on, cells were kept at 4°C on ice. Cells were washed with the medium and counted. Next, cells were stained with L/D-PaCO, L/D-APC-Cy7, aCD3-BV650 and the Cite-Seq antibody cocktail (all 20 TotalSeqC antibodies listed in Table 5) for 30 min at 4°C and then washed with MACS buffer and centrifuged at 400 g for 5 min. The cell pellet was resuspended in 400 µl of MACS buffer, and cells were transferred into a FACS tube with a pre-separation filter (30 µm). Approximately 200,000 live CD3 positive cells were sorted with the BD™ Aria Fusion into reaction tubes filled with 500 µl of medium with a flow rate of 1. Cells were counted, and approximately 15,000 cells were used for further analysis. Then, single-cell libraries for ADTs, RNA and TCR were made according to the manufacturer's protocol with the 10x Chromium Next GEM Single Cell 5' Library and Gel Bead Kit v1.1 in cooperation with Jenny Krause from the lab AG Gagliani.

Libraries were pooled as follows: the eight CITE(AB) and eight GEX(RNA) libraries were pooled together with a concentration of 2 nM each at a ratio of 1:6, and all TCR libraries were pooled together at a concentration of 2 nM. Libraries were frozen and later sent to sequencing. Sequencing was done at the Competence Centre for Genomic Analysis (CCGA, Kiel, Germany). Sequencing data were prepared, demultiplexed and aligned to the human genome using the cellranger pipeline from 10X Genomics. Data were filtered (genes were observed in at least 1% of all cells; duplets and damaged cells were excluded; normalization) and analyzed with the Seurat R package in close cooperation with

Christian Casar (Bioinformatics Core, UKE Hamburg). For a better comparison, all samples were randomly downsampled to the cell number of the lowest sample (4,400 cells per sample).

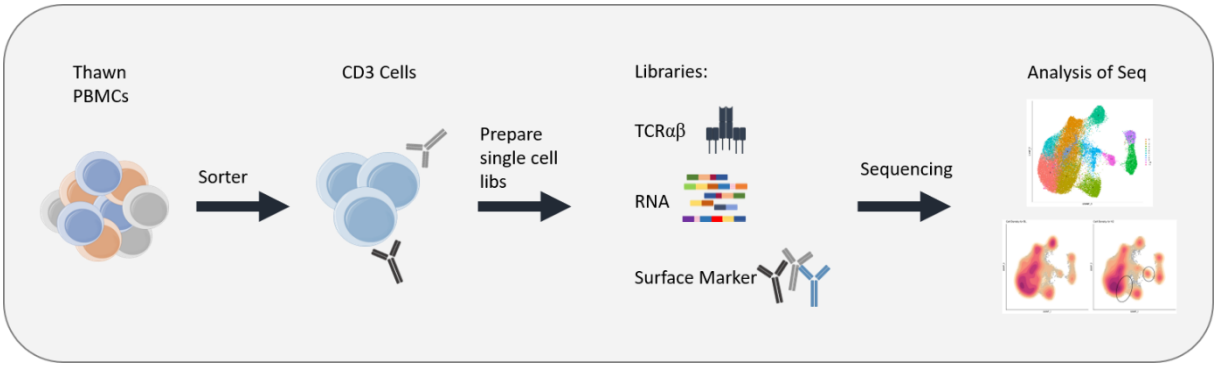

Figure 43. Scheme of the Cite-Seq experiment setup and execution.

5.1.13. Gating strategies and downstream FACS analysis

As described in section 5.1.6 and shown in Table 2, deep immunophenotyping was performed using a flow cytometry-based analysis. The antigens used for each panel can be found in Table 2. For manual gating and conformation of the SPADEVizR populations, FlowJo™ v10 software and Rstudio were used. All of the samples from one staining panel were loaded into one workspace, and the compensation for each sample was adjusted individually. Next, singlets, lymphocytes, time gates and live CD45 or live CD45high gates were applied to all samples and adjusted if necessary (Fig. 12). For the T cell subpopulation analysis, only CD45high cells were analyzed, while CD45 positive cells were used for the analysis of innate and B cells.

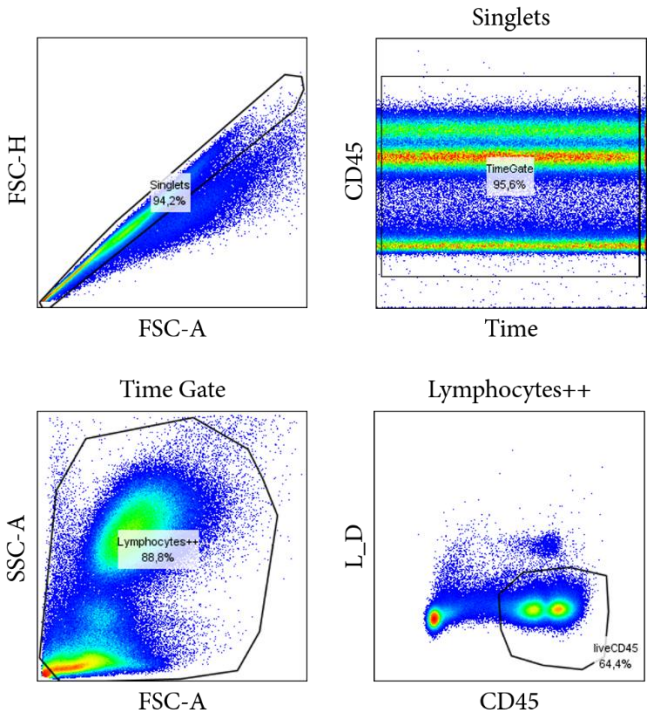

Figure 44. General gating strategy.

Data from the live CD45 cells, including their compensation data, were exported and loaded into RStudio. Cells were transformed and normalized channel by channel. Normalization was verified by FlowJo, and samples or channels were excluded as necessary. The normalized flow cytometric data were further used for either classical manual gating or SPADE[227] and SPADEVizR[228] analysis in R. Population, which were altered according to SPADEVizR were confirmed in FlowJo. The significance of both the manually gated and SPADE populations was confirmed with GraphPAD or RStudio. In this thesis, manual gating was performed for different staining panels:

- Panel I: CD3 positive cells, CD4, CD8+, double positive (DP), double negative (DN), central memory (CM), effector memory (EM), naïve and effector cells (Fig.13). Additionally, the proportion from CD4+/CD8+/DP/DN of CD28, CD57, CD160, CD161, CD272 and CD279 positive cells were gated.
- Panel II: CD3, CD4, CD8, CD25, CD44, CD45Ra, CD49a, CD49b, CD62L, CD69, CD103 and LAG-3 positive cells.
- Panel III: Tregs, CD39, CD73, CD127, effector (HLA-DR+) and naïve (CD45Ra+) positive cells (Fig. 45).

- Panel IV: CD3, CD4, CD8, Foxp3, Granzyme B, IFNγ, TNFα, IL-4, IL-10 and IL-17 positive cells (Fig. 45).
- Panel VIII: TH1-like, TH2-like and TH17-like and "real" TH17 cells were gated from CD4+ cells according to surface marker expression, as Figure 45 shows.

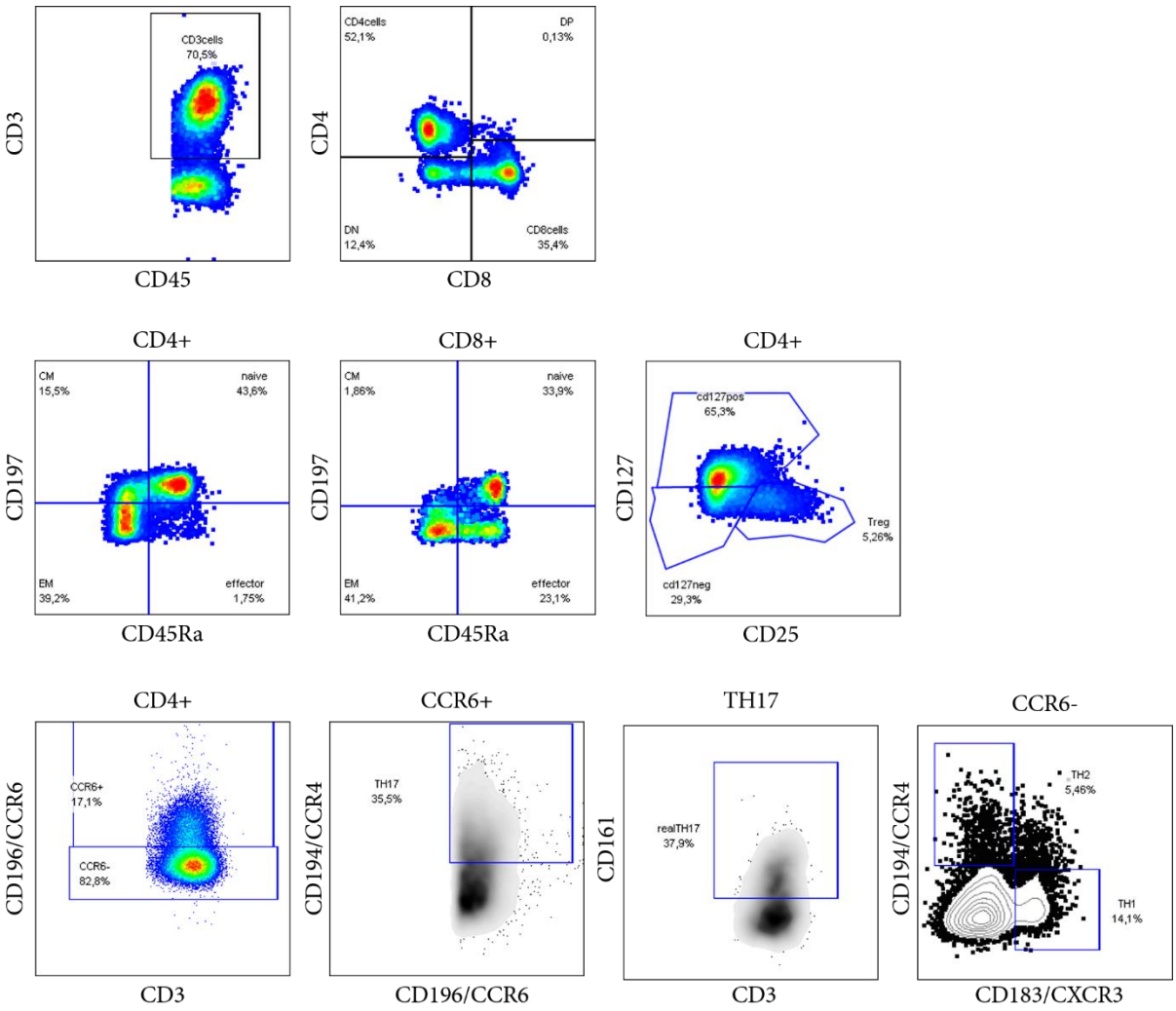

Figure 45. Gating strategy for T cells.

- Panel V: Monocytes, TNFα, IL-10, IL-1b, IL-8, IL-6 and IL-12 positive cells (Fig. 14).
- Panel VI: B cells, Baffr+, naïve, natural memory and switched memory B cells (Fig. 14).
- Panel VII: NK cells, pDCs and cDC2 (Figure 46).

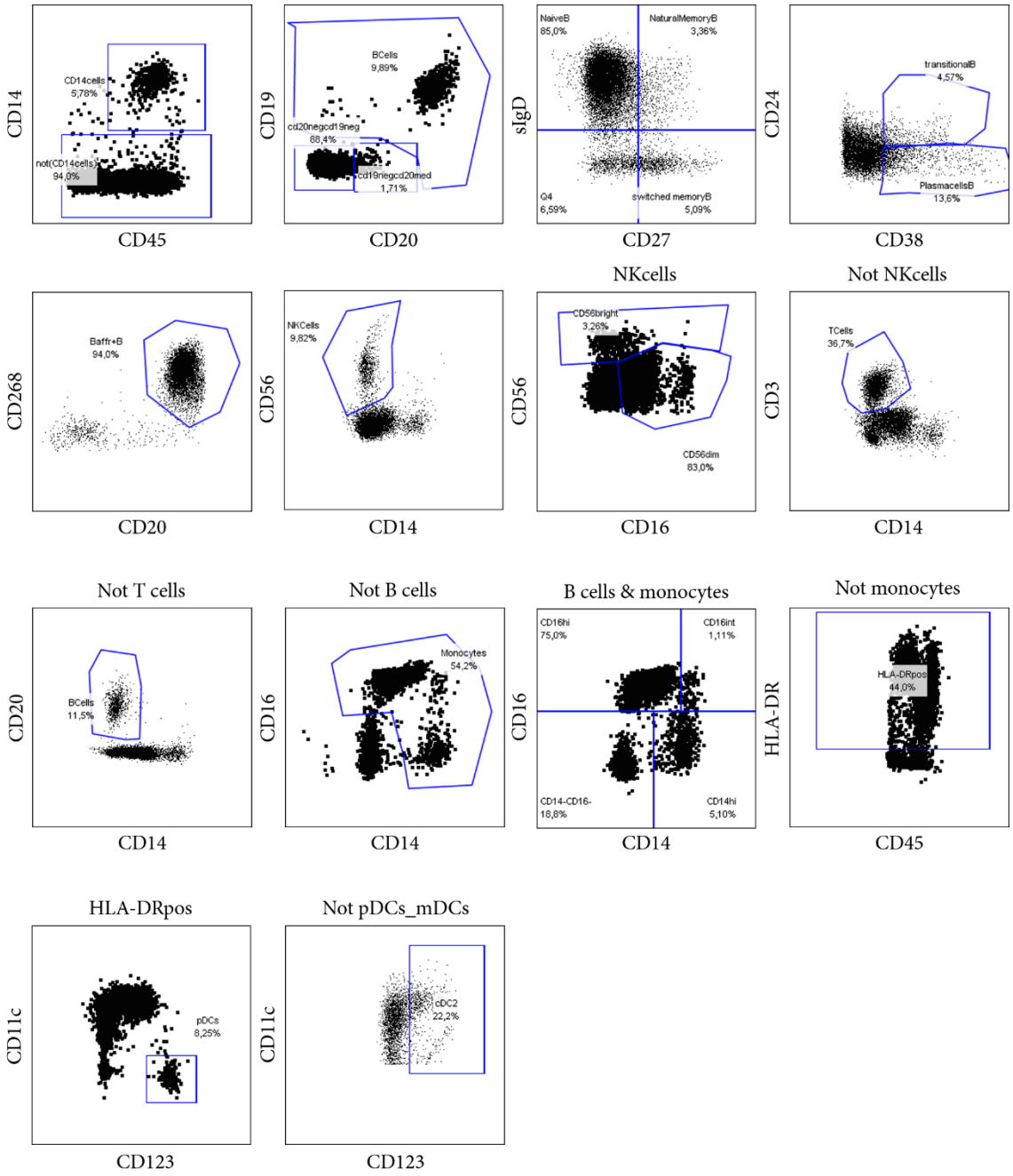

Figure 46. Gating strategy for non-T cell panels.

5.1.14. Statistics

The statistical analysis was performed with GraphPad Prism (V.8.) and RStudio. The statistical tests used are indicated in the respective figure legends. Data are presented as mean ± SD. Significant differences were indicated as $p < 0.0001$: ****; $p < 0.001$: ***; $p < 0.01$: **; or $p < 0.05$: *.

5.2. Patient characteristics

Table 3. FTM Proband characteristics

Cohort	FTM		
Age at BL	29,3	**Time points**	2,8
3M (mean months after HRT start)	2,7	**HRT (testosterone syringe)**	15
6M (mean months after HRT start)	5,7	**HRT (testosterone gel)**	4
T3/4 (mean months after HRT start)	10,5	**additional GnRH-Analoga**	1
side diseases (count, if more than once)	hypothyroidism (2), depression (2), schizophrenia , low blood pressure , autism spectrum disorder , morbus basedow , irritable bowel , hashimoto , alopecia universalis , pseudo croup	**medication (count, if more than once)**	L-Thyroxin (5), duspatalin, sertralin, valsartan, citalopram, perazin, benazepril, omeprazol, salufalk, cetirizin, venlafaxin, dekristol, folsan

Table 4. Patient characteristics of male and female AIH, PBC, Healthy

Disease	Sex	Age	Count	Height [cm]	Weight [kg]	Immun-suppressiva [yes]	BMI	Fibroscan [kPa]
PBC	female	53,0	11	165,3	73,3	0	28,29	4,95
PBC	male	71,5	6	174,5	85,0	1	22,48	6,73
AIH	female	55,8	4	166,5	67,3	3	22,87	6,05
AIH	male	48,3	8	184,0	86,2	6	25,96	7,33
PBC/AIH Overlap	female	53,0	4	164,0	73,7	3	33,83	4,63
PBC/AIH Overlap	male	48,7	3	185,5	82,5	2	24,25	5,93
AIH/NASH	female	65,0	1	167,0	90,0	1	32,27	4,40
Healthy (HC)	female	51,4	10	170,7	74,5	0	25,42	//
Healthy (HC)	male	46,3	8	186,6	88,1	0	25,33	//
all	female	53,2	30	167,9	73,7	7	26,93	//
all	male	53,2	25	183,8	86,1	9	24,98	//

Table 5. Patient characteristics of explant liver tissue

Diagnosis	PSC	AIH or AIH/NASH	Ethyltox or Ethyltox/HCC	Cyst Liver	NAFLD
Count	3	1/1	1/1	1	1
Mean Age	66	61,5	57,5	65	52
Sex	male	female/male	female	female	male

5.3. Materials

Table 5. Consumables

Article	Cataloge Number	Company
FACS Tubes	551.579	Sarstedt AG, Germany
Cryotubes 1.8 ml	379	Sarstedt AG, Germany
Pipette tips 0.2ml - 25ml	e.g. 760012	Sarstedt AG, Germany
Suspension 96-well plate	833.925.500	Sarstedt AG, Germany
Flat Bottom Plate (6-, 12-, 24-, 48-, 96-wells)	e.g. 83.3920.300	Sarstedt AG, Germany
Tubes 1.5ml - 5ml	e.g. 72.690.001	Sarstedt AG, Germany
Tubes 15ml, 25ml	e.g. 188271	Greiner Bio-One, Germany
Cell Strainer 100 µm	542000	Greiner Bio-One, Germany
LS columns	130-042-401	Miltenyi Biotec
Multiply-µStrip Pro 8-strip	72.991.002	Sarstedt AG, Germany
Syringes 1 mL, 2 mL, 10 mL	e.g. 9166017V	B. Braun
Pre-Separation Filters	130-041-407	Miltenyi Biotec
Tube, 5 ml, 75x12 mm, PS	Ref. 55.476.005	Sarstedt AG, Germany
Dimension Vista® Small Sample Container (SSC)	Ref. KS860	Siemens, Germany

Table 6. Devices

Article	Cataloge Number	Company
Eppendorf 5920R	5948000010	Eppendorf, Germany
Eppendorf 5810R	5810000010	Eppendorf, Germany
Eppendorf 5427R	5409000010	Eppendorf, Germany
Microbiolgy Safety Cabinet Class II		ThermoFisher, USA
MCO-18AIC CO2 Incubator	SA-MCO18	Sanyo, Japan
MCO-19AIC CO2 Incubator	SA-MCO19	Sanyo, Japan
GFL 1083 water bath	1083	GFL GmbH, Germany
Biorevo BZ-9000 Fluorescence Microscope		Keyence, Japan
T100 Thermal Cycler	1861096	Bio-Rad, USA
Biometra TRIO Thermal Cycler		Biometra
BDTM LSR II		BD, USA
BD LSRFortessaTM		BD, USA
BD FACSAriaTM Fusion		BD, USA
Pipetboy Acu 2	155000	Integra Biosciences, Germany
Eppendorf Research® plus (diff. sizes)	e.g. 3123000012	Eppendorf, Germany
Vortex-Genie 2	SI-0236	Scientific Industries, USA
Eppendorf ThermoMixer® Comfort	5382000015	Eppendorf, Germany
NanoDropTM 2000	ND-2000	ThermoFisher, USA
Tecan Infinite microplate reader		Tecan, Switzerland
ViiATM 7 Real-Time PCR System		Applied Biosystems, USA

Table 7. Antibodies and Cytokines

Article	Type	Catalogue Number	Company
CD103	Antibody	350218	Biolegend, USA
CD117	Antibody	313206	Biolegend, USA
CD11c	Antibody	301641	Biolegend, USA
CD123	Antibody	306010	Biolegend, USA
CD127	Antibody	351326	Biolegend, USA
CD127	Antibody	351322	Biolegend, USA
CD14	Antibody	301838	Biolegend, USA
CD14	Antibody	301804	Biolegend, USA
CD16	Antibody	302018	Biolegend, USA
CD16	Antibody	302039	Biolegend, USA
CD160	Antibody	341210	Biolegend, USA
CD161	Antibody	339916	Biolegend, USA
CD161	Antibody	339904	Biolegend, USA
CD183	Antibody	353732	Biolegend, USA
CD19	Antibody	302252	Biolegend, USA
CD194	Antibody	359410	Biolegend, USA
CD196	Antibody	353406	Biolegend, USA
CD197	Antibody	353218	Biolegend, USA
CD199	Antibody	358911	Biolegend, USA
CD1c	Antibody	331520	Biolegend, USA
CD20	Antibody	302322	Biolegend, USA
CD20	Antibody	302330	Biolegend, USA
CD20	Antibody	302303	Biolegend, USA
CD223	Antibody	369304	Biolegend, USA
CD24	Antibody	311116	Biolegend, USA
CD25	Antibody	302630	Biolegend, USA
CD268	Antibody	316914	Biolegend, USA
CD27	Antibody	302816	Biolegend, USA
CD272	Antibody	344511	Biolegend, USA
CD279	Antibody	329924	Biolegend, USA
CD28	Antibody	302926	Biolegend, USA
CD294	Antibody	350125	Biolegend, USA
CD3	Antibody	317324	Biolegend, USA
CD3	Antibody	317336	Biolegend, USA
CD38	Antibody	303512	Biolegend, USA
CD39	Antibody	328212	Biolegend, USA
CD4	Antibody	317426	Biolegend, USA
CD4	Antibody	300548	Biolegend, USA
CD43	Antibody	343208	Biolegend, USA
CD44	Antibody	338808	Biolegend, USA
CD45	Antibody	304036	Biolegend, USA

CD45	Antibody	304048	Biolegend, USA
CD45RA	Antibody	304138	Biolegend, USA
CD49a	Antibody	328312	Biolegend, USA
CD49b	Antibody	359306	Biolegend, USA
CD49d	Antibody	304303	Biolegend, USA
CD56	Antibody	318328	Biolegend, USA
CD57	Antibody	359619	Biolegend, USA
CD62L	Antibody	304843	Biolegend, USA
CD69	Antibody	310914	Biolegend, USA
CD69	Antibody	310926	Biolegend, USA
CD73	Antibody	344004	Biolegend, USA
CD8	Antibody	301028	Biolegend, USA
CD8	Antibody	301048	Biolegend, USA
CD8	Antibody	300930	Biolegend, USA
Foxp3	Antibody	320214	Biolegend, USA
Granzyme B	Antibody	515403	Biolegend, USA
HLA-DR	Antibody	307642	Biolegend, USA
HLA-DR	Antibody	307604	Biolegend, USA
IFNγ	Antibody	502530	Biolegend, USA
IgD	Antibody	348203	Biolegend, USA
TCR Vα24-J18	Antibody	342921	Biolegend, USA
TNFα	Antibody	502938	Biolegend, USA
TCRγδ	Antibody	655410	BD, USA
β7-integrin	Antibody	121010	Biolegend, USA
IL-17A	Antibody	512328	Biolegend, USA
IL-10	Antibody	501404	Biolegend, USA
IL-8	Antibody	511411	Biolegend, USA
IL-6	Antibody	501112	Biolegend, USA
IL-4	Antibody	500824	Biolegend, USA
IL-1β	Antibody	511710	Biolegend, USA
IL-12/IL-23 p40	Antibody	501822	Biolegend, USA
Vα7.2	Antibody	351708	Biolegend, USA
CD25	Antibody	302643	Biolegend, USA
CD127	Antibody	351352	Biolegend, USA
CD194	Antibody	359423	Biolegend, USA
CD183	Antibody	353745	Biolegend, USA
CD279	Antibody	329955	Biolegend, USA
CD223	Antibody	369333	Biolegend, USA
CD152	Antibody	369619	Biolegend, USA
TIGIT	Antibody	372725	Biolegend, USA
CD4	Antibody	344649	Biolegend, USA
CD8	Antibody	344751	Biolegend, USA
HLA-DR	Antibody	307659	Biolegend, USA

TCR gd	Antibody	331229	Biolegend, USA
CD56	Antibody	362557	Biolegend, USA
CD314	Antibody	320835	Biolegend, USA
CD45RA	Antibody	304157	Biolegend, USA
CD197	Antibody	353247	Biolegend, USA
CD49b	Antibody	359311	Biolegend, USA
CD3	unstained antibody	317302	Biolegend, USA
CD28	unstained antibody	302902	Biolegend, USA
Proleukin, IL-2	cytokine		Novartis Pharma, Switzerland
IL-1β	cytokine	130-093-898	Miltenyi Biotec, Germany
TNFα	cytokine	300-01A	PeproTech, USA
IFNγ	cytokine	300-02	PeproTech, USA
C0034 CD3	TotalSeq™ C Antibody	300479	Biolegend, USA
C0072 CD4	TotalSeq™ C Antibody	300567	Biolegend, USA
C0046 CD8	TotalSeq™ C Antibody	344753	Biolegend, USA
C0085 CD25	TotalSeq™ C Antibody	302649	Biolegend, USA
C0148 CD197 (CCR7)	TotalSeq™ C Antibody	353251	Biolegend, USA
C0390 CD127 (IL-7Rα)	TotalSeq™ C Antibody	351356	Biolegend, USA
C0063 CD45RA	TotalSeq™ C Antibody	304163	Biolegend, USA
C0147 CD62L	TotalSeq™ C Antibody	304851	Biolegend, USA
C0071 CD194 (CCR4)	TotalSeq™ C Antibody	359425	Biolegend, USA
C0140 CD183 (CXCR3)	TotalSeq™ C Antibody	353747	Biolegend, USA
C0143 CD196 (CCR6)	TotalSeq™ C Antibody	353440	Biolegend, USA
C0168 CD57 Recombinant	TotalSeq™ C Antibody	393321	Biolegend, USA
C0170 CD272 (BTLA)	TotalSeq™ C Antibody	344527	Biolegend, USA
C0088 CD279 (PD-1)	TotalSeq™ C Antibody	329963	Biolegend, USA
C0149 CD161	TotalSeq™ C Antibody	339947	Biolegend, USA
C0386 CD28	TotalSeq™ C Antibody	302963	Biolegend, USA
C0581 TCR Vα7.2	TotalSeq™ C Antibody	351735	Biolegend, USA
C0584 TCR Vα24-Jα18	TotalSeq™ C Antibody	342925	Biolegend, USA
C0139 TCR γ/δ	TotalSeq™ C Antibody	331231	Biolegend, USA
C0032 CD154	TotalSeq™ C Antibody	310849	Biolegend, USA

Table 8. Reagents

Article	Cataloge Number	Manufacturers
RPMI 1640	11875085	ThermoFisher, USA
X-Vivo™ 15	881024	Biozym, Germany
Biocoll	L6113	Biochrom, Germany
OptiPrep™	OptiPrepTM	Sigma-Aldrich, USA
RBC Lysis/Fixation Solution (10X)	422401	Biolegend, USA
Monensin Solution (1000X)	420701	Biolegend, USA
Brefeldin A Solution (1000X)	00-4506-51	eBioscience, USA
Pacific Orange NHS-Ester	P30253	ThermoFisher, USA
Fixable Viability Dye eFluor™ 506	65-0866-14	eBioscience, USA
Alexa Fluor™ 750 NHS-Ester	A20011	ThermoFisher, USA
Fetal calf serum (FCS)	A15-101	PAA Laboratories, USA
Penicillin-Streptomycin (10'000 U/ml)	15140122	ThermoFisher, USA
DMSO	D4540	Sigma-Aldrich, USA
ABTS™		Sigma-Aldrich, USA
β-Mercaptoethanol		Sigma-Aldrich, USA
Cholera Toxin		Sigma-Aldrich, USA
Collagen R solution		SERVA
Collagenase NB 4G Proved Grade		Nordmark, Germany
EGF recombinant human		PeproTech, USA
Epinephrine		Sigma-Aldrich, USA
Ethanol, absolute		Th. Geyer, Germany
Ham's F-12 Nutrient Mix		ThermoFisher, USA
HGF recombinant human		PeproTech, USA
Hydrocortisone		Sigma-Aldrich, USA
Hydrogen peroxide (30 %)		Merck, Germany
Insulin solution human		Sigma-Aldrich, USA
Insulin-Transferrin-Selenium (ITS) (100X)		ThermoFisher, USA
Ionomycin calcium salt		Sigma-Aldrich, USA
L-Glutamine (200 mM)		ThermoFisher, USA
Adenine		Sigma-Aldrich, USA
Methanol		J.T.Baker, Germany
OneComp eBeads™ Compensation Beads		ThermoFisher, USA
Paraformaldehyde solution (4 % in PBS)		Morphisto, Germany
TaqMan™ Fast Advanced Master Mix		ThermoFisher, USA
Triton R X 100		Carl Roth, Germany
Trypan blue solution (0.4 %)		ThermoFisher, USA
TrypLE Express Enzym (1X)	12604013	ThermoFisher, USA

Tween R 20		J.T.Baker, Germany
Water	0082423E	B. Braun
DPBS	14190144	ThermoFisher, USA
Charcoal, Dextran Coated	C6241-5G	Sigma-Aldrich, USA

Table 9. Buffer and Medium

Buffer & Medium	Ingredients	Concentrations/Amounts
PBS	NaCl	137 mM
	KCl	2.7 mM
	Na2HPO4	6.5 mM
	KH2PO4	1.5 mM
FACS-Buffer	EDTA	2 mM
	FCS	2%
	NaN3	0.01 %
	in PBS	
MACS-Buffer	EDTA	2 mM
	BSA	1%
	in PBS	
Saponin Buffer	Saponin	0.3 %
	BSA	0.1 %
	in PBS	
PMA-solution	in DMSO	1 mg/m
Ionomycin-solution	in DMSO	1 mg/ml
LPS-solution	in PBS	5 mg/ml
H69-medium	DMEM / HAM F12	67,5ml / 22,5ml
100ml	DCC-FCS	10 ml
	Hydrocortisone	100 µl
	Triiodothyronine	1 ml
	EGF	10 µl
	Adenine	1 ml
	Epinephrine	40 µl
	Insulin-Transferrin 100x	750 µl
	L-Glutamine	16,25 µl
	Pen/Strep	0,375 ml
Primary Cholangiocyte	DMEM / HAM F12	43 ml / 43 ml
Medium	DCC-FCS	10 ml
100ml	HGF	10 µl
	Cholera Toxin	1 ml
	Hydrocortisone	1 ml
	Triiodothyronine	1 ml

	EGF	10 µl
	Insulin	0,25 ml
	Pen/Strep	1 ml
	AmphoB	50 µl
Lymphocyte Medium	RPMI	
	DCC-FCS	5-10%
	Pen/Strep	1%

Table 10. TaqMan Assays

Article	Cataloge Number	Company
AR	00171172_m1	ThermoFisher, USA
Ar	00442688_m1	ThermoFisher, USA
CCL 2	00234140_m1	ThermoFisher, USA
CCL 20	00355476_m1	ThermoFisher, USA
CCR 7	01013469_m1	ThermoFisher, USA
CYP19A 1	00903411_m1	ThermoFisher, USA
ESR 1	00174860_m1	ThermoFisher, USA
ESR 2	01100353_m1	ThermoFisher, USA
Esr1	00433149_m1	ThermoFisher, USA
Esr2	00599821_m1	ThermoFisher, USA
GIMAP7	04990082_s1	ThermoFisher, USA
GPER 1	01922715_s1	ThermoFisher, USA
Gper1	02620446_s1	ThermoFisher, USA
Gprc 6a	00467618_m1	ThermoFisher, USA
GPRC6A	01026851_m1	ThermoFisher, USA
Hprt	03024075_m1	ThermoFisher, USA
HPRT 1	02800695_m1	ThermoFisher, USA
IFNG	00989291_m1	ThermoFisher, USA
IL10	00961622_m1	ThermoFisher, USA
IL13	00174379_m1	ThermoFisher, USA
IL17A	00174383_m1	ThermoFisher, USA
IL1B	1555410_m1	ThermoFisher, USA
IL4	00174122_m1	ThermoFisher, USA
IL6	00174131_m1	ThermoFisher, USA
IL8	00174103_m1	ThermoFisher, USA
JUNB	00357891_s1	ThermoFisher, USA
KRT 19	00761767_s1	ThermoFisher, USA
KRT 7	00559840_m1	ThermoFisher, USA
RORC	01076122_m1	ThermoFisher, USA
SLC 39A9	04276955_m1	ThermoFisher, USA
Slc39a9	00470907_m1	ThermoFisher, USA

SRD 5A1	00971645_g1	ThermoFisher, USA
SRD 5A2	00936406_m1	ThermoFisher, USA
SRD 5a3	00430680_g1	ThermoFisher, USA
TBX 21	00203436_m1	ThermoFisher, USA
TNF	01113624_g1	ThermoFisher, USA

Table 11. Kits

Article	Cataloge Number	Company
CellTrace™ Violet Cell Proliferation Kit	C34557	ThermoFisher, USA
Pan T Cell Isolation Kit, human	130-096-535	Miltenyi Biotec, Germany
Pan Monocyte Isolation Kit, human	130-096-537	Miltenyi Biotec, Germany
Pan-DC Enrichment Kit, human	130-100-777	Miltenyi Biotec, Germany
CD4 MicroBeads, human	130-045-101	Miltenyi Biotec, Germany
CD8 MicroBeads, human	130-045-201	Miltenyi Biotec, Germany
Chromium Next GEM Single Cell 5' Library and Gel Bead Kit v1.1	1000165	10x Genomics, USA
Chromium Next GEM Chip G Single Cell Kit	1000223	10x Genomics, USA
High-Capacity cDNA Reverse Transcription Kit	4368814	ThermoFisher, USA
NucleoSpin R RNA	REF 740210.20	MACHEREY-NAGEL, Germany
PAXgene Blood RNA Kit	762174	Qiagen, Netherlands
Human TNF-α Standard ABTS ELISA	900-K25	PeproTech, USA
Human IFN-γ Standard ABTS ELISA	900-K27	PeproTech, USA
ELISA MAX™ Deluxe Set Human CCL20	441404	Biolegend, USA
Human MCP-1 (CCL2) Standard ABTS ELISA	900-K31	PeproTech, USA
Human IL-6 Standard TMB ELISA	900-T16	PeproTech, USA
Human IL-8(CXCL8) ABTS ELISA	900-K18	PeproTech, USA
Human Testosterone ELISA Kit	CSB E05099h	Cusabio, USA
Mouse/Rat Testosterone, Total ELISA	SKU: TE187S-100	Calbiotech, USA

Table 12. Software

Article	Company
FlowJoTM v10	BD, USA
BD FACSDivaTM v8	BD, USA
Office 2016	Microsoft Corporation, USA
R (Version 4.0.2)	The R Foundation
Rstudio (Version 1.1.463)	Rstudio PBC
R packages: readxl, tidyverse, ggplot2, xlsx, flowCore, flowVS, dplyr, flowStats, seurat, pheatmap, spade, SPADEVizR	
GraphPad Prism v9	GraphPad Software, USA
LEGENDplexTM Software	Biolegend, USA
Endnote X9	Alfasoft GmbH

6. References

1 Sattler, S. The Role of the Immune System Beyond the Fight Against Infection. *Adv Exp Med Biol* **1003**, 3-14, doi:10.1007/978-3-319-57613-8_1 (2017).

2 Yatim, K. M. & Lakkis, F. G. A brief journey through the immune system. *Clin J Am Soc Nephrol* **10**, 1274-1281, doi:10.2215/CJN.10031014 (2015).

3 Parkin, J. & Cohen, B. An overview of the immune system. *Lancet* **357**, 1777-1789, doi:10.1016/S0140-6736(00)04904-7 (2001).

4 Brodin, P. & Davis, M. M. Human immune system variation. *Nat Rev Immunol* **17**, 21-29, doi:10.1038/nri.2016.125 (2017).

5 Dupic, T., Marcou, Q., Walczak, A. M. & Mora, T. Genesis of the alphabeta T-cell receptor. *PLoS Comput Biol* **15**, e1006874, doi:10.1371/journal.pcbi.1006874 (2019).

6 Dong *et al.* Structural basis of assembly of the human T cell receptor-CD3 complex. *Nature* **573**, 546-552, doi:10.1038/s41586-019-1537-0 (2019).

7 Mousset, C. M. *et al.* Comprehensive Phenotyping of T Cells Using Flow Cytometry. *Cytometry A* **95**, 647-654, doi:10.1002/cyto.a.23724 (2019).

8 Brummelman, J., Pilipow, K. & Lugli, E. The Single-Cell Phenotypic Identity of Human CD8(+) and CD4(+) T Cells. *Int Rev Cell Mol Biol* **341**, 63-124, doi:10.1016/bs.ircmb.2018.05.007 (2018).

9 Bettelli, E., Korn, T. & Kuchroo, V. K. Th17: the third member of the effector T cell trilogy. *Curr Opin Immunol* **19**, 652-657, doi:10.1016/j.coi.2007.07.020 (2007).

10 Saito, S., Nakashima, A., Shima, T. & Ito, M. Th1/Th2/Th17 and regulatory T-cell paradigm in pregnancy. *Am J Reprod Immunol* **63**, 601-610, doi:10.1111/j.1600-0897.2010.00852.x (2010).

11 Singh, A. K., Rhost, S., Lofbom, L. & Cardell, S. L. Defining a novel subset of CD1d-dependent type II natural killer T cells using natural killer cell-associated markers. *Scand J Immunol* **90**, e12794, doi:10.1111/sji.12794 (2019).

12 Rouxel, O. & Lehuen, A. Mucosal-associated invariant T cells in autoimmune and immune-mediated diseases. *Immunol Cell Biol* **96**, 618-629, doi:10.1111/imcb.12011 (2018).

13 Paul, S., Shilpi & Lal, G. Role of gamma-delta (gammadelta) T cells in autoimmunity. *J Leukoc Biol* **97**, 259-271, doi:10.1189/jlb.3RU0914-443R (2015).

14 Schutyser, E., Struyf, S. & Van Damme, J. The CC chemokine CCL20 and its receptor CCR6. *Cytokine Growth Factor Rev* **14**, 409-426, doi:10.1016/s1359-6101(03)00049-2 (2003).

15 Afshan, G., Afzal, N. & Qureshi, S. CD4+CD25(hi) regulatory T cells in healthy males and females mediate gender difference in the prevalence of autoimmune diseases. *Clin Lab* **58**, 567-571 (2012).

16 Narsale, A., Moya, R. & Davies, J. D. Human CD4(+) CD25(+) CD127(hi) cells and the Th1/Th2 phenotype. *Clin Immunol* **188**, 103-112, doi:10.1016/j.clim.2018.01.003 (2018).

17 Topham, D. J. & Reilly, E. C. Tissue-Resident Memory CD8(+) T Cells: From Phenotype to Function. *Front Immunol* **9**, 515, doi:10.3389/fimmu.2018.00515 (2018).

18 Ichikawa, T. *et al.* CD103(hi) Treg cells constrain lung fibrosis induced by CD103(lo) tissue-resident pathogenic CD4 T cells. *Nat Immunol* **20**, 1469-1480, doi:10.1038/s41590-019-0494-y (2019).

19 Cheuk, S. *et al.* CD49a Expression Defines Tissue-Resident CD8(+) T Cells Poised for Cytotoxic Function in Human Skin. *Immunity* **46**, 287-300, doi:10.1016/j.immuni.2017.01.009 (2017).
20 Boisvert, M., Chetoui, N., Gendron, S. & Aoudjit, F. Alpha2beta1 integrin is the major collagen-binding integrin expressed on human Th17 cells. *Eur J Immunol* **40**, 2710-2719, doi:10.1002/eji.201040307 (2010).
21 Deaglio, S. *et al.* Adenosine generation catalyzed by CD39 and CD73 expressed on regulatory T cells mediates immune suppression. *J Exp Med* **204**, 1257-1265, doi:10.1084/jem.20062512 (2007).
22 Takenaka, M. C., Robson, S. & Quintana, F. J. Regulation of the T Cell Response by CD39. *Trends Immunol* **37**, 427-439, doi:10.1016/j.it.2016.04.009 (2016).
23 Wang, J. *et al.* Fibrinogen-like Protein 1 Is a Major Immune Inhibitory Ligand of LAG-3. *Cell* **176**, 334-347 e312, doi:10.1016/j.cell.2018.11.010 (2019).
24 Anderson, A. C., Joller, N. & Kuchroo, V. K. Lag-3, Tim-3, and TIGIT: Co-inhibitory Receptors with Specialized Functions in Immune Regulation. *Immunity* **44**, 989-1004, doi:10.1016/j.immuni.2016.05.001 (2016).
25 Fujio, K., Yamamoto, K. & Okamura, T. Overview of LAG-3-Expressing, IL-10-Producing Regulatory T Cells. *Curr Top Microbiol Immunol* **410**, 29-45, doi:10.1007/82_2017_59 (2017).
26 Gattinoni, L. *et al.* A human memory T cell subset with stem cell-like properties. *Nat Med* **17**, 1290-1297, doi:10.1038/nm.2446 (2011).
27 Liu, W. *et al.* CD127 expression inversely correlates with FoxP3 and suppressive function of human CD4+ T reg cells. *J Exp Med* **203**, 1701-1711, doi:10.1084/jem.20060772 (2006).
28 Fish, E. N. The X-files in immunity: sex-based differences predispose immune responses. *Nat Rev Immunol* **8**, 737-744, doi:10.1038/nri2394 (2008).
29 Bernin, H. & Lotter, H. Sex bias in the outcome of human tropical infectious diseases: influence of steroid hormones. *J Infect Dis* **209 Suppl 3**, S107-113, doi:10.1093/infdis/jit610 (2014).
30 Sellau, J., Groneberg, M. & Lotter, H. Androgen-dependent immune modulation in parasitic infection. *Semin Immunopathol* **41**, 213-224, doi:10.1007/s00281-018-0722-9 (2019).
31 Grebely, J. *et al.* The effects of female sex, viral genotype, and IL28B genotype on spontaneous clearance of acute hepatitis C virus infection. *Hepatology* **59**, 109-120, doi:10.1002/hep.26639 (2014).
32 Bouman, A., Heineman, M. J. & Faas, M. M. Sex hormones and the immune response in humans. *Hum Reprod Update* **11**, 411-423, doi:10.1093/humupd/dmi008 (2005).
33 Cutolo, M. *et al.* Sex hormones influence on the immune system: basic and clinical aspects in autoimmunity. *Lupus* **13**, 635-638, doi:10.1191/0961203304lu1094oa (2004).
34 Klein, S. L. & Flanagan, K. L. Sex differences in immune responses. *Nat Rev Immunol* **16**, 626-638, doi:10.1038/nri.2016.90 (2016).
35 Vom Steeg, L. G., Attreed, S. E., Zirkin, B. & Klein, S. L. Testosterone treatment of aged male mice improves some but not all aspects of age-associated increases in influenza severity. *Cell Immunol* **345**, 103988, doi:10.1016/j.cellimm.2019.103988 (2019).
36 Guess, T. E., Rosen, J., Castro-Lopez, N., Wormley, F. L., Jr. & McClelland, E. E. An inherent T cell deficit in healthy males to C. neoformans infection may begin to

explain the sex susceptibility in incidence of cryptococcosis. *Biol Sex Differ* **10**, 44, doi:10.1186/s13293-019-0258-2 (2019).
37 Zychlinsky Scharff, A. *et al.* Sex differences in IL-17 contribute to chronicity in male versus female urinary tract infection. *JCI Insight* **5**, doi:10.1172/jci.insight.122998 (2019).
38 Tenover, J. S. Effects of testosterone supplementation in the aging male. *J Clin Endocrinol Metab* **75**, 1092-1098, doi:10.1210/jcem.75.4.1400877 (1992).
39 Ferrucci, L. *et al.* Low testosterone levels and the risk of anemia in older men and women. *Arch Intern Med* **166**, 1380-1388, doi:10.1001/archinte.166.13.1380 (2006).
40 Markle, J. G. *et al.* Sex differences in the gut microbiome drive hormone-dependent regulation of autoimmunity. *Science* **339**, 1084-1088, doi:10.1126/science.1233521 (2013).
41 Bianchi, I., Lleo, A., Gershwin, M. E. & Invernizzi, P. The X chromosome and immune associated genes. *J Autoimmun* **38**, J187-192, doi:10.1016/j.jaut.2011.11.012 (2012).
42 Souyris, M. *et al.* TLR7 escapes X chromosome inactivation in immune cells. *Sci Immunol* **3**, doi:10.1126/sciimmunol.aap8855 (2018).
43 Souyris, M., Mejia, J. E., Chaumeil, J. & Guery, J. C. Female predisposition to TLR7-driven autoimmunity: gene dosage and the escape from X chromosome inactivation. *Semin Immunopathol* **41**, 153-164, doi:10.1007/s00281-018-0712-y (2019).
44 Invernizzi, P. *et al.* Frequency of monosomy X in women with primary biliary cirrhosis. *Lancet* **363**, 533-535, doi:10.1016/S0140-6736(04)15541-4 (2004).
45 Miozzo, M. *et al.* Preferential X chromosome loss but random inactivation characterize primary biliary cirrhosis. *Hepatology* **46**, 456-462, doi:10.1002/hep.21696 (2007).
46 Invernizzi, P. *et al.* X chromosome monosomy: a common mechanism for autoimmune diseases. *J Immunol* **175**, 575-578, doi:10.4049/jimmunol.175.1.575 (2005).
47 Ngo, S. T., Steyn, F. J. & McCombe, P. A. Gender differences in autoimmune disease. *Front Neuroendocrinol* **35**, 347-369, doi:10.1016/j.yfrne.2014.04.004 (2014).
48 Bove, R. & Chitnis, T. The role of gender and sex hormones in determining the onset and outcome of multiple sclerosis. *Mult Scler* **20**, 520-526, doi:10.1177/1352458513519181 (2014).
49 Hemmer, B., Archelos, J. J. & Hartung, H. P. New concepts in the immunopathogenesis of multiple sclerosis. *Nat Rev Neurosci* **3**, 291-301, doi:10.1038/nrn784 (2002).
50 McFarland, H. F. & Martin, R. Multiple sclerosis: a complicated picture of autoimmunity. *Nat Immunol* **8**, 913-919, doi:10.1038/ni1507 (2007).
51 Chitnis, T. The role of testosterone in MS risk and course. *Mult Scler* **24**, 36-41, doi:10.1177/1352458517737395 (2018).
52 Sicotte, N. L. *et al.* Testosterone treatment in multiple sclerosis: a pilot study. *Arch Neurol* **64**, 683-688, doi:10.1001/archneur.64.5.683 (2007).
53 Murphy, G. & Isenberg, D. Effect of gender on clinical presentation in systemic lupus erythematosus. *Rheumatology (Oxford)* **52**, 2108-2115, doi:10.1093/rheumatology/ket160 (2013).
54 Danchenko, N., Satia, J. A. & Anthony, M. S. Epidemiology of systemic lupus erythematosus: a comparison of worldwide disease burden. *Lupus* **15**, 308-318, doi:10.1191/0961203306lu2305xx (2006).

55 Ramirez Sepulveda, J. I. *et al.* Sex differences in clinical presentation of systemic lupus erythematosus. *Biol Sex Differ* **10**, 60, doi:10.1186/s13293-019-0274-2 (2019).
56 Eloranta, M. L. & Ronnblom, L. Cause and consequences of the activated type I interferon system in SLE. *J Mol Med (Berl)* **94**, 1103-1110, doi:10.1007/s00109-016-1421-4 (2016).
57 Webb, K. *et al.* Sex and Pubertal Differences in the Type 1 Interferon Pathway Associate With Both X Chromosome Number and Serum Sex Hormone Concentration. *Front Immunol* **9**, 3167, doi:10.3389/fimmu.2018.03167 (2018).
58 Lahita, R. G., Bradlow, H. L., Ginzler, E., Pang, S. & New, M. Low plasma androgens in women with systemic lupus erythematosus. *Arthritis Rheum* **30**, 241-248, doi:10.1002/art.1780300301 (1987).
59 Carbone, M. & Neuberger, J. M. Autoimmune liver disease, autoimmunity and liver transplantation. *J Hepatol* **60**, 210-223, doi:10.1016/j.jhep.2013.09.020 (2014).
60 European Association for the Study of the, L. EASL Clinical Practice Guidelines: Autoimmune hepatitis. *J Hepatol* **63**, 971-1004, doi:10.1016/j.jhep.2015.06.030 (2015).
61 Grant, C. R. & Liberal, R. Liver immunology: How to reconcile tolerance with autoimmunity. *Clin Res Hepatol Gastroenterol* **41**, 6-16, doi:10.1016/j.clinre.2016.06.003 (2017).
62 Invernizzi, P. Liver auto-immunology: the paradox of autoimmunity in a tolerogenic organ. *J Autoimmun* **46**, 1-6, doi:10.1016/j.jaut.2013.08.006 (2013).
63 Lleo, A. *et al.* Evolving Trends in Female to Male Incidence and Male Mortality of Primary Biliary Cholangitis. *Sci Rep* **6**, 25906, doi:10.1038/srep25906 (2016).
64 Lleo, A., Marzorati, S., Anaya, J. M. & Gershwin, M. E. Primary biliary cholangitis: a comprehensive overview. *Hepatol Int* **11**, 485-499, doi:10.1007/s12072-017-9830-1 (2017).
65 Rubel, L. R., Rabin, L., Seeff, L. B., Licht, H. & Cuccherini, B. A. Does primary biliary cirrhosis in men differ from primary biliary cirrhosis in women? *Hepatology* **4**, 671-677, doi:10.1002/hep.1840040418 (1984).
66 Abdulkarim, M. *et al.* Sex differences in clinical presentation and prognosis in patients with primary biliary cholangitis. *Scand J Gastroenterol* **54**, 1391-1396, doi:10.1080/00365521.2019.1683226 (2019).
67 Al-Chalabi, T., Underhill, J. A., Portmann, B. C., McFarlane, I. G. & Heneghan, M. A. Impact of gender on the long-term outcome and survival of patients with autoimmune hepatitis. *J Hepatol* **48**, 140-147, doi:10.1016/j.jhep.2007.08.013 (2008).
68 van Gerven, N. M. *et al.* HLA-DRB1*03:01 and HLA-DRB1*04:01 modify the presentation and outcome in autoimmune hepatitis type-1. *Genes Immun* **16**, 247-252, doi:10.1038/gene.2014.82 (2015).
69 Heneghan, M. A., Yeoman, A. D., Verma, S., Smith, A. D. & Longhi, M. S. Autoimmune hepatitis. *Lancet* **382**, 1433-1444, doi:10.1016/S0140-6736(12)62163-1 (2013).
70 Bovensiepen, C. S. *et al.* TNF-Producing Th1 Cells Are Selectively Expanded in Liver Infiltrates of Patients with Autoimmune Hepatitis. *J Immunol* **203**, 3148-3156, doi:10.4049/jimmunol.1900124 (2019).
71 Trivedi, P. J. *et al.* Good maternal and fetal outcomes for pregnant women with primary biliary cirrhosis. *Clin Gastroenterol Hepatol* **12**, 1179-1185 e1171, doi:10.1016/j.cgh.2013.11.030 (2014).
72 Schramm, C. *et al.* Pregnancy in autoimmune hepatitis: outcome and risk factors. *Am J Gastroenterol* **101**, 556-560, doi:10.1111/j.1572-0241.2006.00479.x (2006).

73 Westbrook, R. H., Yeoman, A. D., Kriese, S. & Heneghan, M. A. Outcomes of pregnancy in women with autoimmune hepatitis. *J Autoimmun* **38**, J239-244, doi:10.1016/j.jaut.2011.12.002 (2012).
74 Bremer, L., Schramm, C. & Tiegs, G. Immunology of hepatic diseases during pregnancy. *Semin Immunopathol* **38**, 669-685, doi:10.1007/s00281-016-0573-1 (2016).
75 Prough, R. A., Clark, B. J. & Klinge, C. M. Novel mechanisms for DHEA action. *J Mol Endocrinol* **56**, R139-155, doi:10.1530/JME-16-0013 (2016).
76 Burger, H. G. Androgen production in women. *Fertil Steril* **77 Suppl 4**, S3-5, doi:10.1016/s0015-0282(02)02985-0 (2002).
77 Zouboulis, C. C. & Degitz, K. Androgen action on human skin -- from basic research to clinical significance. *Exp Dermatol* **13 Suppl 4**, 5-10, doi:10.1111/j.1600-0625.2004.00255.x (2004).
78 Davey, R. A. & Grossmann, M. Androgen Receptor Structure, Function and Biology: From Bench to Bedside. *Clin Biochem Rev* **37**, 3-15 (2016).
79 menZimmerman, Y., Eijkemans, M. J., Coelingh Bennink, H. J., Blankenstein, M. A. & Fauser, B. C. The effect of combined oral contraception on testosterone levels in healthy women: a systematic review and meta-analysis. *Hum Reprod Update* **20**, 76-105, doi:10.1093/humupd/dmt038 (2014).
80 Vermeulen, A., Goemaere, S. & Kaufman, J. M. Testosterone, body composition and aging. *J Endocrinol Invest* **22**, 110-116 (1999).
81 Haring, R. *et al.* Age-specific reference ranges for serum testosterone and androstenedione concentrations in women measured by liquid chromatography-tandem mass spectrometry. *J Clin Endocrinol Metab* **97**, 408-415, doi:10.1210/jc.2011-2134 (2012).
82 Friedrich, N. *et al.* Reference ranges for serum dehydroepiandrosterone sulfate and testosterone in adult men. *J Androl* **29**, 610-617, doi:10.2164/jandrol.108.005561 (2008).
83 Rothman, M. S. *et al.* Reexamination of testosterone, dihydrotestosterone, estradiol and estrone levels across the menstrual cycle and in postmenopausal women measured by liquid chromatography-tandem mass spectrometry. *Steroids* **76**, 177-182, doi:10.1016/j.steroids.2010.10.010 (2011).
84 Swerdloff, R. S., Dudley, R. E., Page, S. T., Wang, C. & Salameh, W. A. Dihydrotestosterone: Biochemistry, Physiology, and Clinical Implications of Elevated Blood Levels. *Endocr Rev* **38**, 220-254, doi:10.1210/er.2016-1067 (2017).
85 Clarke, B. L. & Khosla, S. Androgens and bone. *Steroids* **74**, 296-305, doi:10.1016/j.steroids.2008.10.003 (2009).
86 Sinnesael, M., Boonen, S., Claessens, F., Gielen, E. & Vanderschueren, D. Testosterone and the male skeleton: a dual mode of action. *J Osteoporos* **2011**, 240328, doi:10.4061/2011/240328 (2011).
87 Estrada, M., Espinosa, A., Muller, M. & Jaimovich, E. Testosterone stimulates intracellular calcium release and mitogen-activated protein kinases via a G protein-coupled receptor in skeletal muscle cells. *Endocrinology* **144**, 3586-3597, doi:10.1210/en.2002-0164 (2003).
88 Cutolo, M. *et al.* Androgen and estrogen receptors are present in primary cultures of human synovial macrophages. *J Clin Endocrinol Metab* **81**, 820-827, doi:10.1210/jcem.81.2.8636310 (1996).

89 Prossnitz, E. R. & Barton, M. Signaling, physiological functions and clinical relevance of the G protein-coupled estrogen receptor GPER. *Prostaglandins Other Lipid Mediat* **89**, 89-97, doi:10.1016/j.prostaglandins.2009.05.001 (2009).
90 Olsen, N. J., Olson, G., Viselli, S. M., Gu, X. & Kovacs, W. J. Androgen receptors in thymic epithelium modulate thymus size and thymocyte development. *Endocrinology* **142**, 1278-1283, doi:10.1210/endo.142.3.8032 (2001).
91 Death, A. K. *et al.* Dihydrotestosterone promotes vascular cell adhesion molecule-1 expression in male human endothelial cells via a nuclear factor-kappaB-dependent pathway. *Endocrinology* **145**, 1889-1897, doi:10.1210/en.2003-0789 (2004).
92 Huang, C. K. *et al.* New therapy via targeting androgen receptor in monocytes/macrophages to battle atherosclerosis. *Hypertension* **63**, 1345-1353, doi:10.1161/HYPERTENSIONAHA.113.02804 (2014).
93 Benten, W. P. *et al.* Functional testosterone receptors in plasma membranes of T cells. *FASEB J* **13**, 123-133, doi:10.1096/fasebj.13.1.123 (1999).
94 Thomas, P., Converse, A. & Berg, H. A. ZIP9, a novel membrane androgen receptor and zinc transporter protein. *Gen Comp Endocrinol* **257**, 130-136, doi:10.1016/j.ygcen.2017.04.016 (2018).
95 Benten, W. P., Lieberherr, M., Sekeris, C. E. & Wunderlich, F. Testosterone induces Ca2+ influx via non-genomic surface receptors in activated T cells. *FEBS Lett* **407**, 211-214, doi:10.1016/s0014-5793(97)00346-3 (1997).
96 Pi, M., Parrill, A. L. & Quarles, L. D. GPRC6A mediates the non-genomic effects of steroids. *J Biol Chem* **285**, 39953-39964, doi:10.1074/jbc.M110.158063 (2010).
97 Sakkiah, S., Ng, H. W., Tong, W. & Hong, H. Structures of androgen receptor bound with ligands: advancing understanding of biological functions and drug discovery. *Expert Opin Ther Targets* **20**, 1267-1282, doi:10.1080/14728222.2016.1192131 (2016).
98 Edelsztein, N. Y. & Rey, R. A. Importance of the Androgen Receptor Signaling in Gene Transactivation and Transrepression for Pubertal Maturation of the Testis. *Cells* **8**, doi:10.3390/cells8080861 (2019).
99 Pietri, E. *et al.* Androgen receptor signaling pathways as a target for breast cancer treatment. *Endocr Relat Cancer* **23**, R485-498, doi:10.1530/ERC-16-0190 (2016).
100 Leung, J. K. & Sadar, M. D. Non-Genomic Actions of the Androgen Receptor in Prostate Cancer. *Front Endocrinol (Lausanne)* **8**, 2, doi:10.3389/fendo.2017.00002 (2017).
101 Bennett, N. C., Gardiner, R. A., Hooper, J. D., Johnson, D. W. & Gobe, G. C. Molecular cell biology of androgen receptor signalling. *Int J Biochem Cell Biol* **42**, 813-827, doi:10.1016/j.biocel.2009.11.013 (2010).
102 Koryakina, Y., Ta, H. Q. & Gioeli, D. Androgen receptor phosphorylation: biological context and functional consequences. *Endocr Relat Cancer* **21**, T131-145, doi:10.1530/ERC-13-0472 (2014).
103 Ueda, T., Bruchovsky, N. & Sadar, M. D. Activation of the androgen receptor N-terminal domain by interleukin-6 via MAPK and STAT3 signal transduction pathways. *J Biol Chem* **277**, 7076-7085, doi:10.1074/jbc.M108255200 (2002).
104 Bagchi, G. *et al.* Androgens transduce the G alphas-mediated activation of protein kinase A in prostate cells. *Cancer Res* **68**, 3225-3231, doi:10.1158/0008-5472.CAN-07-5026 (2008).
105 Lee, L. F. *et al.* Interleukin-8 confers androgen-independent growth and migration of LNCaP: differential effects of tyrosine kinases Src and FAK. *Oncogene* **23**, 2197-2205, doi:10.1038/sj.onc.1207344 (2004).

106 Garcia, R. *et al.* Constitutive activation of Stat3 by the Src and JAK tyrosine kinases participates in growth regulation of human breast carcinoma cells. *Oncogene* **20**, 2499-2513, doi:10.1038/sj.onc.1204349 (2001).
107 Turkson, J. *et al.* Stat3 activation by Src induces specific gene regulation and is required for cell transformation. *Mol Cell Biol* **18**, 2545-2552, doi:10.1128/mcb.18.5.2545 (1998).
108 Yang, L. *et al.* Induction of androgen receptor expression by phosphatidylinositol 3-kinase/Akt downstream substrate, FOXO3a, and their roles in apoptosis of LNCaP prostate cancer cells. *J Biol Chem* **280**, 33558-33565, doi:10.1074/jbc.M504461200 (2005).
109 Liu, P., Li, S., Gan, L., Kao, T. P. & Huang, H. A transcription-independent function of FOXO1 in inhibition of androgen-independent activation of the androgen receptor in prostate cancer cells. *Cancer Res* **68**, 10290-10299, doi:10.1158/0008-5472.CAN-08-2038 (2008).
110 Liu, X., Qing, S., Che, K., Li, L. & Liao, X. Androgen receptor promotes oral squamous cell carcinoma cell migration by increasing EGFR phosphorylation. *Onco Targets Ther* **12**, 4245-4252, doi:10.2147/OTT.S200718 (2019).
111 Converse, A., Zhang, C. & Thomas, P. Membrane Androgen Receptor ZIP9 Induces Croaker Ovarian Cell Apoptosis via Stimulatory G Protein Alpha Subunit and MAP Kinase Signaling. *Endocrinology* **158**, 3015-3029, doi:10.1210/en.2017-00087 (2017).
112 Shihan, M., Bulldan, A. & Scheiner-Bobis, G. Non-classical testosterone signaling is mediated by a G-protein-coupled receptor interacting with Gnalpha11. *Biochim Biophys Acta* **1843**, 1172-1181, doi:10.1016/j.bbamcr.2014.03.002 (2014).
113 Shihan, M., Chan, K. H., Konrad, L. & Scheiner-Bobis, G. Non-classical testosterone signaling in spermatogenic GC-2 cells is mediated through ZIP9 interacting with Gnalpha11. *Cell Signal* **27**, 2077-2086, doi:10.1016/j.cellsig.2015.07.013 (2015).
114 Thomas, P., Pang, Y., Dong, J. & Berg, A. H. Identification and characterization of membrane androgen receptors in the ZIP9 zinc transporter subfamily: II. Role of human ZIP9 in testosterone-induced prostate and breast cancer cell apoptosis. *Endocrinology* **155**, 4250-4265, doi:10.1210/en.2014-1201 (2014).
115 Henze, L., Schwinge, D. & Schramm, C. The Effects of Androgens on T Cells: Clues to Female Predominance in Autoimmune Liver Diseases? *Front Immunol* **11**, 1567, doi:10.3389/fimmu.2020.01567 (2020).
116 Gubbels Bupp, M. R. & Jorgensen, T. N. Androgen-Induced Immunosuppression. *Front Immunol* **9**, 794, doi:10.3389/fimmu.2018.00794 (2018).
117 McCrohon, J. A. *et al.* Androgen receptor expression is greater in macrophages from male than from female donors. A sex difference with implications for atherogenesis. *Circulation* **101**, 224-226, doi:10.1161/01.cir.101.3.224 (2000).
118 Mantalaris, A. *et al.* Localization of androgen receptor expression in human bone marrow. *J Pathol* **193**, 361-366, doi:10.1002/1096-9896(0000)9999:9999<::AID-PATH803>3.0.CO;2-W (2001).
119 Laffont, S. *et al.* Androgen signaling negatively controls group 2 innate lymphoid cells. *J Exp Med* **214**, 1581-1592, doi:10.1084/jem.20161807 (2017).
120 Chen, W. *et al.* Human mast cells express androgen receptors but treatment with testosterone exerts no influence on IgE-independent mast cell degranulation elicited by neuromuscular blocking agents. *Exp Dermatol* **19**, 302-304, doi:10.1111/j.1600-0625.2009.00969.x (2010).

121 Fijak, M. *et al.* Influence of Testosterone on Inflammatory Response in Testicular Cells and Expression of Transcription Factor Foxp3 in T Cells. *Am J Reprod Immunol* **74**, 12-25, doi:10.1111/aji.12363 (2015).
122 Liva, S. M. & Voskuhl, R. R. Testosterone acts directly on CD4+ T lymphocytes to increase IL-10 production. *J Immunol* **167**, 2060-2067, doi:10.4049/jimmunol.167.4.2060 (2001).
123 adtBebo, B. F., Jr., Schuster, J. C., Vandenbark, A. A. & Offner, H. Androgens alter the cytokine profile and reduce encephalitogenicity of myelin-reactive T cells. *J Immunol* **162**, 35-40 (1999).
124 Viselli, S. M., Olsen, N. J., Shults, K., Steizer, G. & Kovacs, W. J. Immunochemical and flow cytometric analysis of androgen receptor expression in thymocytes. *Mol Cell Endocrinol* **109**, 19-26, doi:10.1016/0303-7207(95)03479-q (1995).
125 Lundell, A. C. *et al.* Dihydrotestosterone levels at birth associate positively with higher proportions of circulating immature/naive CD5(+) B cells in boys. *Sci Rep* **7**, 15503, doi:10.1038/s41598-017-15836-1 (2017).
126 Walecki, M. *et al.* Androgen receptor modulates Foxp3 expression in CD4+CD25+Foxp3+ regulatory T-cells. *Mol Biol Cell* **26**, 2845-2857, doi:10.1091/mbc.E14-08-1323 (2015).
127 Rubinow, K. B. *et al.* Circulating sex steroids coregulate adipose tissue immune cell populations in healthy men. *Am J Physiol Endocrinol Metab* **313**, E528-E539, doi:10.1152/ajpendo.00075.2017 (2017).
128 Hewagama, A., Patel, D., Yarlagadda, S., Strickland, F. M. & Richardson, B. C. Stronger inflammatory/cytotoxic T-cell response in women identified by microarray analysis. *Genes Immun* **10**, 509-516, doi:10.1038/gene.2009.12 (2009).
129 Dunn, S. E. *et al.* Peroxisome proliferator-activated receptor (PPAR)alpha expression in T cells mediates gender differences in development of T cell-mediated autoimmunity. *J Exp Med* **204**, 321-330, doi:10.1084/jem.20061839 (2007).
130 Zhang, M. A. *et al.* Peroxisome proliferator-activated receptor (PPAR)alpha and -gamma regulate IFNgamma and IL-17A production by human T cells in a sex-specific way. *Proc Natl Acad Sci U S A* **109**, 9505-9510, doi:10.1073/pnas.1118458109 (2012).
131 Zhang, M. A. *et al.* Antagonizing Peroxisome Proliferator-Activated Receptor alpha Activity Selectively Enhances Th1 Immunity in Male Mice. *J Immunol* **195**, 5189-5202, doi:10.4049/jimmunol.1500449 (2015).
132 Malkin, C. J. *et al.* The effect of testosterone replacement on endogenous inflammatory cytokines and lipid profiles in hypogonadal men. *J Clin Endocrinol Metab* **89**, 3313-3318, doi:10.1210/jc.2003-031069 (2004).
133 Olsen, N. J. & Kovacs, W. J. Evidence that androgens modulate human thymic T cell output. *J Investig Med* **59**, 32-35, doi:10.2310/jim.0b013e318200dc98 (2011).
134 Fan, Y. *et al.* Low intraprostatic DHT promotes the infiltration of CD8+ T cells in BPH tissues via modulation of CCL5 secretion. *Mediators Inflamm* **2014**, 397815, doi:10.1155/2014/397815 (2014).
135 Yang, Y. *et al.* CD8+ T cells promote proliferation of benign prostatic hyperplasia epithelial cells under low androgen level via modulation of CCL5/STAT5/CCND1 signaling pathway. *Sci Rep* **7**, 42893, doi:10.1038/srep42893 (2017).
136 Giltay, E. J. *et al.* In vivo effects of sex steroids on lymphocyte responsiveness and immunoglobulin levels in humans. *J Clin Endocrinol Metab* **85**, 1648-1657, doi:10.1210/jcem.85.4.6562 (2000).

137 Kissick, H. T. *et al.* Androgens alter T-cell immunity by inhibiting T-helper 1 differentiation. *Proceedings of the National Academy of Sciences* **111**, 9887-9892, doi:10.1073/pnas.1402468111 (2014).
138 Vasanthakumar, A. *et al.* Sex-specific adipose tissue imprinting of regulatory T cells. *Nature*, doi:10.1038/s41586-020-2040-3 (2020).
139 Jia, T. *et al.* Association of Autophagy in the Cell Death Mediated by Dihydrotestosterone in Autoreactive T Cells Independent of Antigenic Stimulation. *J Neuroimmune Pharmacol* **10**, 620-634, doi:10.1007/s11481-015-9633-x (2015).
140 Massa, M. G. *et al.* Testosterone Differentially Affects T Cells and Neurons in Murine and Human Models of Neuroinflammation and Neurodegeneration. *Am J Pathol* **187**, 1613-1622, doi:10.1016/j.ajpath.2017.03.006 (2017).
141 Schwinge, D. *et al.* Testosterone suppresses hepatic inflammation by the downregulation of IL-17, CXCL-9, and CXCL-10 in a mouse model of experimental acute cholangitis. *J Immunol* **194**, 2522-2530, doi:10.4049/jimmunol.1400076 (2015).
142 Dalal, M., Kim, S. & Voskuhl, R. R. Testosterone therapy ameliorates experimental autoimmune encephalomyelitis and induces a T helper 2 bias in the autoantigen-specific T lymphocyte response. *J Immunol* **159**, 3-6 (1997).
143 Wekerle, H., Kojima, K., Lannes-Vieira, J., Lassmann, H. & Linington, C. Animal models. *Ann Neurol* **36 Suppl**, S47-53, doi:10.1002/ana.410360714 (1994).
144 Matsuura, W. *et al.* SLC39A9 (ZIP9) regulates zinc homeostasis in the secretory pathway: characterization of the ZIP subfamily I protein in vertebrate cells. *Biosci Biotechnol Biochem* **73**, 1142-1148, doi:10.1271/bbb.80910 (2009).
145 *GTEx Portal*, <https://gtexportal.org/home/gene/SLC39A9> (2021).
146 Yang, M., Xu, Z. & Zhuang, Z. Macrophages affect immune inflammation and proliferation in benign prostatic hyperplasia via androgen receptor and CD40/CD40L signaling pathway. *Tissue Cell* **64**, 101343, doi:10.1016/j.tice.2020.101343 (2020).
147 Yao, G. & Shang, X. J. A comparison of modulation of proliferation of thymocyte by testosterone, dehydroisoandrosterone and androstenedione in vitro. *Arch Androl* **51**, 257-265, doi:10.1080/014850190924115 (2005).
148 Yao, G., Liang, J., Han, X. & Hou, Y. In vivo modulation of the circulating lymphocyte subsets and monocytes by androgen. *Int Immunopharmacol* **3**, 1853-1860, doi:10.1016/j.intimp.2003.09.002 (2003).
149 Hamzeh, M. & Robaire, B. Effect of testosterone on epithelial cell proliferation in the regressed rat epididymis. *J Androl* **30**, 200-212, doi:10.2164/jandrol.108.006171 (2009).
150 Peng, Y. *et al.* Testosterone induces renal tubular epithelial cell death through the HIF-1alpha/BNIP3 pathway. *J Transl Med* **17**, 62, doi:10.1186/s12967-019-1821-7 (2019).
151 Arnold, J. T., Le, H., McFann, K. K. & Blackman, M. R. Comparative effects of DHEA vs. testosterone, dihydrotestosterone, and estradiol on proliferation and gene expression in human LNCaP prostate cancer cells. *Am J Physiol Endocrinol Metab* **288**, E573-584, doi:10.1152/ajpendo.00454.2004 (2005).
152 Hofling, M. *et al.* Testosterone inhibits estrogen/progestogen-induced breast cell proliferation in postmenopausal women. *Menopause* **14**, 183-190, doi:10.1097/01.gme.0000232033.92411.51 (2007).
153 Ferri, S. *et al.* A multifaceted imbalance of T cells with regulatory function characterizes type 1 autoimmune hepatitis. *Hepatology* **52**, 999-1007, doi:10.1002/hep.23792 (2010).

154 Longhi, M. S. *et al.* Expansion and de novo generation of potentially therapeutic regulatory T cells in patients with autoimmune hepatitis. *Hepatology* **47**, 581-591, doi:10.1002/hep.22071 (2008).
155 Rong, G. *et al.* Imbalance between T helper type 17 and T regulatory cells in patients with primary biliary cirrhosis: the serum cytokine profile and peripheral cell population. *Clin Exp Immunol* **156**, 217-225, doi:10.1111/j.1365-2249.2009.03898.x (2009).
156 Chen, J. *et al.* Regulatory T cells with a defect in inhibition on co-stimulation deteriorated primary biliary cholangitis. *Oncotarget* **8**, 108406-108417, doi:10.18632/oncotarget.22658 (2017).
157 Fijak, M. *et al.* Testosterone replacement effectively inhibits the development of experimental autoimmune orchitis in rats: evidence for a direct role of testosterone on regulatory T cell expansion. *J Immunol* **186**, 5162-5172, doi:10.4049/jimmunol.1001958 (2011).
158 Zhang, B. *et al.* BAFF promotes regulatory T-cell apoptosis and blocks cytokine production by activating B cells in primary biliary cirrhosis. *Braz J Med Biol Res* **46**, 433-439, doi:10.1590/1414-431X20132665 (2013).
159 Canale, F. P., Ramello, M. C. & Montes, C. L. CD39 as a marker of pathogenic CD8+ T cells in cancer and other chronic inflammatory diseases. *Oncoscience* **5**, 65-66, doi:10.18632/oncoscience.404 (2018).
160 Fuseini, H. *et al.* Testosterone Decreases House Dust Mite-Induced Type 2 and IL-17A-Mediated Airway Inflammation. *J Immunol* **201**, 1843-1854, doi:10.4049/jimmunol.1800293 (2018).
161 Yasuda, K., Takeuchi, Y. & Hirota, K. The pathogenicity of Th17 cells in autoimmune diseases. *Semin Immunopathol* **41**, 283-297, doi:10.1007/s00281-019-00733-8 (2019).
162 Kunzmann, L. K. *et al.* Monocytes as potential mediators of pathogen-induced Th17 differentiation in patients with primary sclerosing cholangitis (PSC). *Hepatology*, doi:10.1002/hep.31140 (2020).
163 Bae, H. R. *et al.* Chronic expression of interferon-gamma leads to murine autoimmune cholangitis with a female predominance. *Hepatology* **64**, 1189-1201, doi:10.1002/hep.28641 (2016).
164 Arellano, G., Ottum, P. A., Reyes, L. I., Burgos, P. I. & Naves, R. Stage-Specific Role of Interferon-Gamma in Experimental Autoimmune Encephalomyelitis and Multiple Sclerosis. *Front Immunol* **6**, 492, doi:10.3389/fimmu.2015.00492 (2015).
165 Carbajal, K. S. *et al.* Th Cell Diversity in Experimental Autoimmune Encephalomyelitis and Multiple Sclerosis. *J Immunol* **195**, 2552-2559, doi:10.4049/jimmunol.1501097 (2015).
166 Kleiveland, C. R. in *The Impact of Food Bioactives on Health: in vitro and ex vivo models* (eds Kitty Verhoeckx *et al.*) 161-167 (Springer International Publishing, 2015).
167 Idriss, H. T. & Naismith, J. H. TNF alpha and the TNF receptor superfamily: structure-function relationship(s). *Microsc Res Tech* **50**, 184-195, doi:10.1002/1097-0029(20000801)50:3<184::AID-JEMT2>3.0.CO;2-H (2000).
168 Ma, W. *et al.* Targeting androgen receptor with ASC-J9 attenuates cardiac injury and dysfunction in experimental autoimmune myocarditis by reducing M1-like macrophage. *Biochem Biophys Res Commun* **485**, 746-752, doi:10.1016/j.bbrc.2017.02.123 (2017).

169 Jordan, A. R., Racine, R. R., Hennig, M. J. & Lokeshwar, V. B. The Role of CD44 in Disease Pathophysiology and Targeted Treatment. *Front Immunol* **6**, 182, doi:10.3389/fimmu.2015.00182 (2015).
170 de Araujo-Souza, P. S. *et al.* Differential interferon-gamma production by naive and memory-like CD8 T cells. *J Leukoc Biol* **108**, 1329-1337, doi:10.1002/JLB.2AB0420-646R (2020).
171 Otsuki, N., Kamimura, Y., Hashiguchi, M. & Azuma, M. Expression and function of the B and T lymphocyte attenuator (BTLA/CD272) on human T cells. *Biochem Biophys Res Commun* **344**, 1121-1127, doi:10.1016/j.bbrc.2006.03.242 (2006).
172 Sawaf, M. *et al.* Defective BTLA functionality is rescued by restoring lipid metabolism in lupus CD4+ T cells. *JCI Insight* **3**, doi:10.1172/jci.insight.99711 (2018).
173 Oster, C. *et al.* BTLA Expression on Th1, Th2 and Th17 Effector T-Cells of Patients with Systemic Lupus Erythematosus Is Associated with Active Disease. *Int J Mol Sci* **20**, doi:10.3390/ijms20184505 (2019).
174 Al-Othman, N., Hammad, H. & Ahram, M. Dihydrotestosterone regulates expression of CD44 via miR-328-3p in triple-negative breast cancer cells. *Gene* **675**, 128-135, doi:10.1016/j.gene.2018.06.094 (2018).
175 Al-Othman, N. *et al.* Role of CD44 in breast cancer. *Breast Dis* **39**, 1-13, doi:10.3233/BD-190409 (2020).
176 Poch, T. *et al.* Single-cell atlas of hepatic T cells reveals expansion of liver-resident naive-like CD4+ T cells in primary sclerosing cholangitis. *J Hepatol*, doi:10.1016/j.jhep.2021.03.016 (2021).
177 Ichiki, Y. *et al.* T cell immunity in autoimmune hepatitis. *Autoimmun Rev* **4**, 315-321, doi:10.1016/j.autrev.2005.01.005 (2005).
178 Larbi, A. & Fulop, T. From "truly naive" to "exhausted senescent" T cells: when markers predict functionality. *Cytometry A* **85**, 25-35, doi:10.1002/cyto.a.22351 (2014).
179 Effros, R. B. Telomere/telomerase dynamics within the human immune system: effect of chronic infection and stress. *Exp Gerontol* **46**, 135-140, doi:10.1016/j.exger.2010.08.027 (2011).
180 Nunes, C. *et al.* Expansion of a CD8(+)PD-1(+) replicative senescence phenotype in early stage CLL patients is associated with inverted CD4:CD8 ratios and disease progression. *Clin Cancer Res* **18**, 678-687, doi:10.1158/1078-0432.CCR-11-2630 (2012).
181 Henson, S. M. *et al.* KLRG1 signaling induces defective Akt (ser473) phosphorylation and proliferative dysfunction of highly differentiated CD8+ T cells. *Blood* **113**, 6619-6628, doi:10.1182/blood-2009-01-199588 (2009).
182 Verma, K. *et al.* Human CD8+ CD57- TEMRA cells: Too young to be called "old". *PLoS One* **12**, e0177405, doi:10.1371/journal.pone.0177405 (2017).
183 Reinke, S. *et al.* Terminally differentiated CD8(+) T cells negatively affect bone regeneration in humans. *Sci Transl Med* **5**, 177ra136, doi:10.1126/scitranslmed.3004754 (2013).
184 Yap, M. *et al.* Expansion of highly differentiated cytotoxic terminally differentiated effector memory CD8+ T cells in a subset of clinically stable kidney transplant recipients: a potential marker for late graft dysfunction. *J Am Soc Nephrol* **25**, 1856-1868, doi:10.1681/ASN.2013080848 (2014).
185 Di Mitri, D. *et al.* Reversible senescence in human CD4+CD45RA+CD27- memory T cells. *J Immunol* **187**, 2093-2100, doi:10.4049/jimmunol.1100978 (2011).

186 Tian, Y. *et al.* Unique phenotypes and clonal expansions of human CD4 effector memory T cells re-expressing CD45RA. *Nat Commun* **8**, 1473, doi:10.1038/s41467-017-01728-5 (2017).
187 Betjes, M. G., Meijers, R. W., de Wit, E. A., Weimar, W. & Litjens, N. H. Terminally differentiated CD8+ Temra cells are associated with the risk for acute kidney allograft rejection. *Transplantation* **94**, 63-69, doi:10.1097/TP.0b013e31825306ff (2012).
188 Bruns, H. *et al.* Anti-TNF immunotherapy reduces CD8+ T cell-mediated antimicrobial activity against Mycobacterium tuberculosis in humans. *J Clin Invest* **119**, 1167-1177, doi:10.1172/JCI38482 (2009).
189 Mehling, M. *et al.* FTY720 therapy exerts differential effects on T cell subsets in multiple sclerosis. *Neurology* **71**, 1261-1267, doi:10.1212/01.wnl.0000327609.57688.ea (2008).
190 Efremova, M., Vento-Tormo, M., Teichmann, S. A. & Vento-Tormo, R. CellPhoneDB: inferring cell-cell communication from combined expression of multi-subunit ligand-receptor complexes. *Nat Protoc* **15**, 1484-1506, doi:10.1038/s41596-020-0292-x (2020).
191 Schwefel, D. *et al.* Structural insights into the mechanism of GTPase activation in the GIMAP family. *Structure* **21**, 550-559, doi:10.1016/j.str.2013.01.014 (2013).
192 Barnes, M. J. *et al.* Loss of T cell and B cell quiescence precedes the onset of microbial flora-dependent wasting disease and intestinal inflammation in Gimap5-deficient mice. *J Immunol* **184**, 3743-3754, doi:10.4049/jimmunol.0903164 (2010).
193 Schulteis, R. D. *et al.* Impaired survival of peripheral T cells, disrupted NK/NKT cell development, and liver failure in mice lacking Gimap5. *Blood* **112**, 4905-4914, doi:10.1182/blood-2008-03-146555 (2008).
194 Saunders, A. *et al.* Putative GTPase GIMAP1 is critical for the development of mature B and T lymphocytes. *Blood* **115**, 3249-3257, doi:10.1182/blood-2009-08-237586 (2010).
195 Yano, K. *et al.* Gimap3 and Gimap5 cooperate to maintain T-cell numbers in the mouse. *Eur J Immunol* **44**, 561-572, doi:10.1002/eji.201343750 (2014).
196 Ciucci, T. & Bosselut, R. Gimap and T cells: a matter of life or death. *Eur J Immunol* **44**, 348-351, doi:10.1002/eji.201344375 (2014).
197 Filen, S. & Lahesmaa, R. GIMAP Proteins in T-Lymphocytes. *J Signal Transduct* **2010**, 268589, doi:10.1155/2010/268589 (2010).
198 Nitta, T. *et al.* IAN family critically regulates survival and development of T lymphocytes. *PLoS Biol* **4**, e103, doi:10.1371/journal.pbio.0040103 (2006).
199 Rincon, M. & Flavell, R. A. AP-1 transcriptional activity requires both T-cell receptor-mediated and co-stimulatory signals in primary T lymphocytes. *EMBO J* **13**, 4370-4381 (1994).
200 Carr, T. M., Wheaton, J. D., Houtz, G. M. & Ciofani, M. JunB promotes Th17 cell identity and restrains alternative CD4(+) T-cell programs during inflammation. *Nat Commun* **8**, 301, doi:10.1038/s41467-017-00380-3 (2017).
201 Li, B., Tournier, C., Davis, R. J. & Flavell, R. A. Regulation of IL-4 expression by the transcription factor JunB during T helper cell differentiation. *EMBO J* **18**, 420-432, doi:10.1093/emboj/18.2.420 (1999).
202 Zhang, Y., Zhang, Y., Gu, W. & Sun, B. TH1/TH2 cell differentiation and molecular signals. *Adv Exp Med Biol* **841**, 15-44, doi:10.1007/978-94-017-9487-9_2 (2014).

203 Katagiri, T., Kameda, H., Nakano, H. & Yamazaki, S. Regulation of T cell differentiation by the AP-1 transcription factor JunB. *Immunol Med*, 1-12, doi:10.1080/25785826.2021.1872838 (2021).
204 Wu, J. *et al.* Regulatory T cells sense effector T-cell activation through synchronized JunB expression. *FEBS Lett* **593**, 1020-1029, doi:10.1002/1873-3468.13393 (2019).
205 Yamazaki, S. *et al.* The AP-1 transcription factor JunB is required for Th17 cell differentiation. *Sci Rep* **7**, 17402, doi:10.1038/s41598-017-17597-3 (2017).
206 Katagiri, T. *et al.* JunB plays a crucial role in development of regulatory T cells by promoting IL-2 signaling. *Mucosal Immunol* **12**, 1104-1117, doi:10.1038/s41385-019-0182-0 (2019).
207 Yukawa, M. *et al.* AP-1 activity induced by co-stimulation is required for chromatin opening during T cell activation. *J Exp Med* **217**, doi:10.1084/jem.20182009 (2020).
208 Naito, T., Tanaka, H., Naoe, Y. & Taniuchi, I. Transcriptional control of T-cell development. *Int Immunol* **23**, 661-668, doi:10.1093/intimm/dxr078 (2011).
209 Chuang, H. C. & Tan, T. H. MAP4K Family Kinases and DUSP Family Phosphatases in T-Cell Signaling and Systemic Lupus Erythematosus. *Cells* **8**, doi:10.3390/cells8111433 (2019).
210 Bentz, E. K. *et al.* Gene expression signatures of breast tissue before and after cross-sex hormone therapy in female-to-male transsexuals. *Fertil Steril* **94**, 2688-2696, doi:10.1016/j.fertnstert.2010.04.024 (2010).
211 Jiang, X. *et al.* The immunobiology of mucosal-associated invariant T cell (MAIT) function in primary biliary cholangitis: Regulation by cholic acid-induced Interleukin-7. *J Autoimmun* **90**, 64-75, doi:10.1016/j.jaut.2018.01.007 (2018).
212 Setsu, T. *et al.* Persistent reduction of mucosal-associated invariant T cells in primary biliary cholangitis. *J Gastroenterol Hepatol* **33**, 1286-1294, doi:10.1111/jgh.14076 (2018).
213 Bottcher, K. *et al.* MAIT cells are chronically activated in patients with autoimmune liver disease and promote profibrogenic hepatic stellate cell activation. *Hepatology* **68**, 172-186, doi:10.1002/hep.29782 (2018).
214 Hua, F. *et al.* Elevation of Vdelta1 T cells in peripheral blood and livers of patients with primary biliary cholangitis. *Clin Exp Immunol* **186**, 347-355, doi:10.1111/cei.12852 (2016).
215 Martins, E. B., Graham, A. K., Chapman, R. W. & Fleming, K. A. Elevation of gamma delta T lymphocytes in peripheral blood and livers of patients with primary sclerosing cholangitis and other autoimmune liver diseases. *Hepatology* **23**, 988-993, doi:10.1002/hep.510230508 (1996).
216 Hammerich, L. & Tacke, F. Role of gamma-delta T cells in liver inflammation and fibrosis. *World J Gastrointest Pathophysiol* **5**, 107-113, doi:10.4291/wjgp.v5.i2.107 (2014).
217 Ujiie, H. & Shevach, E. M. gammadelta T Cells Protect the Liver and Lungs of Mice from Autoimmunity Induced by Scurfy Lymphocytes. *J Immunol* **196**, 1517-1528, doi:10.4049/jimmunol.1501774 (2016).
218 Huber, S. A., Kupperman, J. & Newell, M. K. Hormonal regulation of CD4(+) T-cell responses in coxsackievirus B3-induced myocarditis in mice. *J Virol* **73**, 4689-4695, doi:10.1128/JVI.73.6.4689-4695.1999 (1999).
219 Liu, J., Nan, H., Brutkiewicz, R. R., Casasnovas, J. & Kua, K. L. Sex discrepancy in the reduction of mucosal-associated invariant T cells caused by obesity. *Immun Inflamm Dis* **9**, 299-309, doi:10.1002/iid3.393 (2021).

220 Chen Yu, S. L., Nicholas Giroux, Rose Mathew, Shengli Ding, Joan Kalnitsky, Elizabeth W. Petzold, Hong Chung, Grecia Rivera Palomino, Tomer Rotstein, Rui Xi, Emily R. Ko, Ephraim L. Tsalik, Gregory D. Sempowski, Thomas N. Denny, Thomas W. Burke, Micah T. McClain, Christopher W. Woods, Xiling Shen, Daniel R. Saban. *Mucosal Associated Invariant T (MAIT) Cell Responses Differ by Sex in COVID-19*, <https://www.biorxiv.org/content/10.1101/2020.12.01.407148v1.abstract> (2020/12/01).

221 Pradhan, A. & Olsson, P. E. Sex differences in severity and mortality from COVID-19: are males more vulnerable? *Biol Sex Differ* **11**, 53, doi:10.1186/s13293-020-00330-7 (2020).

222 Mohamed, M. S., Moulin, T. C. & Schioth, H. B. Sex differences in COVID-19: the role of androgens in disease severity and progression. *Endocrine* **71**, 3-8, doi:10.1007/s12020-020-02536-6 (2021).

223 Wei, Y. *et al.* Alterations of gut microbiome in autoimmune hepatitis. *Gut* **69**, 569-577, doi:10.1136/gutjnl-2018-317836 (2020).

224 Zheng, D., Liwinski, T. & Elinav, E. Interaction between microbiota and immunity in health and disease. *Cell Res* **30**, 492-506, doi:10.1038/s41422-020-0332-7 (2020).

225 University Hospital of Ghent. *Free & Bioavailable Testosterone calculator*, <http://www.issam.ch/freetesto.htm> (access (05.11.2020)).

226 Vermeulen, A., Verdonck, L. & Kaufman, J. M. A critical evaluation of simple methods for the estimation of free testosterone in serum. *J Clin Endocrinol Metab* **84**, 3666-3672, doi:10.1210/jcem.84.10.6079 (1999).

227 Qiu, P. *et al.* Extracting a cellular hierarchy from high-dimensional cytometry data with SPADE. *Nat Biotechnol* **29**, 886-891, doi:10.1038/nbt.1991 (2011).

228 Gautreau, G. *et al.* SPADEVizR: an R package for visualization, analysis and integration of SPADE results. *Bioinformatics* **33**, 779-781, doi:10.1093/bioinformatics/btw708 (2017).

List of Tables & Figures

Figures

Tables

Declaration on oath

DECLARATION ON OATH

I hereby certify, on oaths, that I have written this dissertation myself and that I have not used any aids other than those specified. The submitted written version corresponds to that on the electronic storage medium. I confirm that this dissertation was not submitted in a previous doctoral procedure.

EIDESSTATTLICHE VERSICHERUNG

Hiermit versichere ich an Eides statt, die vorliegende Dissertation selbst verfasst und keine anderen als die angegebenen Hilfsmittel benutzt zu haben. Die eingereichte schriftliche Fassung entspricht der auf dem elektronischen Speichermedium. Ich versichere, dass diese Dissertation nicht in einem früheren Promotionsverfahren eingereicht wurde.

Date, Signature

Danksagung

Zunächst geht ein Riesendankeschön an Dr. Dorothee Schwinge, die mich in den letzten Jahren so toll als Betreuerin und ganz tolle Kollegin unterstützt hat. Ohne dich hätte ich diese Zeit nicht so schön „überstanden“. Tausend Dank!!!

Bei Prof. Dr. Christoph Schramm möchte ich mich sehr für die gesamte tolle Betreuung und das tolle Projekt, an dem ich arbeiten durfte bedanken!

Danke euch beiden für alles!!

Ein mega riesen mega Danke geht an alle Menschen, die in unserem wunderschönen Laborflur arbeiten!! Ohne euch hätte ich das nicht geschafft. Insbesondere möchte ich den tollen TA’s für ihre Unterstützung danken! Vielen Dank liebe Sabrina, Gela, Jenny, Nina, Marko und Nicola!

Zudem auch ein fettes Danke an alle anderen Kollegen und Kolleginnen ohne die es nur halb so lustig gewesen wäre und die auch immer geholfen haben. Besonderen Dank geht hier an die liebe Steffi, Anna, Fenja, Tobi und meinen Medizini Jasper!

Ein riesen Danke geht auch an alle die anderen Arbeitsgruppen, mit denen ich zusammenarbeiten durfte und die das Projekt erst so spannend gemacht haben. Besonders an das Transit Team rund um Johannes Fuß, die uns diese tollen Proben ermöglicht haben.

Ein besonderer Dank geht auch an meine lieben Eltern und meine tolle Schwester, sowie meine gesamte inzwischen erweitere tolle Familie und all meine lieben Freunde. Vielen Dank für eure Unterstützung und die Bereicherung meines Nicht-Labor-Lebens ☺! Last but not least, ein nicht in Worten fassbares Danke an meinem geliebten Mann, ohne dich hätte ich das nicht geschafft!

Ich hoffe ich habe niemand vergessen, auf jeden Fall einfach ein fettes Danke an alle die das hier lesen!!!